SYNTHESIS AND CHARACTERIZATION OF SOME NOVEL SUPPORTED METAL CATALYSTS TO CONTROL CARBON MONOXIDE EMISSION FROM AUTOMOBILE VEHICLE EXHAUST

Thesis submitted by

Souvik Das

Master of Chemical Engineering

Class Roll no: 002210302006

Exam Roll no: M4CHE24006

Session: 2022-2024

Registration Number: 163436 Of 2022-2023

Under the guidance of

Dr. (Prof) Ujjaini Sarkar

Professor

Chemical Engineering Department

Jadavpur university

Kolkata, India-700032

DECLARATION OF ORIGINALITY AND COMPLIANCE OF ACADEMIC ETHICS

I hereby declare that this thesis contains literature survey and original research work by the undersigned candidate, as part of his "***Master of Engineering in Chemical Engineering***" studies. All information in this document have been obtained and presented in accordance with academic rules and ethical conduct.

I also declare that, as required by these rules and conduct, I have fully cited and referenced all material and results that are not original to research work.

Name: SOUVIK DAS

Roll No: 002210302006

Registration No.: 163436

Thesis Title: SYNTHESIS AND CHARACTERIZATION OF SOME NOVEL SUPPORTED METAL CATALYSTS TO CONTROL CARBON MONOXIDE EMISSION FROM AUTOMOBILE VEHICLE EXHAUST.

Signature: Souvik Das

Date: 30/05/2024

CERTIFICATE

This is to certify that Mr. Souvik Das, Final year Masters of Chemical Engineering (M.ChE) examination student of Department of Chemical Engineering, Jadavpur University, Class Roll No. 002210302006, Registration No. 163436 of 2022- 2023, Examination Roll No. M4CHE24006 has completed the Project work titled, "Synthesis And Characterization Of Some Novel Supported Metal Catalysts To Control Carbon Monoxide Emission From Automobile Vehicle Exhaust" under the guidance of Dr. (Prof.) Ujjaini Sarkar during his Master's Curriculum. This work has not been reported earlier anywhere and can be approved for submission in partial fulfilment of the course work.

Ujjaini Sarkar 29.5.2024

Dr.(Prof.) Ujjaini sarkar
Project Supervisor, Professor
Chemical Engineering Department,
Jadavpur University

Professor
HEMICAL ENGINEERING DEPARTMENT
JADAVPUR UNIVERSITY
Kolkata-700 032

29/5/24

Dr.(Prof.) Papita Das
Head of the Department
Chemical Engineering Department,
Jadavpur university

HEAD
CHEMICAL ENGINEERING DEPARTMENT
JADAVPUR UNIVERSITY
Kolkata-700 032

Dipan Laha 29/5/24

Dean
Faculty of Engineering & Technology
Jadavpur University

DEAN
Faculty of Engineering & Technology
JADAVPUR UNIVERSITY
KOLKATA-700 032

CERTIFICATE OF APPROVAL

This thesis is hereby approved as creditable study of an engineering subject carried out and presented in a manner satisfactory to warrant its acceptance as prerequisite to the degree for which it has been submitted. It is understood by this approval that undersigned don't endorse or approve any statement made, opinion expressed or conclusion drawn therein but approve the thesis only for purpose of which it is submitted.

Souvik Das 30/5/24

Souvik Das

Roll No: 002210302006

Exam Roll No: M4CHE24006

Registration No: 163436

Department of Chemical Engineering

Jadavpur University

ACKNOWLEDGEMENT

I consider it as my privilege to express gratitude and respect to all those who guided and inspired me in the completion of my 1st Phase of term paper. The undertaking of this project inculcated a strong sense of research inside me and I also came to know about so many new things.

I am highly obliged and grateful to my Project Coordinator **Dr. (Prof.) Ujjaini Sarkar, Professor at Department of Chemical Engineering, Jadavpur university, Kolkata** for her excellent guidance, endless encouragement, and cooperation extended to me from the onset of this task until its successful completion.

I am very grateful to **Dr.(Prof.) Papita Das, Head of the Chemical Engineering Department, Jadavpur University** for all the necessary help I got during my project work.

I am also indebted to **Jadavpur University, Dept. of Chemical Engineering**, for supporting me and giving me the opportunity to use the equipment to do my research. I would like to acknowledge **Mr. Dhruba Sakha, IIT Kharagpur, Chemical engineering Department** for their contribution to analysis BET. I would like to thank **IACS ,Kolkata** and **CGCRI, Kolkata** helping me to analysis FTIR Spectroscopy. Also, I would like to thank **Mr. Sudhir Ghosh, Metallurgy Department**, Jadavpur University helping to analysis XRD and **Physics Department**, Jadavpur University helping me in FE-SEM Analysis.

My sincere appreciation also extends to all my lab mates, **Miss Deblina Sengupta, Mr. Debojyoti Das** and **Miss. Ashima Mondal** who have provided assistance on various occasions. I would also like to extend my thanks to our Lab assistant Mr. Rakesh Day, who has helped me a lot throughout my work.

I am grateful to my parents and all of my family members who encouraged and supported me all through and helped me in all respect.

Souvik Das 30/5/24

Souvik Das

ABSTRACT

Catalytic oxidation of carbon monoxide (CO) has been receiving attention due to higher amount of CO emission from automobile vehicle exhaust [Internal Combustion (IC) engine] which affects human health and environment to a great extent. The main focus of this piece of research is to synthesize a dedicated catalyst to control carbon monoxide emission selectively, in presence of carbon dioxide, hydrocarbons, and oxides of nitrogen and sulphur. A series of three catalysts is prepared. At first the supports were prepared. The CeO_2-Al_2O_3 supported Cu catalyst is synthesized using conventional one step incipient wet impregnation method [named as Cu/CA]. Next, another CeO_2-Al_2O_3 supported Cu catalyst is prepared using the same method where copper nitrate hydrate is used as a precursor for both support and the catalyst [named as Cu/CA-T]. A reference Cu/Al_2O_3 catalyst is also prepared. A detailed characterization study is undertaken to gain insight into the impact of the support morphology on the surface, structural and chemical properties. The catalysts are specifically characterized using a Scanning Electron Microscopy (SEM) for morphological details, X-ray Powder Diffraction (XRD) to identify the molecular structure, Fourier-Transform Infrared Spectroscopy (FTIR) based analysis to identify the functional groups, CHNS for elemental analysis, Thermo-Gravimetric Analysis (TGA) to establish the thermal stability and Brunauer–Emmett–Teller Analysis (BET) to find out the surface area to volume ratio and pore-size distribution. Finally, the synthesized catalysts are tested to determine their capability of removal of CO from automobile exhaust pipe. This study focus on the behaviour of catalysts at varying temperatures, gas compositions and flow rates, characteristic of automobile exhaust environments.

Table of Contents

Chapter No and Name	Section Heading	Page No
Chapter 1: Control of Carbon Monoxide from vehicular Exhaust: Background	1.1. Background	1-1 – 1-4
	1.2. Automobile Pollution	1-4 – 1-5
	1.3. Generation of CO from Automobile Exhaust	1-6 – 1-7
	1.3.1. Generation of CO during cold start condition	1-7 – 1-9
	1.4. Carbon Monoxide (CO)	1-9
	1.4.1. Physical and Chemical Characteristics	1-9 -1-10
	1.4.2. Environmental concerns	1-11
	1.4.2.1. Health impact on Human being	1-11 – 1-12
	1.4.2.2. Health impacts on Animals and Birds	1-12 – 1-13
	1.4.3. Toxicity or Toxicological Effect	1-13 – 1-15
	1.5. Methods of control of CO in Automobile Exhaust	1-15 – 1-16
	1.5.1. National Efforts to control CO	1-16 – 1-18
	1.5.2. Control by Catalytic converter	1-18
	1.5.2.1. Construction of Catalytic Converter	1-18 – 1.19
	1.5.2.2. Mechanism of Catalytic Converter	1-19 – 1-20
	1.5.3. Alternate of Source of Fuel	1-20 -1-21
Chapter 2: Control of Carbon Monoxide from vehicular exhaust: Review of literature, research gaps and objectives	2.0. Research gaps	2-1 – 2-4
	2.1. Statement of the problem	2-4
	2.2. Objective: Overall and Specific	2-4
	2.3. Literature Review	2-5 – 2-10
	3.0. Introduction	3-1 -3-2
	3.1. Selective Catalysts chosen	3-2 -3-4

Chapter 3: Control of Carbon monoxide from vehicular exhaust: Synthesis of Selective Catalysts	3.2. Methods of Synthesis	3-7
	3.2.1. Synthesis of Catalyst 1 (Cu/CA) by IWI method	3-7
	3.2.2. Synthesis of Catalyst 2 (Cu/CA-T) by T-IWI method	3-7 – 3-8
	3.2.3. Synthesis of Catalyst 3 (Cu/A) by IWI method	3-8
	3.2.4. Synthesis of Catalyst 4 (Cu/CA-S) by Solution gelation method	3-9
Chapter 4: Control of Carbon Monoxide from vehicular exhaust: Physical and Chemical Characterization of Synthesized catalysts	4.1. CHNS based Elemental analysis	4-1 – 4-4
	4.2. Fourier Transform Infrared Spectroscopy (FT-IR) based analysis	4-5 – 4-10
	4.3. Thermogravimetric (TGA) analysis	4-11 – 4-16
	4.4. Surface area and Pore volume analysis	4-17 – 4-26
	4.5. X-Ray Diffraction (XRD) analysis	4-27 – 4-36
	4.6. Field Emission Scanning Electron Microscopy (FESEM) analysis	4-37 – 4-42
Chapter 5: Control of Carbon Monoxide from vehicular exhaust: In-situ control using portable paced bed filled with synthesized catalysts	5.0. Introduction	5-1
	5.1. IC Engine details and Generation of CO	5-2 – 5-4
	5.1.1. Generation of CO (Carbon Monoxide)	5-5 – 5-6
	5.2. Design of the Experiments	5-7 – 5-10
	5.2.1. Parameters for Testing	5-10
	5.3. Results and Discussion	5-11 – 5-23
Chapter 6: Conclusion and recommendations for Future works	6.1. Conclusion	6-01 – 6-02
	6.2. Recommendation for Future work	6-02 – 6-03
Chapter 7: References	References	7-01 – 7-03

List of Figures

Chapter No and Name	Figure Heading	Page No.
Chapter 1: Introduction	1.1. Sources of emissions of air pollution	1-2
	1.2. Contribution of Toxic elements from Vehicular Exhaust	1-3
	1.3. Symptoms of CO poisoning	1-12
	1.4. Schematic Diagram of Catalytic Converter	1-19
	1.5. Conversion of CO to CO_2 using catalysts	1-20
Chapter 3: Control of Carbon monoxide from vehicular exhaust: Synthesis of Selective Catalysts	3.1. Precursors in use (a) Aluminium (Gamma) nano powder, (b) Copper Nitrate Hydrate, (c) Cerium Nitrate Hexahydrate, (d) Aluminium iso-Propoxide	3-6
	3.2. (a) Catalyst 1 (Cu/CA), (b) Catalyst 2 (Cu/CA-T), (c) Catalyst 3 (Cu/A), (d) Catalyst 4 (Cu/CA-S)	3-10
Chapter 4: Control of Carbon Monoxide from vehicular exhaust: Physical and Chemical Characterization of Synthesized catalysts	4.1. Schematic diagram of the principle of working of a CHNS analyser	4-2
	4.2. Bar diagram representing weight percentage of Carbon, Hydrogen, Nitrogen and Sulphur for the four (4) nos. of catalysts synthesized	4-4
	4.3. Fourier transform infrared (FTIR) spectra of (a) Cu/CA, (b) Cu/CA-T and (c) Cu/A	4-8
	4.4. Consolidated FT-IR plots to compare the transmittance peaks for Cu/CA, Cu/CA-T and Cu/A	4-9
	4.5. TGA plots of synthesized (a) Cu/CA, (b) Cu/CA-T, (c) Cu/A	4-13 – 4-15
	4.6. Consolidated TGA plots of synthesized (a)Cu-CA, (b)Cu-CAT, (c) Cu-A	4-16
	4.7. Nitrogen adsorption-desorption isotherms of (a) Cu/CA, (b) Cu/CAT and (c) Cu/A	4-19 – 4-21
	4.8. BJH pore size distribution curves of (a) Cu/CA, (b) Cu/CAT and (c) Cu/A	4-22 – 4-23

	4.9. Density Functional Theory [DFT] based pore size distribution model curves of (a) Cu/CA, (b) Cu/CAT, (c) Cu/A	4-25 – 4-26
	4.10. XRD patterns of (a) Cu/CA, (b) Cu/CA-T, (c) Cu/A and (d) Cu/CA-S	4-33 -4-36
	4.11. FESEM images and particle size distribution histogram of synthesized catalysts: (a) Cu/CA, (b) Cu/CA-T, (c) Cu/A, (d) Cu/CA-S	4-39 – 4-42
Chapter 5: Control of Carbon Monoxide from vehicular exhaust: In-situ control using portable paced bed filled with synthesized catalysts	5.1. Schematic diagram of an IC engine	5-3
	5.2. Inner Structure of the catalytic converter present in a car exhaust pipe	5-4
	5.3. The vehicle [Make: Maruti-Suzuki; Model: 800 DX] used for testing	5-6
	5.4. Raw material of the external structure of the cylindrical packed bed (Aluminium Mesh)	5-8
	5.5. Cylindrical envelopes for storing the cotton beds packed with synthesized catalysts.	5-8
	5.6. Catalysts dispersed over the cotton bed for (a) Cu/CA, (b) Cu/CAT, (c) Cu/A	5-9
	5.7. Cylindrical packed-bed stuffed with well-dispersed synthesized catalysts	5-10
	5.8. Installation of the packed-bed filled with catalysts at the tailpipe	5-11
	5.9. Pictures of monitoring of CO, testing and recording the data-sets	5-13
	5.10. Comparison plots of CO emissions with various quantity of catalysts and accelerated speed: (a) Quantity=0.5 gm, Speed=10 km/h, (b) Quantity=0.5 gm, Speed=20 km/h, (c) Quantity= 1.0 gm, Speed= 10 km/h, (d) Quality=1.0 gm, Speed=20 km/h	5-20 – 5-21

List of Tables

Chapter No and Names	Table Headings	Page No
Chapter 1: Control of Carbon Monoxide from vehicular exhaust: Background	1.1. Basic Properties	1-9 -1-10
	1.2. Toxicity data for carbon monoxide on mammals and birds	1-14 – 1-15
	1.3. Emission norms in India parallel to EU emission standards	1-16 – 1-17
	1.4. Pollution load estimated in different city in India, CPCB	1-17 – 1-18
Chapter 2: Control of Carbon Monoxide from vehicular exhaust: Review of literature, research gaps and objectives	2.1. Review of Literature	2-5 – 2-10
Chapter 3: Control of Carbon monoxide from vehicular exhaust: Synthesis of Selective Catalysts	3.1. Physical and chemical properties of the precursors and used compounds during the synthesis of various catalysts	3-5
	3.2. Details of the protocol followed during synthesis of the catalysts	3-11 – 3-13
Chapter 4: Control of Carbon Monoxide from vehicular exhaust: Physical and Chemical Characterization of Synthesized catalysts	4.1. Weight percentages of carbon, Hydrogen, Nitrogen and Sulphur	4-4
	4.2. Identification of Functional groups present in the three catalysts using Figure 4.3 (a, b, c) along with actual and normalized peak areas	4-11 -4-12
	4.3. Estimated data of Surface area, Pore volume and pore radius of the synthesized catalysts	4-24
	4.4. Phase analysis data of (a) Cu/CA, (b) Cu/CA-T, (c) Cu/A and (d) Cu/CA-S	4-31 -4-32
	4.5. Average crystalline size of the synthesized catalysts	4-32

	4.6. Percentage of Crystallinity index of the catalysts	4-32
Chapter 5: Control of Carbon Monoxide from vehicular exhaust: In-situ control using portable paced bed filled with synthesized catalysts	5.1. CO emission testing without using any catalyst [control]	5-11 -5-12
	5.2. Control of CO emissions using Catalyst 1 (Cu/CA)	5-13 -5-15
	5.3. Control of CO emissions using Catalyst 2 (Cu/CA-T)	5-15 – 5-17
	5.4. Control of CO emissions using Catalyst 3 (Cu/A)	5-17 – 5-19

Chapter 1

Control of Carbon Monoxide from vehicular exhaust: *Background*

1.1 Background

Air pollution in India is a serious environmental concern. Among the 30 most polluted cities in the world, 21 were in India in 2019. As per a study based on 2016 data, 140 million peoples in India breath air which is 10 times more toxic than the WHO safe limit. Urban people suffers more than the rural. In 2022 According to the World Air Quality Report, 2023 by the Swiss organisation IQAir, India ranked third worst country out of 134 countries (Mishra 2023).The air (prevention and control of pollution) act was passed in 1981 to regulate air pollution but has failed to reduce pollution because of poor enforcement of the rules. Kolkata is the second most polluted city in the world, according to a recent report of HEI SoGA. First is our national capital Delhi.

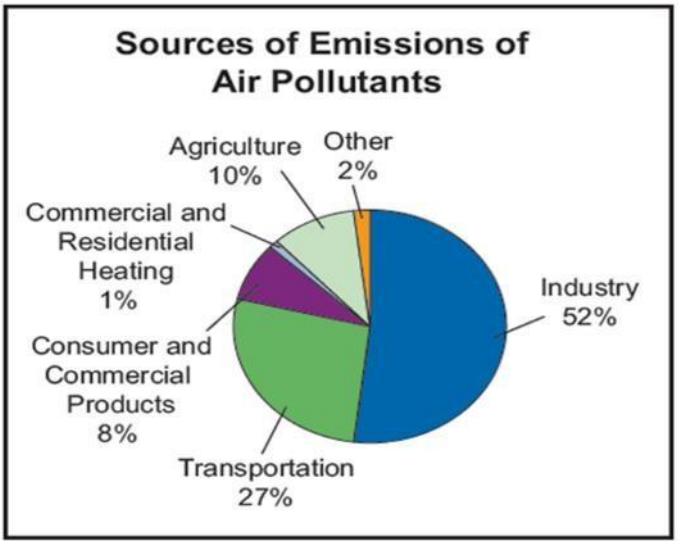


Figure 1.1: Sources of emissions of air pollutants.

The automobile sectors are the fastest growing source of air pollution and carbon emission. 27% of the air pollution contributes by the automobile sector. **Figure 1.1** shows the sources of air pollution. Due to economic growth and due to higher standard of living, annual vehicle sales in India increases. A report says annual car sales in India are projected to increase from the current 3.5 million to about 10.5 million- a three times increase by 2030, which will increase the exposure to vehicular exhaust emission. According to study, vehicles annually contribute about 290 gigagrams (Gg) of PM2.5 . At the same time, around 8% of total greenhouse gas (GHG) emissions in India from the transport sector. Automobile pollution level in our city, Kolkata is also alarming. West Bengal pollution control board has indicated that the automobiles contribute to particulate of the size of 1.1 micron and account for nearly 50% of the air pollution load in Kolkata (Chowdhury 2015).

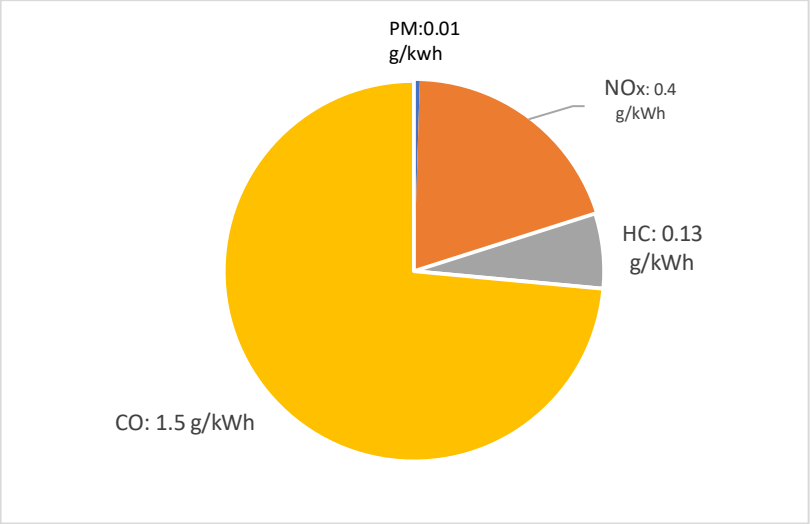


Figure 1.2: Contribution of toxic elements from vehicular exhaust

The automobile pollutants come in a variety of forms, including carbon monoxide (CO), carbon di-oxide (CO_2), hydrocarbon compounds (HC), nitrogen oxides (NO_x), Sulphur oxides (SO_X) and particulate matter. FIG 2 shows the contribution of this pollutants release from the automobile exhaust. Automobile exhaust contains toxic gases primarily due to the incomplete combustion process in the engine. When fuel, such as gasoline or diesel burns, it produces this type of toxic gases. Among all of this, automobile exhaust contributes 64% of the CO (Badr and Probert 1994). CO is a poisonous gas that is emitted from the exhaust system of a combustible engine of an automobile that uses petrol or diesel as a fuel is odourless, colourless, tasteless and non-irritating. Carbon monoxide (CO) produce during the incomplete combustion of fuel and in the time of engine starting up period (cold start period). Petrol engines are produced more CO than the diesel engines. CO emissions from automobile contribute to air pollution, leading to health issues and environmental damage. CO can be harmful to humans when inhaled in large quantities, as it reduces the blood's ability to carry oxygen. It combines with the haemoglobin present in blood cells and

haemoglobin present in blood cells and converted into carboxy-haemoglobin, which reduces the oxygen carrying capacity of the human body. So, it is important to reduce the CO more than the other pollutants. Catalytic converter is used to reduce the toxicity of pollutants.

Catalytic converter is an emission control device, installed in the exhaust pipe, used to reduce the toxic gas emissions from an internal combustion engine. To control the exhaust pollution various types of catalysts in catalytic converters have been investigated. Nobel metals and base metal catalysts are used to capture the pollutants. Catalytic reaction is occurred between the catalyst and the toxic pollutant. Oxidation or reduction reaction occurs and the toxic gases convert to less toxic gases (Mishra 2023).

There are many types of catalysts (e.g. Noble metal catalysts, Base metal catalyst, Perovskite, hopcalite catalyst, Monal catalyst, spinal catalyst) and catalytic converter (e.g. Two-way, Three-way, Four-way) are present in market but a dedicated catalyst for CO emission control is not available in market(Dey and Mehta 2020). At this point of time only noble metals are used in catalytic converter. So increasing cost of noble metal catalysts are concern in the synthesis of catalytic oxidation of CO over non noble metal catalysts. Thus, it is a requirement of synthesis a dedicated base metal catalysts which can control CO emission in every situation, in all types of weather condition and it will be existed for a long period of time and cost effective.

1.2 Automobile Pollution

Automobile pollution is the main concern in 21st century. The emission from vehicles are increases with the increasing of populations. The world is more concern about the automobile pollution due to automobile pollution exhaust. In 1951 the total number of vehicles present in India is 3 million and it increases up to 326.3 million in fiscal year 2020. A report says the annual vehicles sales in India are projected to increase from the current 3.5 million to about 10.5 million-a three time increase by 2030, which will increase exposure to vehicular exhaust emissions. India has the

third largest road network in the world. Automobile vehicles emit several pollutants depending upon the quality of the fuel, air to fuel ratio and the engine efficiency, age of the vehicles. Emission level of the pollutants also depending upon the vehicle types and its maintenance. The major pollutant gases are carbon monoxide (CO), Nitrogen oxides (NO_x), Sulphur oxides (SO_X), air toxics, namely benzene (C_6H_6), 1,3-butadiene (C_4H_6), particulate matter (PM) etc.

The predominant pollutants in petrol driven vehicles are hydrocarbons and carbon monoxide and predominant pollutants from diesel vehicles are oxides of nitrogen and particulates.

The automobile pollutions have been identified as one of the major contributors in the deteriorating air quality in the urban and semi-urban areas. Reasons for increasing vehicular pollution problems in urban India are as follows:

1. High vehicle density in congested areas.
2. People uses older, outdated and second used vehicles which emits maximum pollutants in air.
3. Inadequate inspection, service and maintenance facilities.
4. Uses of low quality of fuels.
5. Predominance of private vehicles especially cars and two wheelers, owing to unsatisfactory public transport system, thereby causing higher idling emissions and traffic congestion.

The automobile pollution is the source of two-third air pollution in the urban area. Emissions came from three sources the exhaust system, fuel system and crankcase ventilation gases. Among the emitted gases, CO is the most poisonous gas, it also emits in the cold start condition. In cold start condition 75% of the emitted gases is carbon monoxide. It is a big challenge to control the emission of CO from automobile exhaust.

1.3. Generation of CO from Automobile Exhaust

Carbon monoxide (CO) is produced from automobile exhaust primarily through the incomplete combustion of carbon-containing fuels, such as gasoline or diesel. In an internal combustion engine, fuel is mixed with air and ignited in the combustion chamber. Ideally, this process should result in complete combustion, where the fuel is entirely oxidized to carbon dioxide (CO_2) and water vapor (H_2O). However, combustion in engines may not always be complete. This can happen due to various factors such as insufficient oxygen supply, improper fuel-to-air ratio, inefficient combustion chamber design, or engine malfunction. Factors such as engine load, speed, temperature, ignition timing, and fuel quality can affect combustion efficiency and CO emissions. When combustion is incomplete, carbon-containing molecules in the fuel (like hydrocarbons) may not fully oxidize, leading to the formation of carbon monoxide (CO) instead of carbon dioxide (CO_2).

Some crucial factors of incomplete combustions are described below:

A. Fuel-Air Mixture Ratios:

The stoichiometric air-fuel ratio, defined as the ideal ratio for complete combustion, varies for different fuels. Deviations from the stoichiometric ratio, either rich (excess fuel) or lean (excess air), can lead to incomplete combustion and elevated CO emissions. Engine management systems adjust fuel injection timing and duration to maintain optimal air-fuel ratios under varying operating conditions.

B. Combustion Chamber Design:

The design of the combustion chamber influences airflow, turbulence, and fuel atomization, affecting combustion efficiency. Swirl, tumble, and squish patterns are employed to promote thorough mixing of air and fuel, minimizing CO formation. Advanced engine designs, such as direct injection and stratified charge combustion, optimize fuel delivery and combustion kinetics to reduce CO emissions.

C. Engine Malfunctions:

Mechanical issues such as worn piston rings, faulty spark plugs, and malfunctioning oxygen sensors can disrupt combustion processes, leading to increased CO emissions. Regular maintenance and diagnostic checks are essential to ensure proper engine operation and minimize emissions. In cases of incomplete combustion, some carbon atoms from the fuel molecules may not fully oxidize to form CO2. Instead, they combine with only one oxygen atom, forming carbon monoxide (CO). This process can be represented by the following chemical reaction:

$$2C_8H_{18} + 25O_2 \rightarrow 16CO + 18H_2O + other\ byproducts$$

This reaction demonstrates the incomplete combustion of octane, a component of gasoline, resulting in the production of carbon monoxide along with water vapor and other byproducts.

The resulting exhaust gases, including carbon monoxide, are expelled from the engine through the exhaust system. Once expelled from the vehicle's exhaust system, carbon monoxide is released into the environment. It can contribute to air pollution, especially in areas with high traffic congestion.

1.3.1 Generation of CO during cold start condition:

During the cold start period of an internal combustion engine, carbon monoxide (CO) emissions can be significantly higher compared to when the engine reaches operating temperature. The high tailpipe emissions (60%-80% of CO) would occur from a vehicle even equipped a catalytic converter within the first few minutes or approximately first few kilometres after a vehicle start (Dey and Mehta 2020). This is due to several factors:

Fuel Enrichment: During cold starts, the engine control unit (ECU) often enriches the fuel mixture to facilitate ignition and ensure smooth operation. This enrichment increases the fuel-to-air ratio, resulting in a richer mixture than the stoichiometric ratio. Therefore, incomplete combustion may occur, leading to higher CO emissions.

Cold Catalyst Inefficiency: Catalytic converters require a certain operating temperature to reach optimal efficiency. During cold starts, the catalytic converter is not yet warmed up, and its effectiveness in converting CO to less harmful substances like carbon dioxide (CO_2) is reduced. This allows more CO to escape into the atmosphere during the initial phase of engine operation.

Cold Engine Operation: Cold engines are less efficient in combustion compared to engines operating at normal operating temperatures. The fuel atomization and vaporization may be incomplete, leading to poor combustion and increased CO emissions.

Shorter Exhaust Path: During cold starts, the exhaust system may not reach its full operating temperature. This means that the exhaust gases spend less time in the catalytic converter, reducing the opportunity for CO conversion.

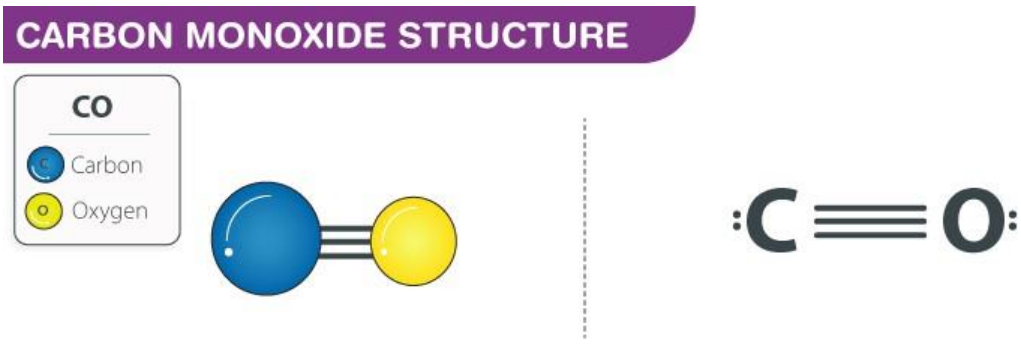
Increased Idling Time: In cold weather conditions, drivers often let their vehicles idle for longer periods to warm up the engine and cabin. Extended idling increases fuel consumption and CO emissions, especially if the engine is not operating at its optimal temperature.

The difference between CO emissions during the cold start and hot start depends after the speed-time pattern, capacity of engine and operating catalysts, emission factors of CO were about 3-4 times lower than warm engine conditions (Dey, Dhal et al. 2019). The first phase of cold start period is characterized by the highest cold-start emissions due to significant fuel-air ratio enrichment and lower temperatures of the engine, lubricant, and catalytic converter. Subsequently, emissions decline during the second phase of the cold-start transient as catalyst and engine temperatures gradually increase, along with lower enrichments of the air-fuel mixture ratio. The third phase exhibits the lowest cold-start emissions as operating temperatures are achieved and air-fuel mixture values approach the stoichiometric ratio. A rice fuel-air mixture produces very high amount of CO emission. In the time of cold start period temperature of the combustion chamber is low (around ambient temperature). At this temperature, 10%-30% of fuel vaporizes when injected into the combustion chamber. That means remain fuels are in liquid phase.

Therefore, 8-15 times the stoichiometric amount of additional fuel is injected to produce enough vapours for perfect ignition. The fuel vapours are ignited by the spark plug and most of the liquid fuel vaporizes and exit the engine partially combusted, containing relatively large amount of CO compare to other pollutants. Due to this a dedicated catalyst is required to control the CO emission during the cold start period. The main requirement from the catalyst was that it should have to work at low temperature (Dey and Mehta 2020).

1.4. Carbon Monoxide (CO)

Carbon monoxide (CO) is a colourless, odourless, and tasteless gas that is produced by incomplete combustion of carbon-containing fuels such as coal, wood, natural gas, and gasoline. It is highly toxic to humans and animals when encountered in high concentrations because it binds with haemoglobin in the blood, reducing its ability to carry oxygen. This can lead to carbon monoxide poisoning, which can be fatal. Carbon monoxide consists of one carbon atom and one oxygen atom connected by a triple bond. It is the simplest carbon oxide. In coordination complexes, the carbon monoxide ligand is called carbonyl. It is a key ingredient in many processes in industrial chemistry.



1.4.1. Physical and Chemical Characteristics

Table 1.1: Basic Properties

Molar mass	28.010 g-mol^{-1}
Density	1.250 kg/m^3 at 0°C, 1 atm

	1.145 Kg/m^3 at 25°C, 1 atm
Solubility in water	27.6 mg/L (25°C)
Henry's law constant (k_H)	-9.8×10^{-6} cm^3/mol
Refractive index (N_D)	1.0003364
Dipole moment	0.122 D
Heat capacity (C_P)	29.1 J/(k-mol)
Standard molar entropy($S°_{298}$)	197.7 J/(K-mol)
Standard enthalpy of formation ($\Delta_f H°_{298}$)	-110.5 KJ/mol
Standard enthalpy of combustion ($\Delta_c H°_{298}$)	-283.0 KJ/mol

Carbon monoxide (CO) has several physical and chemical characteristics:

Physical State: At standard temperature and pressure (STP), carbon monoxide is a colourless, odourless, and tasteless gas. It is lighter than air, with a density of about 0.9687 kg/m³.

Melting Point: Carbon monoxide has a relatively low melting point of -205.02°C (-337.04°F), which means it can exist as a solid at very low temperatures.

Boiling Point: The boiling point of carbon monoxide is relatively low at -191.5°C (-312.7°F), which means it exists as a gas under typical conditions.

Solubility: Carbon monoxide is sparingly soluble in water, with about 27.9 milligrams of CO dissolving in one litre of water at 0°C.

Flammability: Carbon monoxide is highly flammable. It burns in air with a blue flame, producing carbon dioxide (CO2) as a product of combustion.

Toxicity: Carbon monoxide is highly toxic to humans and animals. It binds to haemoglobin in the blood, reducing its ability to carry oxygen, leading to carbon monoxide poisoning.

Chemical Reactivity: Carbon monoxide is chemically reactive. It can react with oxygen in the presence of a catalyst to form carbon dioxide (CO2) in the process known as oxidation. It can also react with halogens and certain metals under appropriate conditions.

Stability: Carbon monoxide is relatively stable under normal conditions, but it can decompose at high temperatures to form carbon and oxygen.

1.4.2 Environmental Concerns

Uncontrollable emission of CO from automobile exhaust is a big concern of today's world. Carbon monoxide (CO) is one of the most unnoticed poisons of the 21th century. CO has serious health impacts on human, animals, birds as well as in microorganism levels. Not only the living beings, environments are also affected due to CO poisoning. Toxicity in soil and air, global warming, acid rain are some impacts in nature which is faced due to CO emission. CO is less soluble in water so waterbodies and aquatic animals are less effected.

1.4.2.1. Health impact on Human beings

Inhalation is the main exposure route for CO to human body. Exposure to CO can occur when we are in outdoors. City people are affected more due to presence of high traffic. When CO inhaled to the body, it is first dissolved in blood and quickly bound with haemoglobin (Hb) which is present in the blood and formed carboxy Haemoglobin (CO-Hb). When we take breath mainly oxygen is come to blood and make the bond with haemoglobin. But binding of carbon monoxide with Hb occurs with nearly same speed as with which oxygen binds to Hb. But the bond between CO and Hb is about 245 times stronger than O_2-Hb bonds. Thus, carbon monoxide competes with oxygen for haemoglobin binding sites, always win the race and remains bounded with Hb for longer period. O_2 dissociated easily from Hb but CO cannot. In this way percentage of CO-Hb increases in body continuously. On the other hand, less amount of Haemoglobin binding sites is available to pair with oxygen. So, this kind of situation is leading towards an undersupply of Oxygen into the blood and tissues. The result is arterial hypoxaemia and it leads towards death. The infants, the elders who has heart and respiratory diseases are affected due to CO-Hb formation in body. Cardiovascular injury, neurological problems, hypertension can happen from CO-Hb formation (Raub 1999).

Symptoms of CO poisoning at low concentration include:

- Fatigue in healthy individuals
- Chest pain and heart disease

At moderate concentrations:

- Angina
- Impaired vision
- Reduced brain function

At higher concentrations:

- Impaired vision and coordination
- Headaches
- Dizziness
- Weakness and tiredness
- Flu like symptoms
- Confusion
- Nausea
- Weak pulse
- Fainting
- Coma



Figure 1.3: Symptoms of CO poisoning

1.4.2.2. Health impacts on Animals and Birds

CO poisoning is a big issue in poultry farm. When chicks are being transported by tracks, they are directly contact with CO which emitted from exhaust of transport vehicles. Mortality rate may be high unless fresh air is provided immediately. At necropsy, the beak and face are cyanotic and a bright pink colour is noted throughout the viscera, particularly at the lungs and bloods are affected more.

Small animals or birds whom have less lung capacity are more sensitive to high level of CO poisoning. Most cases of CO poisoning in animals occur because of human error. A street dog and other street animals are affected more than the other animals

because they are directly contact with road traffic. Affected animals behave like a confused and lethargic way. Some common symptoms among the animals and birds:

(a) Red gums in the mouth
(b) Difficulty in breathing
(c) Exhaustion
(d) Vomiting
(e) Nausea

1.4.3 Toxicity or Toxicological Effect

A. Human: CO is a lethal and toxic gas when we inhaled it in enough quantities. In humans, 1 hour exposure to 0.32% CO will cause unconsciousness and at 0.45% CO will cause death. In research of centres for disease control and prevention (CDC),1994 says that nonlethal symptoms by CO toxicity shows at 1 hour exposure to 1000 to 1200 ppm CO and potential lethal reaction take place at 1 hour exposure to 1500 to 2000 ppm CO in human body. When the level of Carboxy Haemoglobin reaches at 15% or more, symptoms of CO poisoning is shown on human body. In a clean area, where clean air is present, the level of CO in the air will be 1% to 2%, so in human body, COHb also present in endanger level. But when people living in large polluted cities, where automobile emission of CO is very high, typically have COHb levels of 2-3% in human bloods and tissues. CO poisoning also depends on CO concentration, duration of exposure in toxic CO environment, as well as age, size and health status of a person.

B. Mammal: The American veterinary medical association (AVMA 2013) did several studies on CO exposure to mammals. In acute oral inhalation tests over a 4-hour period, LC_{50} values for rat, mouse and guinea pig were 1.807 ppm, 2,444 ppm, 5,818 ppm respectively. If a rat expose to high levels of CO (1500-2500 ppm) for 90 minutes caused hypertension, hypothermia, unconsciousness as well as continuously expose to 200 ppm CO during 18 days caused a decrease in litter size and birth weights. When a domestic pig exposed to 300 ppm CO for 10 days, decreased food intake capacity and the body weight. On a guinea pigs expose to 8% CO concentrate; they collapsed in 40 seconds to 2 minutes

and death occurred within six minutes. When minks and chinchillas exposed in CO environment, collapsed in one minute, breathing problem started in two minutes and cardiac arrest in 5-7 minutes(Morris, Curtis and Widowski 1985). Summarized data is given in the **Table 1.2.**

Table 1.2: Toxicity data for carbon monoxide on mammals and birds

TOXICITY DATA FOR CARBON MONOXIDE				
Test species	Test	Results	Time	Reference
Mammals				
Brown Rat	LC_{50}	8,636 ppm	15 min	(Hartzell et al, 1985)
		5,207 ppm	30 min	(Hartzell et al, 1985)
		4,600-5,000 ppm	30 min	(NIH 2016)
		1,784 ppm	4 hr.	(Rose et al. 1970)
		1,807 ppm	4 hr.	(NIH 2016)
House Mouse		2.414 ppm	4 hr.	(Rose et al. 1970)
		2,444 ppm	4 hr.	(NIH 2016)
Guinea Pig (Cavia porcellus)		5,647 ppm	4 hr.	(Rose et al. 1970)
		5,818 ppm	4 hr.	(NIH 2016)
Human	LC_{LO}	5,000 ppm	5 min	(Tab Biol Per 1933)
		4,000 ppm	30 min	(Lefaux 1968)
Birds				

Japanese Quail (Coturnix japonica)	LD_{50}	2,103 mq/kq	Oral	(Schafer Jr and Bowles Jr 2004)
	LC_{50}	1,938 ppm	Inhalation	(Mineau, Baril et al. 2001)
European Starling	LC_{50}	LC_{50} 2,213 ppm	Inhalation	(Mineau, Baril et al. 2001)
Red-winged Blackbird	LC_{50}	LC_{50} 1,334 ppm	Inhalation	(Mineau, Baril et al. 2001)

(i)LC_{50} is the lethal concentration of a material in air/water that will 50% of the test subjects when administered as a single exposure, (II) LC_{LO} is the lowest concentration of a material in air/water reported to have caused the death of animals or humans, (III) LD_{50} is the lethal dose of a material given orally to test animals that will kill 50% of the population, administered as a single exposure.

C. Birds: In an adult leghorn chicken, CO at 0.1% for 60 minutes caused an increase in tidal volumes and blood pressure decreases. COHb concentrations become 39%. if CO concentration increase to 0.5%, it becomes lethal after an average of 20.5 minutes. LD_{50} values for Japanese Quail, starlings, Red-winged blackbird were 1938 ppm, 2213 ppm, 1334 ppm respectively.

D Terrestrial Invertebrates and Micro-organisms: Insects are generally unaffected to CO. In a study of Baker and Wright 1977, Insects are generally resistant to 100 ppm of CO. Exposure of insects to high levels of CO environment (80% CO, 20% O_2) for 20 days results in the death of all insects.

1.5. Methods of control of CO in automobile exhaust

The emissions from vehicles are increases day by day with increasing of population. The governments and scientists are more concern due to automobile pollution exhaust. Most cities and towns in India are highly polluted due to petrol and

diesel powered two and three wheelers and second-hand vehicles because they contribute 80% of the total CO emission. Government of India and other countries take many actions to control the CO emission year to year. Many rules and regulations are implemented. On the other hand, Scientists are invented catalytic converters and types of catalysts to convert the highly toxic CO and other automobile emitted pollutant to other less toxic gases.

1.5.1. National efforts to control CO

1970 clean air act was the first effort by the Indian government to control automobile pollution. The act mentioned to requirement of 90% reduction in CO emission from automobiles. First emission standard regulated in 1991, after that revision in norms occurred in 1996, 1998,2000. Since 2000, India has started adopting European emission norms as discussed in **Table 1.3**. With updating the norms year by years, the standard for CO emission was decreased for petrol and diesel driven two, three wheelers and all kinds of light and heavy vehicles. All vehicle manufacturers must follow the norms. At present, Bharat stage VI (BS-VI) is parallel to Euro 6 regulations since 2020. Bharat stage emission standards are emission standards enforced by the government of India to control and reduce the air pollutants from the standards and the time frame for the implementation are decided by the central pollution control board under the Ministry of Environment and Forest.

In the year 2020, the last updated CO emission limit is 0.50 gm/km. If a vehicle surpasses the CO emissions limit in India, it could face penalties, such as fine, restrictions on usage or even being banned from the road until the issue is fixed. Additionally, the manufacturer might be required to recall the vehicles and make necessary modifications to ensure they meet the emission standards.

Table 1.3: Emission norms in India parallel to EU emission standards

Norms	**European**	**Year**	**CO (g/Km)**

1991 Norms	_	_	14.3 - 27.1
1996 Norms	_	_	8.68 - 12.40
1998 Norms	_	_	4.34 - 6.20
India Stage 2000 Norms	Euro 1	2000	2.72
Bharat Stage-II	Euro 2	2001	2.2
Bharat Stage-III	Euro 3	2005	2.3
Bharat Stage-IV	Euro 4	2010	1.0
Bharat Stage-V	Euro 5	2017	0.63
Bharat Stage-VI	Euro 6	2020	0.50

Table 1.4: Pollution load estimated in different city in India, CPCB

City	**Pollution load in metric ton per day**
	CO
Delhi	412.84
Mumbai	179.55
Kolkata	129.50

Chennai	167.00
Bangalore	209.04
Hyderabad	153.95
Kanpur	27.73
Agra	16.93

1.5.2. Control by Catalytic Converter

The first catalytic converter was invented by Eugene Houdry, a French mechanical Engineer in 1930. Catalytic converter is an automobile pollution control device. It is a vital component of a vehicle's exhaust system, installed in the inner surface of exhaust pipe which is corrected with IC engine. It reduces harmful emissions like carbon monoxide (CO), hydrocarbons (HC), Nitrogen oxides (NO_X), Sulphur oxide (SO_X) into less harmful gases. If catalytic converter is not installed in the vehicles or catalytic converter is malfunctioning, it can lead to higher emissions of these pollutants, causing the vehicles to surpass CO emissions limits set by government norms. In India, the use of catalytic converters is mandated by law for certain categories of vehicles to reduce harmful emissions. In 1995, a law was passed in India to install catalytic converters in new petrol passenger cars, starting initially in the four metro cities of Delhi, Kolkata, Mumbai and Chennai. Now it is mandatory to preinstall catalytic converter in most of the vehicles in India.

1.5.2.1. Construction of catalytic converter

Catalytic converter consists of a metal housing containing a honeycomb structure made of ceramic or metal coated with catalysts materials. **Figure 1.4** shows the schematic diagram of catalytic converter. Mainly catalytic converter made with three things- (a) catalyst support, (b) The wash coat, (c) The catalyst.

(a) Catalyst support- The catalyst support is made up of ceramic which has high heat resistivity. The structure of support is like honeycomb because it provides a large surface area.

(b) The wash coat- A wash coat is a carrier for the catalytic materials. The surface area of the wash coat is large and it made with Al_2O_3, TiO_2, SiO_2 mixtures. The coat must retain its surface area and prevent sintering of the catalytic metal particles even at high temperature.

(c) The Catalyst- Catalysts are the main part of catalytic converter. It oxidises the CO and Converted to low toxic gas like CO_2. There are many types of catalyst like Nobel metal catalysts, base metal catalyst, Perovskite metal oxide catalyst, hopcalites, available in market. There are many types of methods to prepare this catalyst. Some methods are Incipient wet impregnation (IWI), solution-gelation, co-precipitation, Co-impregnation methods etc. Platinum, Palladium and Rhodium are the novel metals used broadly as catalysts. Cerium, Iron, Copper, Manganese and Nickel are used as base metals in catalysts. Although each has certain limitations. In our catalyst preparation we focus on base metal catalysts because they are non-precious and cost effective (Dey and Mehta 2020).

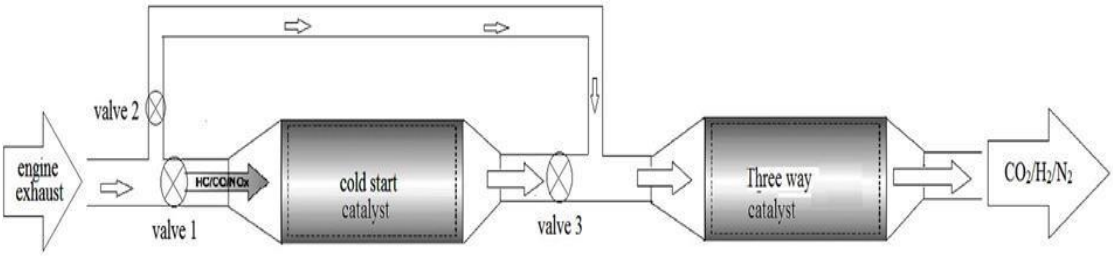


Figure 1.4: Schematic diagram of Catalytic converter

1.5.2.2. Mechanism of catalytic converter

The mechanism by which automobile catalysts extract CO in a catalytic converter involves a serious of chemical reactions. Inside the catalytic converter, there are typically

two main components: a reduction catalyst and an oxidation catalyst. Oxidation catalysts are used to convert CO to CO_2.

The oxidation catalyst, often composed of noble metals and base metals, facilitates the oxidation of Carbon monoxide (CO) into carbon di-oxide (CO_2). The CO is firstly released from IC engine. The CO passes through the catalytic converter and adsorbed by oxidation catalyst. In the next step oxidation catalyst accelerates the reaction between CO and O_2 to form CO_2.

The basic reaction on the catalytic surface is as follows:

$$CO + O_2 = CO_2$$

The reaction occurs at high temperatures, typically by the heat generated from the engine's combustion process. The precious metal catalysts provide the necessary surface for these reactions to take place, increasing the efficiency of the conversion process and reducing harmful emissions in vehicle exhaust (Patel, Subedar and Patel 2022).

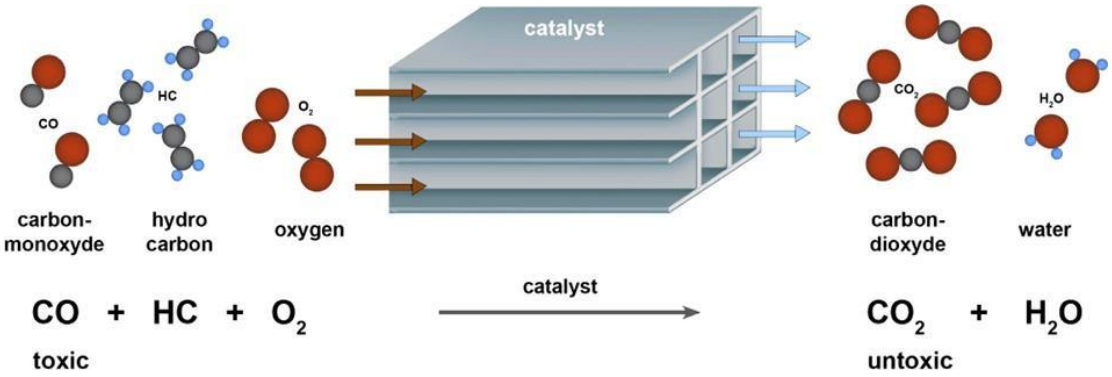


Figure 1.5: Conversion of CO to CO_2 using Catalysts

1.5.3. Alternate source of fuels

The automobile vehicles exhaust pollution control occurred using alternative fuels like LPG, CNG, Hydrogen fuels, bio-ethanol blended fuels etc. Renewable energies have the capability to alternate the conventional fuels. Biofuel may be an alternative. Biofuel derived from biomass-that is plants, algae, domestic or industrial biowaste. Biofuel

production is less time consuming than fossil fuels. Biofuels emit less greenhouse gas when burned in an engine and it is a carbon-neutral fuel**.** In 2018, India released its national policy on biofuels which set blending targets for ethanol (20% blending by 2030) and biodiesel (5% by 2030)(Ravindranath, Lakshmi et al. 2011). Another alternative will be Hydrogen fuel. Hydrogen is a clean fuel, when it consumes in a fuel cell, produce only water. Hydrogen can be produced from natural gas, nuclear power, biomass and renewable power like solar and wind. This quality makes it an attractive fuel option for transportation sector. India has announced a target of net zero carbon emission by 2070. Green hydrogen plays a substantial role towards this target.

Chapter 2

Control of Carbon Monoxide from vehicular exhaust:
Review of literature, research gaps, and objectives

This chapter provides with some relevant information about the literature surveyed and reviewed to conduct the present purview of the research. Several studies to control carbon monoxide emissions from automobile exhaust using metal catalysts have been carried out till date by eminent research groups from all over the world for the last few decades. In this part of the study an effort has been made to review research works that have been carried out on control of carbon monoxide from vehicular exhaust highlighting synthesis of specific catalysts, physical and chemical characterization of the same, along with some state-of-the-art methods of controlling auto-emissions with a specific focus on carbon monoxide (CO). Some of the relevant publications are mentioned in Table 2.1, given at the end of this Chapter, with a short synopsis of the research works carried out by specific research groups along with details of citations.

2.0. Research gaps

The research gaps in this field of study are:

1. Novel methods of synthesis of specific catalysts which would be selective and more active towards control of CO specifically, along with other gases emitted in the vehicular exhaust.
2. Physical and chemical characterization of the synthesized novel supported metal catalysts for controlling carbon monoxide (CO) emissions from automobile vehicle exhaust with state-of-the-art techniques. This is an area that requires further investigation. While significant progress has been made in the development of catalytic converters to reduce CO emissions, there are still several aspects that need to be explored.

a. *Development of new catalyst materials*: The existing catalyst materials used in automotive catalytic converters, such as platinum (Pt), palladium (Pd), and rhodium (Rh), have limitations in terms of cost and efficiency. There is a need to explore alternative catalyst materials, with non-precious metals or metal oxides as precursors or supports, that can offer better performance at a lower cost.

b. *Process optimization of the methods of synthesis of selective catalysts*: The synthesis methods play a crucial role in determining the properties and performance of catalysts. Further research is required to optimize the process parameters of specific synthesis methods, including the choice of support material, metal loading, impregnation techniques, and conditions of heat treatment. This would enable the production of catalysts with enhanced activity, selectivity, and stability.

c. *Characterization techniques*: Accurate characterization of catalysts is essential for understanding their structure-property relationships and identifying the active sites responsible for CO oxidation. Advanced characterization techniques, such as X-ray Diffraction (XRD), Transmission Electron Microscopy (TEM), Scanning Electron Microscopy (SEM), X-ray Photoelectron Spectroscopy (XPS), and Fourier-Transform Infrared Spectroscopy (FT-IR), can provide valuable insights into the catalyst's textural and surface properties. Further exploration of these techniques and their application in case of novel catalytic systems is necessary.

d. *Catalyst performance under realistic conditions*: Evaluating the performance of catalysts under real-world operating conditions is critical. Research should focus on studying the behaviour of catalysts at varying temperatures, gas compositions, and flow rates, characteristic of automobile exhaust environments. Long-term durability and resistance to deactivation due to poisoning by sulphur compounds and other contaminants should also be investigated.

e. *Catalyst design and optimization*: Developing catalysts with improved performance requires a fundamental understanding of the reaction mechanisms involved specifically in the oxidation of CO. Researchers should investigate the role of various parameters, such as distribution of metal particle size, properties of support material, and catalyst morphology, on the activity and selectivity of synthesized catalysts. This would aid in the rational design and optimization of catalysts for efficient control of CO emissions.

Addressing these research gaps would contribute to the development of novel supported metal catalysts that can effectively reduce carbon monoxide emissions from automobile vehicle exhaust, leading to cleaner and more sustainable transportation systems.

2.1. Statement of the problem

Synthesis and characterization of some novel metal supported metal catalysts to control specifically carbon monoxide emissions from automobile vehicular exhaust.

2.2. Objectives: *Overall and Specific*

Supported metal catalysts with superior 'low-temperature activity,' excellent 'thermal stability', and 'high-level selectivity' will be synthesized aiming to reduce harmful carbon monoxide emissions. In this research, some novel supported metal catalysts will be prepared using several methods of synthesis like the Incipient Wet Impregnation (IWI) method, Sol-Gel method, etc. with varying support matrix, metal compositions, and calcination temperatures to convert carbon monoxide to carbon dioxide. Synthesized catalysts will be physically characterized afterward using techniques like CHNS, BET, XRD, SEM, FTIR, XPS, etc and chemical characterisation like Boehm titration [see *Annex I*]. Portable fixed beds will be designed using these catalysts as packing material to be used in tandem with an existing catalytic converter of an automobile vehicle. Design of the portable packed-bed will include optimisation of bed height, diameter, quantity of catalysts and changes in the vehicle running speed for varying the emissions of CO.

Table 2.1: Review of literature

Title of the paper	Journal name	Authors	Year of publication	Volume	Page Number	Description
(1) Application of hopcalite catalyst for controlling carbon monoxide emission at cold-start emission conditions	Journal of Traffic and Transportation Engineering (English Edition)	Dey, Subhashish Dhal, Ganesh Chandra Mohan, Devendra Prasad, Ram	2019	6	419-440	To combat CO pollution, catalytic converters are recommended, but their effectiveness during cold starts, when they are inactive, remains a challenge. Hopcalite (CuMnOx) catalysts offer a promising solution due to their ability to operate efficiently at low temperatures. Additionally, their low cost, availability, and advanced synthesis methods make them attractive for automotive catalyst applications. Despite the abundance of research on this topic, there is a lack of comprehensive reviews addressing this issue, presenting an opportunity to fill this gap and explore the future potential of hopcalite catalysts for exhaust gas purification.
(2) Automobile pollution control using catalysis	Resources, Environment and Sustainability	Dey, S Mehta, NS	2020	2	100006	This paper says that Various techniques are employed to control exhaust gas emissions, including engine modifications, fuel pretreatment, additives, exhaust gas recirculation (EGR), positive crankcase ventilation (PCV), and the use of catalytic converters. Catalytic converters are particularly effective in converting more harmful exhaust

						pollutants into less harmful ones. They utilize different types of catalysts, including noble metals and base metals, for automobile exhaust gas treatment. Catalytic converters have proven effective and consistent in reducing harmful tailpipe emissions, leading to their widespread use in trucks, buses, cars, motorcycles, and other equipped vehicles. This paper will delve into recent developments in catalysis for controlling automobile exhaust pollution, covering various types of catalysts and advancements in the field.
(3) Effect of CO pretreatment on the performance of CuO/CeO2/γ-Al2O3 catalysts in CO+O2 reactions	Applied Catalysis A: General	Wan, Haiqin Li, Dan Dai, Yue Hu, Yuhai Zhang, Yanhua Liu, Lianjun Zhao, Bin Liu, Bin Sun, Keqin Dong, Lin Chen, Yi	2009	360	26-32	This study investigated the impact of CO pretreatment on the characteristics of CuO/CeO2/γ-Al2O3 catalysts through various analytical techniques such as X-ray diffraction (XRD), temperature programmed reduction (TPR), X-ray photoelectron spectroscopy (XPS), and infrared spectroscopy (IR). The catalytic activities of the treated catalysts were evaluated in low-temperature CO oxidation reactions (≤200°C). The performance of CuO/CeO2/γ-Al2O3 catalysts in CO oxidation was found to be influenced by operating temperature, copper oxide loading, and CO pretreatment.
(4) Highly active and stable palladium catalysts on	Environmental Science & Technology	Xie, Shaohua Wang, Zhiwei Tan, Wei	2009	55	7624-7633	This study introduces a novel approach, the two-step incipient wetness impregnation (T-IWI) method, for crafting a distinct and highly

novel ceria–alumina supports for efficient oxidation of carbon monoxide and hydrocarbons		Zhu, Yatong Collier, Samantha Ma, Lu Ehrlich, Steven N Xu, Peng Yan, Yong Xu, Tao				durable CeO2/Al2O3 support (CA-T). Pd supported on CA-T demonstrates significantly heightened low-temperature catalytic activity and superior thermal stability in carbon monoxide (CO) and hydrocarbon (HC) oxidations compared to Pd supported on traditional CeO2/Al2O3 (CA) prepared through one-step IWI method.
(5) Effect of nature of ceria support in CuO/CeO2 catalyst for PROX-CO reaction	Fuel	Maciel, Cristhiane Guimarães de Freitas Silva, Tatiana Hirooka, Marcelo Iuki Belgacem, Mohamed Naceur Assaf, Jose Mansur	2012	97	247-252	Exploring the impact of cerium dioxide (ceria, CeO2) on the selective oxidation of CO is crucial for understanding its catalytic properties. Ceria and ceria-based materials hold immense promise across various applications. These materials excel in enhancing the removal of CO by serving as oxygen storage elements. Moreover, ceria finds widespread usage as a support or additive in catalysts for oxidation reactions due to its exceptional oxygen storage capacity and redox activity.
(6) Elemental analysis of organic compounds with the use of automated CHNS analyzers	Journal of analytical chemistry	Fadeeva, VP Tikhova, VD Nikulicheva, ON	2008	63	1094-1106	This paper says determination of carbon, hydrogen, and nitrogen on automated CHNS analyzers. This paper says that how to analyse the CHNS data for the synthesized catalysts.
(7) Effects of preparation method on catalytic	Journal of Engineering and Innovation	Phutthakoon, Pornpaiboon Kitwikai, Chutipon	2022	15	197-207	CuO/CeO2-Al2O3 catalysts were synthesized using three different methods: impregnation, sol-gel, and coprecipitation, maintaining a fixed weight ratio of

activities of the CuO/CeO2-Al2O3 catalyst for the selective CO oxidation reaction		Chopkongklang, Satapon Wiset, Nannapat Wongkaew, Akkarat				copper oxide, cerium oxide, and alumina. Analysis via N2 adsorption revealed variations in specific surface area and pore size among the different preparation methods. X-ray diffraction analysis showed consistent structures of CuO, CeO2, and Al2O3 regardless of the preparation method employed. Among the methods, catalysts prepared via impregnation exhibited superior catalytic activity in CO oxidation and selective CO oxidation reactions.
(8) Design and development of automotive catalytic converter using non-nobel catalyst for the reduction of exhaust emission: A review	Materials Today: Proceedings	Patel, Kuldip D Subedar, Dattatraya Patel, Femina	2022	57	2465-2472	A multitude of alternative technologies have emerged in automotive engineering to mitigate emissions from engine and auxiliary subsystems. While catalytic converters remain indispensable for minimizing pollutants, the rising costs associated with noble metals as catalysts have spurred further exploration into more economical alternatives. This paper surveys research efforts focusing on affordable catalysts such as perovskite, spinel, monel, and hopcalite, alongside the exploration of design parameters aimed at optimizing exhaust flow to enhance reaction rates within catalytic systems.
(9) Homogeneous precipitation synthesis of CuO–ZrO2–CeO2–Al2O3 nano catalyst used in hydrogen production via	Energy Conversion and Management	Baneshi, Javad Haghighi, Mohammad Jodeiri, Naeimeh Abdollahifar, Mozaffar	2014	87	928-937	The CuO–ZrO2–CeO2–Al2O3 catalysts were meticulously characterized through a comprehensive array of analytical techniques including XRD, FESEM, EDX, BET, and FTIR analysis. XRD examinations revealed that the inclusion of ceria in the nano catalysts led to a

methanol steam reforming for fuel cell applications		Ajamein, Hossein				reduction in the size of copper crystallites. Furthermore, FESEM observations highlighted that ceria played a pivotal role in improving surface homogeneity and reducing particle size across the samples. BET analyse the surface area and the pore volume of the catalysts.
(10) Effective removal of automobile exhausts over flower-like Ce1− xCuxO2 nano catalysts exposed active {100} plane	Journal of Rare Earths	Selvamani, A Shanthi, K Santhanaraj, D Babu, CM Srinivasan, VV Thirukumaran, P Ramkumar, V Shakilaparveen, A Balasubramanian, R	2018	36	603-612	This study details the production and analysis of ceria-based nano catalysts doped with copper ions (Ce1−xCuxO2) featuring 3D flower-like and nanocrystalline structures, tailored for the cleansing of automotive exhaust emissions. Through XRD and Raman spectroscopy, the integration of copper ions into the ceria lattice is confirmed. Imaging via FESEM reveals the distinctive 3D flower-like and nanocrystalline architectures of the catalysts.
(11) Effect of nitrate metal (Ce, Cu, Mn and Co) precursors for the total oxidation of carbon monoxide	Resource-efficient technologies	Dey, Subhashish Dhal, Ganesh Chandra Prasad, Ram Mohan, Devendra	2017	3	293-302	This study investigates various catalyst formulations derived from cobalt nitrate, cerium nitrate, copper nitrate, and manganese nitrate precursors for CO oxidation. Notably, among the synthesized catalysts, those originating from cerium nitrate precursors exhibited superior performance in low-temperature CO oxidation. The catalytic activities were evaluated under diverse calcination conditions, including stagnant air, flowing air, and reactive calcination.

(12) Controlling carbon monoxide emissions from automobile vehicle exhaust using copper oxide catalysts in a catalytic converter	Materials Today Chemistry	Dey, S Dhal, G Chandra	2020	17	100282	This paper says Among the non-noble metals, copper (Cu) is found to be the most capable and highly active catalyst for CO oxidation. This analyses the Chemisorption process of CO over copper oxide, Mechanism of CO oxidation over copper oxide catalysts, deactivation and regeneration process of copper oxide catalysts
(13) Catalytic conversion of carbon monoxide into carbon dioxide over spinel catalysts: An overview	Materials Science for Energy Technologies	Dey, Subhashish Dhal, Ganesh Chandra	2019	2	575-588	Analysis of different types and shape of catalysts used for CO conversion, Mechanism of CO oxidation process over catalysts, Deactivation process of catalytic activity.

Chapter 3

Control of Carbon Monoxide from vehicular exhaust:
Synthesis of selective catalysts

3.0. Introduction

The catalyst, used in an auto-catalytic converter, works through a process called catalysis, where it participates in chemical reactions without being consumed itself. When carbon monoxide (CO) passes through the catalytic bed, which are placed over the catalytic converter, the toxic CO is adsorbed on the active sites of the surface and the pores of the catalysts. Then, a catalytic oxidation reaction takes place on the surface of the catalyst by which CO gets converted to CO_2. Basically, two types of catalysts are present, reduction catalyst and oxidation catalyst. Oxidation catalysts are used to convert CO. The catalyst reduces the activation energy of reactions. There are many kinds of catalyst like two-way catalysts, three-way catalysts present, which work over two or three kinds of pollutants but there is no dedicated catalyst which can only control CO emission. The primary requirement of a dedicated catalyst is high selectivity towards CO oxidation, high surface area to adsorb CO, high CO conversion rate at low as well as at high temperature, high concentration of surface oxygen over the catalyst.

A catalytic converter typically contains precious metals like platinum, palladium and rhodium, which act as the main element of catalyst. Their activities are high at high temperature (>170°C) but most of the CO emission from engine occurs at cold start period and it exhibits low selectivity towards CO oxidation. Also, increasing cost of noble metals is a concern in the synthesis of catalytic oxidation of CO. On the other hand, transition metal catalysts perform an interesting catalytic activity at lower temperature with high selectivity toward oxidation of CO. In comparison to other transition metal oxide catalysts, Cu based catalysts have shown better oxidation state and high redox properties, so we choose this as our main element for the precursors needed for the synthesis of various Cu based catalysts. In this work, CuO-CeO_2-Al_2O_3 catalysts are prepared by selective preparation methods. Also, the catalytic activity of these specifically synthesized catalysts, are tested against oxidation of CO.

3.1. Selective Catalysts chosen

In this work, a heterogeneous catalyst is synthesized. In heterogeneous catalysts, the catalyst is in a different phase from the reactants. The interaction happens between the CO, which is in gaseous phase, and a bimetallic catalyst with a metallic support, which is in solid phase.

Cerium (III) nitrate hexahydrate [$Ce(NO_3)_3.6H_2O$, purity > 99%, Molecular Weight: 432.22, Make: Merck India Ltd., CAS number: 10294-41-4] is used as a precursor for CeO_2 as a direct support or an important component in bimetallic support materials. CeO_2 is a metallic oxide that is both thermally and chemically stable and it has high capability to

store and release oxygen as well as has excellent redox properties (Xie, Wang et al. 2021). Ceria exists in two oxidation states, trivalent (Ce^{3+}) and tetravalent (Ce^{4+}) and the charge transfer can be represented by Ce^{4+}-O^{2-}(Maciel, de Freitas Silva et al. 2012). The ability of ceria to undergo rapid redox reaction is responsible for its oxygen storage capacity and high oxygen mobility resulting in better catalytic performance. Due to its high oxygen storage capability, it creates additional oxygen availability for the oxidation of CO.

Copper (II) nitrate hexahydrate [$Cu(NO_3)_2.H_2O$, purity > 99%, Molecular Weight: 187.56, Make: Merck, CAS No: 13778-31-9] used as the precursor for copper oxide (CuO), which is the main metal catalyst. Cu-based catalyst is widely used because of their good catalytic activity in CO oxidation reaction, abundant resources and low price. Strong interaction between Ceria and Copper improves the catalytic performance due to its synergistic effect linked to metal- support interactions. Also, the catalytic activity toward CO oxidation of CuO can be improved by generating oxygen vacancies of CeO_2 which in turn form interfacial attraction between two metals (Lykaki, Pachatouridou et al. 2018). At low temperature, CO adsorbed on the interface of CeO_2 based CuO reacts with the surface oxygen. Then CO_2 is formed. CO_2 will desorb and leave the surface oxygen vacancy available for O_2 gas to fill in. To enhance this mechanism, high surface area of the catalyst is required. But CeO_2 based CuO usually has low surface area.

Al_2O_3 is used as the second support material to increase the surface area of the catalyst. Dispersion of CeO_2 based CuO occurs over the entire surface of Al_2O_3. The wall dispersed CeO_2 on Al_2O_3 are essential for an increment of oxygen storage capacity.

Alumina (Gamma) nanopowder [γ-Al_2O_3, Molecular Weight: 101.96, Make: Sisco Research Laboratories Pvt. Ltd., CAS Number: 1344-28-1] is used as the precursor for Al_2O_3 in the conventional Incipient Wet Impregnation (IWI) method and the same is modified to two-step Incipient Wet Impregnation (T-IWI) synthesis technique. Aluminium Isopropoxide [$Al[OCH(CH_3)_2]_3$, purity ≥ 98%, Molecular Weight: 204.24, Make: Merck India Ltd., CAS Number: 555-31-7] is used as the precursor for Al_2O_3 in the solution-gelation (SG) synthesis technique. Sol-Gel technique is useful for mixed oxide preparation because this can easily control chemical composition of catalyst and low temperature synthesis. (Aghamohammadi, Haghighi et al. 2017) reported high surface area of the catalyst prepared by Sol-Gel method. Wet-Impregnation is also a widely used method for the synthesis of heterogeneous catalysts due to its simplicity, cost-effectiveness, and production of limited waste. The conditions of synthesis such as rate of stirring the solution, drying and calcination temperature affect the surface structure, pore size and pore-size distribution of the catalysts (Phutthakoon, Kitwikai et al. 2022). During the synthesis, distilled water, concentrated HNO_3 (purity > 98%) are used. The same are also purchased from Merck India Ltd. **Table 3.1** shows the physical and chemical characteristics of the elements used in the synthesis of catalysts.

Table 3.1: Physical and Chemical properties of the precursors and used compounds during the synthesis of various catalysts.

Properties	Copper (II) nitrate anhydrate	Cerium (III) nitrate hexahydrate	Gamma Alumina	Aluminium iso-propoxide
Chemical Formula	$Cu(NO_3)_2.H_2O$	$Ce(NO_3)_3.H_2O$	γ -Al_2O3	$Al(O\text{-}CH(CH_3)_2)$
Molar mass	187.5558 g/mol	432.22 g/mol	101.961 g/mol	204.246 g/mol
Appearance	Blue crystals	White or yellow powder, crystals or chunks	White powder	White solid
Density	3.05 g/cm^3	1.67-1.9 g/cm^3	3.987 g/cm^3	1.035 g/cm^3
Melting point	114°C (237°F,387 K)	65°C	2,072°C (3,762°F, 2,345K)	138-142°C
Boiling point	170°C (338°F,443 K)	200°C	2,977°C (5,391°F,3,250K)	135°C (408 K)
Solubility in water	381g/100ml (at 40°C)	175.4g/100ml (at 25°C)	insoluble	Decomposes
Solubility	Soluble ethanol, ammonia, water; insoluble in ethyl acetate	Soluble in water, alcohol, and acetone	Insoluble in all solvents	Soluble in isopropanol
Magnetic susceptibility	+1570.0×10^{-6} cm^3/mol		-37.0×10^{-6} cm^3/mol	2.1×10^{-5} cm^3/mol
Crystal structure	Orthorhombic	triclinic	Trigonal	monoclinic

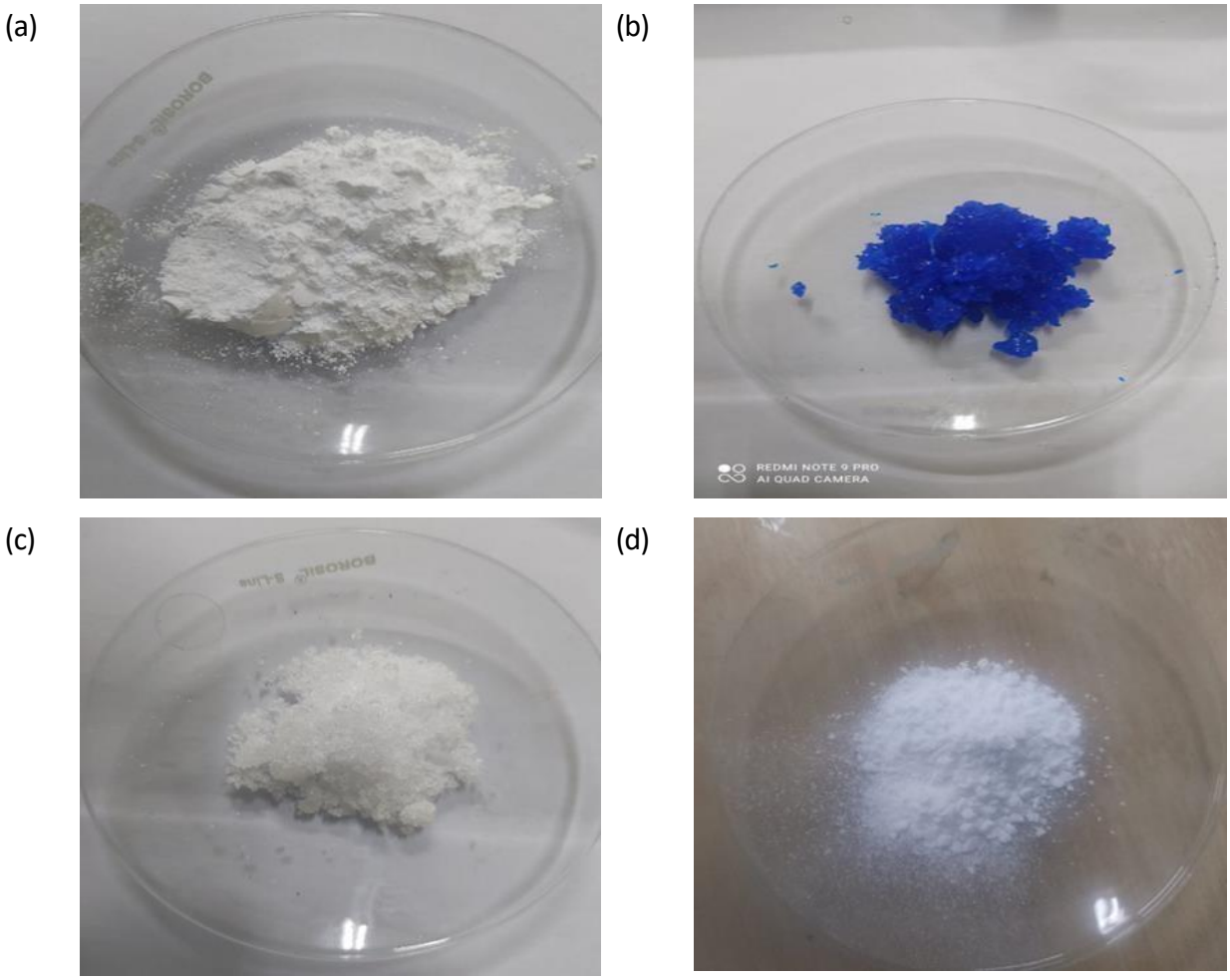


Figure 3.1: Precursors in use (a) Aluminium (Gamma) nano powder, (b) Cupper Nitrate Hydrate, (c) Cerium Nitrate Hexahydrate, (d) Aluminium iso-propoxide.

3.2. Methods of Synthesis

Synthesis of four catalysts with three types of methods like the Incipient Wet Impregnation method (IWI), Two step Incipient Wet Impregnation method (T-IWI) and Solution-Gelation (SG) method are carried out by the following way:

3.2.1. Synthesis of Catalyst 1 (Cu/CA) by IWI method:

At first support is prepared. The stable 30 wt% CeO_2/Al_2O_3 support is prepared by the novel IWI method. Determined concentration of γ-Al_2O_3 is taken onto a crucible. Dropwise distilled water is added to it in order to make a slurry. Partial $Ce(NO_3)_3.6H_2O$ solution with a known concentration (targeting 30 wt% CeO_2) is added dropwise onto the slurry of γ-Al_2O_3 followed by calcination at 550°C for 2 h and designated as CA. The temperature ramp for CeO_2/Al_2O_3 calcination is kept at 2°C/min. Catalysts with 1 wt% Cu on the support (CA) are prepared by IWI method using $Cu(NO_3)_2.H_2O$ as a precursor. $Cu(NO_3)_2.H_2O$ solution with a determined concentration is added dropwise onto the supports followed by drying at 120°C for 1 hour and calcination at 550°C for 2 hours. Cu loaded on CA supports are denoted as Cu/CA. Temperature ramp used for Cu catalyst calcination is 5°C/min.

3.2.2. Synthesis of Catalyst 2 (Cu/CA-T) by T-IWI method:

The stable 30 wt% CeO_2/Al_2O_3 support is prepared by the two step IWI method. . Known concentration of γ-Al_2O_3 is taken onto a crucible. Distilled water is added dropwise to it in order to make it into a slurry. Partial $Ce(NO_3)_3.6H_2O$ solution, with a known concentration

(targeting 10 wt% CeO_2) is added dropwise onto the slurry of γ-Al_2O_3 followed by calcination at 800°C for 2 h. Synthesized 10 wt% CeO_2/Al_2O_3 is denoted as 10CA-800. Afterward, the residual $Ce(NO_3)_3$ solution(20 wt% CeO_2) is added dropwise onto 10CA-800 followed by calcination at 550°C for 2 hours. The temperature ramp for CeO_2/Al_2O_3 calcination is maintained at 2°C/min. The support is named as CA-T. Catalysts with 1 wt% Cu on the support (CA) are prepared by IWI method using $Cu(NO_3)_2.H_2O$ as a precursor. $Cu(NO_3)_2.H_2O$ solution with a known concentration is added dropwise onto the supports followed by drying at 120°C for 1 hour and calcination at 550°C for 2 hours. Cu loaded on CA-T supports are denoted as Cu/CA-T. Temperature ramp used for Cu catalyst calcination is 5°C/min.

3.2.3. Synthesis of Catalyst 3 (Cu/A) by IWI method:

A single metal supported catalyst is prepared as a third sample. It follows conventional one-step IWI method. Pre-determined concentration of γ-Al_2O_3 is taken onto a crucible. Dropwise distilled water is added to it in order to make it into a slurry. Then it is calcinated at 550°C for 2 hours. The support is thus synthesized. Catalysts with 1 wt% Cu on the prepared support are prepared by IWI method using $Cu(NO_3)_2.H_2O$ as a precursor. $Cu(NO_3)_2.H_2O$ solution with a pre-determined concentration is added dropwise onto the support followed by drying at 120°C for 1 hour and calcination at 550°C for 2 hours. Cu loaded on Al_2O_3 supports are denoted as Cu/A. Temperature ramp used for calcination of Cu catalyst is maintained at 5°C/min.

3.2.4. Synthesis of Catalyst 4 (Cu/CA-S) by Solution-Gelation (SG) method:

At first 100 ml distilled water is heated to 80°C and the same temperature is maintained throughout. Aluminium isopropoxide [$Al(O\text{-}i\text{-}Pr)_3$] is added into the hot H_2O and the solution is stirred for 10 minutes with 100 rpm. Then HNO_3 is poured into the solution till the solution turns from opaque to clear. Then the clear solution is cooled to room temperature and stirred for another 30 minutes. After the solution cools down, $Ce(NO_3)_3.6H_2O$ solution, with a pre-determined concentration (targeting 30 wt% of Aluminium isopropoxide), is added to it and the solution is kept under stirring for another 10 minutes. The support is synthesized and the same is named as CA-S. $Cu(NO_3)_2.H_2O$ (1 wt%) is added onto the support and keep stirring for 15 mins with 250 rpm. A sol is formed. The sol is then put into a beaker, under controlled temperature at 50°C. The sol turned into a gel. Next, the gel is cooled to room temperature and kept for 24 hours. After 1 day the gel is transferred to a crucible followed by drying at 110°C for 10 hours and calcination at 500°C for 5 hours. Synthesis of Cu loaded on CA-S is completed and it is named as Cu/CA-S.

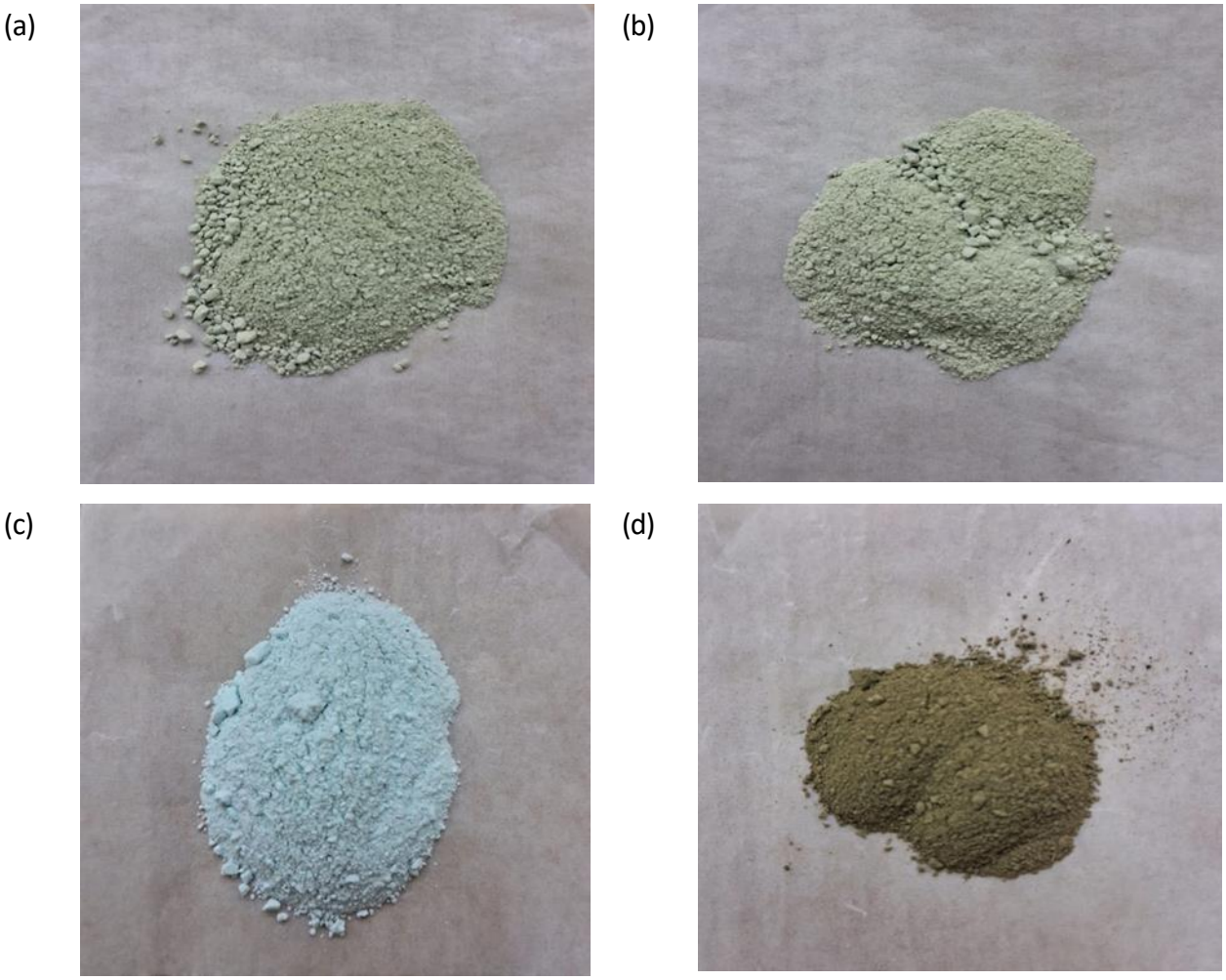


Figure 3.2: (a) Catalyst 1 (Cu/CA), (b) Catalyst 2 (Cu/CA-T), (c) Catalyst 3 (Cu/A), (d) Catalyst 4 (Cu/CA-S).

Table 3.2: Details of the protocol followed during synthesis of the catalysts.

Name of Catalyst	**Method of Synthesis**	**Process of Synthesis**	**Reference**
Cu/CA	Conventional IWI method	The stable 30 wt% CeO_2/Al_2O_3 support is prepared by the novel IWI method. Known concentration of γ-Al_2O_3 is taken onto a crucible. Dropwise distilled water is added to it to make a slurry. Partial $Ce(NO_3)_3.6H_2O$ solution with a known concentration (targeting 30 wt% CeO_2) is added dropwise onto the slurry of γ-Al_2O_3 followed by calcination at 550°C for 2 h and designated as CA. The temperature ramp for CeO_2/Al_2O_3 calcination is kept at 2°C/min. Catalysts with 1 wt% Cu on the support (CA) are prepared by IWI method using $Cu(NO_3)_2.H_2O$ as a precursor. $Cu(NO_3)_2.H_2O$ solution with a known concentration is added dropwise onto the supports followed by drying at 120°C for 1 hour and calcination at 550°C for 2 hours. Cu loaded on CA supports are denoted as Cu/CA. Temperature ramp used for Cu catalyst calcination was 5°C/min.	(Xie, Wang et al. 2021)
Cu/CA-T	Two-Step IWI method	The stable 30 wt% CeO_2/Al_2O_3 support is prepared by the two step IWI method. Known concentration of γ-Al_2O_3 is taken onto a crucible. Dropwise distilled water is	(Xie, Wang et al. 2021)

		added to it in order to make a slurry. Partial $Ce(NO_3)_3.6H_2O$ solution with a known concentration (targeting 10 wt% CeO_2) is added dropwise onto the slurry of γ-Al_2O_3 followed by calcination at 800°C for 2 h. The obtained 10 wt% CeO_2/Al_2O_3 is denoted as 10CA-800. Afterward, the residual $Ce(NO_3)_3$ solution(20 wt% CeO_2) is added dropwise onto 10CA-800 followed by calcination at 550°C for 2 hours. The temperature ramp for CeO_2/Al_2O_3 calcination is kept at 2°C/min. The support is named as CA-T. Catalysts with 1 wt% Cu on the support (CA) are prepared by IWI method using $Cu(NO_3)_2.H_2O$ as a precursor. $Cu(NO_3)_2.H_2O$ solution with a known concentration is added dropwise onto the supports followed by drying at 120°C for 1 hour and calcination at 550°C for 2 hours. Cu loaded on CA-T supports are denoted as Cu/CA-T. Temperature ramp used for Cu catalyst calcination is 5°C/min.	
Cu/A	Conventional IWI method	It follows conventional one-step IWI method. Known concentration of γ-Al_2O_3 is taken onto a crucible. Dropwise distilled water is added to it in order to make a slurry. Then it is calcinated at 550°C for 2 hours. The support is prepared. Catalysts with 1 wt% Cu on the prepared support are prepared by IWI method using $Cu(NO_3)_2.H_2O$ as a precursor. $Cu(NO_3)_2.H_2O$ solution with a known concentration is added dropwise onto the supports followed by drying at 120°C for 1 hour and calcination at 550°C for 2	(Xie, Wang et al. 2021)

		hours. Cu loaded on Al_2O_3 supports are denoted as Cu/A. Temperature ramp used for Cu catalyst calcination is 5°C/min.	
Cu/CA-S	Solution-gelation method	At first 100 ml distilled water is heated to 80°C and control it to this temperature. Aluminium isopropoxide [Al(O-i-Pr)$_3$] is added into the hot H_2O and stirred solution for 10 minutes with 100 rpm. Then HNO_3 is pouring into the solution till solution is turned from opaque to clear. Then the clear solution is cooled to room temperature and stirred for 30 minutes. After the solution became cool, $Ce(NO_3)_3.6H_2O$ solution with a determined concentration (targeting 30 wt% of Aluminium isopropoxide) is added to it and solution kept stirring for 10 minutes. The support is prepared and it is named as CA-S. $Cu(NO_3)_2.H_2O$(1 wt%) was added onto the support and keep stirring for 15 mins with 250 rpm. A sol is formed. The sol is put into a beaker, under controlled temperature at 50°C. sol changes into gel. Next, the gel is cooled to room temperature and placed for 24 hours. After 1 day the gel is transferred to a crucible followed by drying at 110°C for 10 hours and calcination is carried out at 500°C for 5 hours. Synthesis of Cu loaded on CA-S is completed and the same is named as Cu/CA-S.	(Phutthakoon, Kitwikai et al. 2022)

The physical and chemical characterisations of the above synthesized catalysts are required to be carried out so that the physical and chemical properties, which give information on their performance during catalysis reactions, are properly understood. The same is undertaken in the next chapter.

Chapter 4

Control of Carbon Monoxide from vehicular Exhaust: *Physical and Chemical Characterization of synthesized catalysts*

Catalyst characterisation and analysis plays a vital role to development of catalyst, while understanding the catalyst structure. Characterization of catalysts portrays a knowledge of the physical properties, chemical properties, catalytic activity and selectivity. Also, surface area, pore size distribution, composition in the elemental level are determined indirectly using the characterisation outputs with the help of state-of-the-art analytical and graphic software. There are various types of characterisation techniques like X-ray diffraction (XRD), Scanning Electron Microscopy (SEM), Field-Emission Scanning Electron Microscopy (FE-SEM) coupled with Energy Dispersive X-Ray analysis (EDAX), Fourier Transform Infrared Spectroscopy (FT-IR), Thermo-Gravimetric Analysis (TGA), elemental analysis using CHNS Analyzer, Brunauer-Emmett-Teller (BET) surface area analysis, Transmission Electron Microscopy (TEM) analysis, In-situ Raman Spectroscopic Measurements, X-ray

Photoelectron Spectroscopy (XPS) analysis etc. The overall description of characterisation, carried out for the four (4) Nos. catalysts synthesized, are given below.

4.1. CHNS based Elemental analysis

CHNS elemental analysers provide a means for the determination of carbon, hydrogen, nitrogen and sulphur in catalysts and similar types of materials like adsorbents. They are capable of handling a wide variety of sample types, including solids, liquids, volatile and viscous samples. Basic principle of CHNS analyser is to detect the Carbon, Hydrogen, Nitrogen and Sulphur in the catalysts and estimate the weight percentage of the same. In the combustion process, carbon is converted to carbon dioxide; hydrogen to water; nitrogen to nitrogen gas/ oxides of nitrogen and sulphur to sulphur dioxide *(Fadeeva, Tikhova and Nikulicheva 2008)*. **Figure 4.1 s**hows the schematic diagram of CHNS elemental analysis.

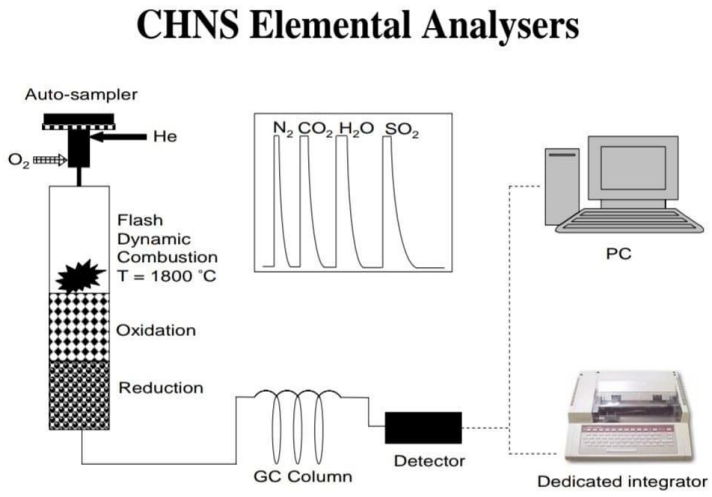


Figure 4.1: Schematic diagram of the principle of working of a CHNS analyser.

The elemental analysis for the four catalysts is obtained from a CHNS Analyzer (**Make:** Elementar, Germany; **Model:** VARIO MICRO CUBE). The combustion tube temperature and the reduction tube temperature are kept at 1150°C and 850°C respectively. The pressure of the carrier Helium gas is maintained at 1100-1200 milli bar and Helium gas flow is maintained at 200 ml/min. At first, two blanks and three standards are run for the system check. Then each of the catalyst samples is run for three times and the average value is taken. Results are shown in **Table 4.1**. The nitrogen content of Cu/CA, Cu/CA-T, Cu/A and Cu/CA-S are 1.75 wt%, 3.17 wt%, 1.051 wt% and 0.87 wt% respectively. Nitrogen contents of Cu/CAT is higher with respect to the other two catalysts. This is because in the Two step Incipient Wet Impregnation (T-IWI) more amount of nitrogenous compound was used [refer *section 3.2.2 of Chapter 3*] as compared to conventional IWI method and sol-gel method. Comparing the carbon content for Cu/CA, Cu/CA-T, Cu/A and Cu/CA-S (Cu/CA: 0.51 wt %; Cu/CA-T: 0.96 wt %; Cu/A: 0.49 wt %; Cu/CA-T: 1.561) [refer **Table 4.1**], Cu/CA-S contained more carbon as compared to the other three catalysts. Overall carbon content in all four samples are found to be quite low and this in turn is expected to help during carbon monoxide adsorption on the catalysts because of the low concentration of carbon on the catalyst surface. The hydrogen content in Cu/CA, Cu/CA-T, Cu/A and Cu/CA-S are found to be 0.875 wt%, 1.625 wt%, 0.450 wt% and 0.893 wt% respectively. Due to low hydrogen content, rate of thermal oxidation must be low so the concentration of oxygen over the catalyst surface will be significantly high which will help in CO oxidation. Sulphur content of Cu/CA, Cu/CA-T, Cu/A and Cu/CA-S are 0.247 wt%, 0.135 wt%, 0.164 wt% and 0.221wt% respectively. Sulphur is a major source of catalyst poisoning as sulphur compounds are strongly chemisorbed on the metal surface. Therefore,

it is ideally desired to be present in very low concentration. CHNS based analysis for the four catalyst samples show that the sulphur content is quite low. Among the four catalysts, sulphur content of Cu/CA-T is minimum so it will be more effective to be used as an automobile catalyst (Arif, Li et al. 2021).

Table 4.1: Weight percentages of Carbon, Hydrogen, Nitrogen and Sulphur

Name of Elements	**Catalyst 1(Cu/CA)**	**Catalyst 2(Cu/CAT)**	**Catalyst 3(Cu/A)**	**Catalyst 4(Cu/CA-S)**
Carbon	0.51	0.96	0.49	1.561
Hydrogen	0.875	1.625	0.450	0.893
Nitrogen	1.75	3.17	1.051	0.87
Sulphur	0.247	0.135	0.164	0.221

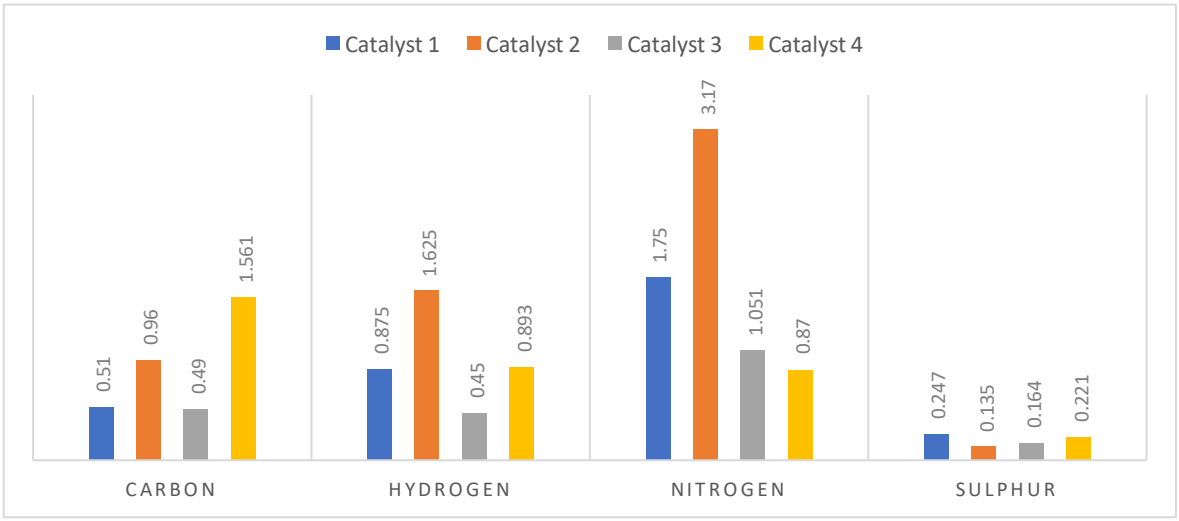


Figure 4.2 Bar diagram representing weight percentages of Carbon, Hydrogen, Nitrogen and Sulphur for the Four (4) nos. of catalysts synthesized.

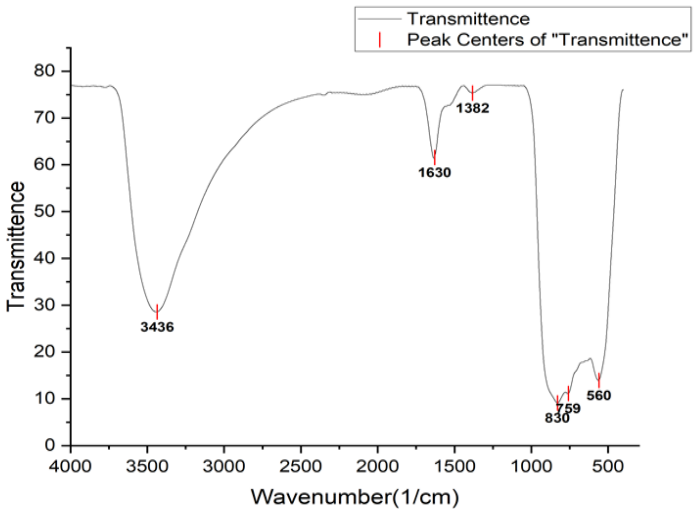
4.2. Fourier Transform Infrared Spectroscopy (FT-IR) based analysis

Fourier Transform Infrared Spectroscopy (FT-IR) based analysis, for the sample Cu-CA, is carried out on a FTIR spectrometer (**Make:** Perkin Elmer**, Model No.** FT-IR C120947) availed on a time-sharing basis from *The Indian Association for the Cultivation of Science, Kolkata*, and for the samples Cu-CAT and Cu-A, the same is carried out on a FT-IR spectrometer (**Make:** Perkin Elmer; **Model No.** FT-IR C120947) availed on a time-sharing basis from the *Central Glass and Ceramic Research Institute, Kolkata*. FTIR spectra are recorded at 4 cm^{-1} resolution with 45 scans per sample. The FTIR spectroscopy analysis is represented by the percentage transmittance versus wave number in cm^{-1}. The spectral analysis of Cu-CA given in **Figure 4.3 (a)** shows a band at 3436 cm^{-1}. This probably signifies the strong and broad vibrational bonds of O-H (Escribano, López et al. 2008). Another bond at 1630 cm^{-1} is due to the O-H stretching and bending vibrations. The band at 1382 cm^{-1} signifies weak O=N=O stretching. The bands at 830 and 560 cm^{-1} could be attributed to broad adsorption bonds of Al-O and Cu-O-Al, and vibration of Cu-O stretching respectively. Spectral analysis of Cu-CAT, given in **Figure 4.3 (b)**, shows a band at 3436 cm^{-1}. This probably signifies the strong and broad vibrational bonds of O-H (*Escribano,* López *et al. 2008*). Another bond at 1622 cm^{-1} is due to O-H stretching and bending vibrations. The band at 1411 cm^{-1} signifies weak O=N=O stretching. Various bands are attributed to very weak N-H vibrations [1124 cm^{-1}], broad adsorption bonds of Al-O, Cu-O-Al [766 cm^{-1}], vibrations of Cu-O stretching [617 cm^{-1}] and cerium doped oxide samples [474 cm^{-1}] respectively (Topsøe and Topsøe 1999). Spectral analysis of Cu-A, given in **Figure 4.3 (c)**, shows a band at 3420 cm^{-1}. This probably signifies the strong and broad vibrational bond

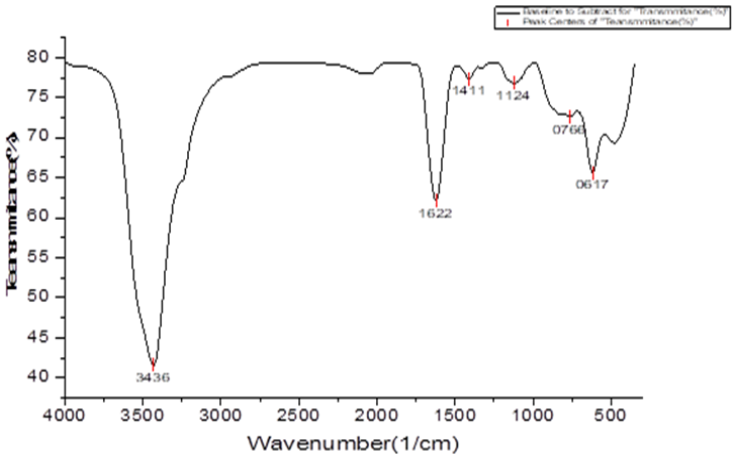
of O-H (Escribano, López et al. 2008). Another band at 1629 cm^{-1} is due to O-H stretching and bending vibrations. The band at 1417 cm^{-1} signifies weak O=N=O stretching. The bands at 1122 cm^{-1}, 824 cm^{-1} and 621 cm^{-1} could be attributed to very weak N-H vibration, broad adsorption bonds of Al-O, Cu-O-Al and vibration of Cu-O stretching respectively (Arif, Li et al. 2021).

There are similar types of bands detected in three catalysts but the peak areas corresponding to each of the wavenumbers are uniquely different. Around the range of wavenumbers 3400-3500 cm^{-1}, peaks of Cu-CA, Cu-CAT and Cu-A are identified but the peak area of Cu-CA (1.19%) is observed to be greater than the transmittance peak area of Cu-CAT (0.80%) and Cu-A (0.86%). Cu-CA shows broader peak compared to the other two catalysts. Another similar band around 1620 cm^{-1} is detected where the Cu-CA has the highest peak area. The decreasing order of peak area is Cu-CA (0.88%) > Cu-A (0.64%) > Cu-CAT (0.46%). The third similar type of band detected around 1400 cm^{-1} where the peak area decreases from Cu-CA (0.98%) to Cu-CAT (0.66%), and to Cu-A (0.50%). In this case Cu-A shows a sharp peak as compared to the other two. Some other peaks are also found similar for all three catalysts and some for any two of the catalysts. From the **Figure 4.3 (a)**, **Figure 4.3 (b)**, and **Figure 4.3 (c)** we can notice several cases where the bands broadened and overlapped. This may be happened due to the presence of compounds formed due to surface-complexation around the specific peaks. A consolidated curve is shown in **Figure 4.4** which compares the FT-IR peaks of the three catalyst samples (Baneshi, Haghighi et al. 2014).

(a)


Transmittence
Peak Centers of "Transmittence"
Transmittence
Wavenumber(1/cm)
3436
1630
1382
830
759
560

(b)


Wavenumber(1/cm)
3436
1622
1411
1124
0796
0617

(c)

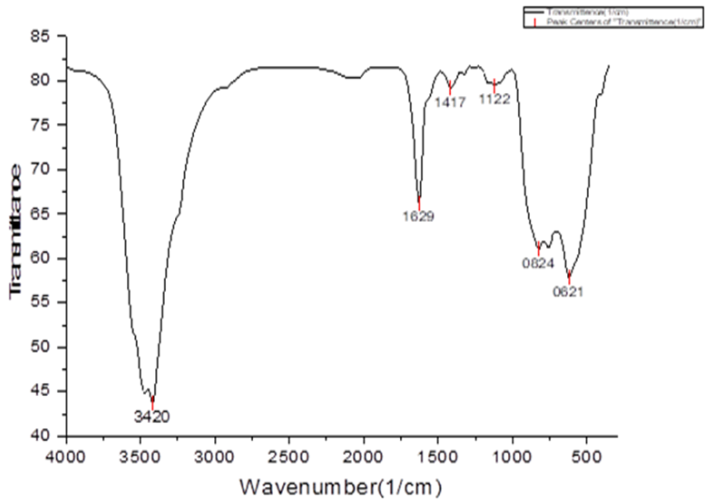


Figure 4.3: Fourier transform infrared (FTIR) spectra of (a)Cu/CA, (b)Cu/CA-T, and (c)Cu/A.

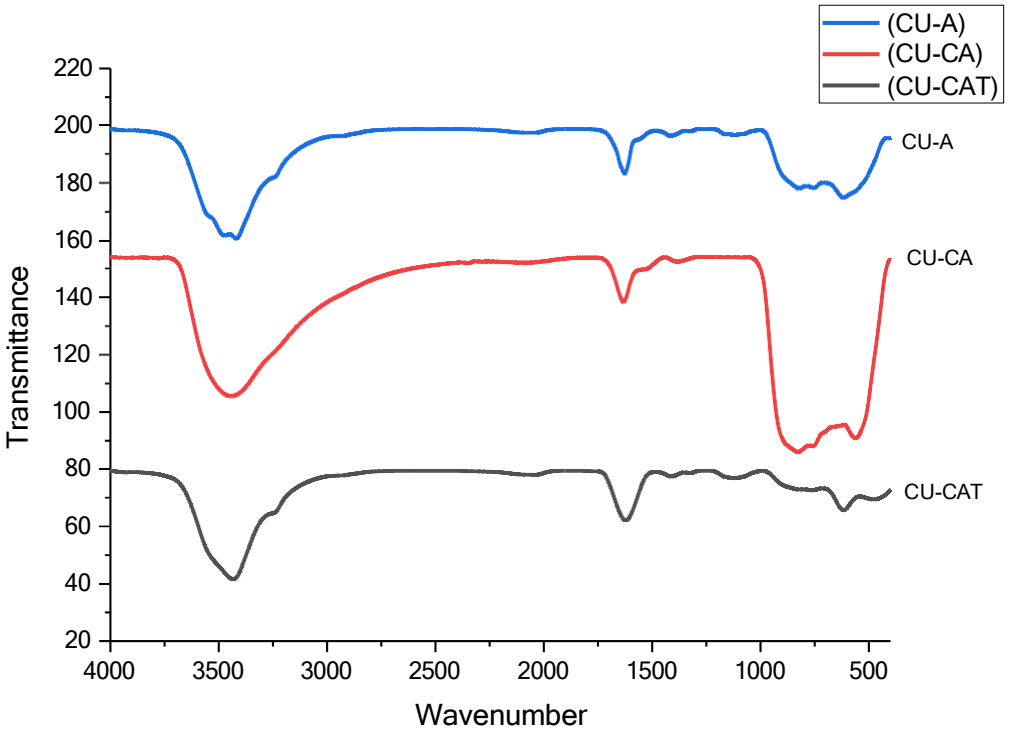


Figure 4.4: Consolidated FT-IR plots to compare the transmittance peaks for Cu-CA, Cu-CAT, and Cu-A.

Table 4.2: Identification of Functional groups present in the three catalysts using Figures 4.3 (a, b, c) along with actual and normalized peak areas.

Cu-CA				**Cu-CAT**				**Cu-A**			
Wavelength (cm^{-1})	*Functional Group*	*Area*	*Normalized Area*	*Wavelength (cm^{-1})*	*Functional Group*	*Area*	*Normalized Area*	*Wavelength (cm^{-1})*	*Functional Group*	*Area*	*Normalized Area*
3436	Strong and broad vibrational bonds of O-H	1.19	9.15	3436	Strong and broad vibrational bonds of O-H	0.80	2.16	3420	Strong and broad vibrational bonds of O-H	0.86	1.91
1630	O-H stretching and bending vibrations	0.88	6.76	1622	O-H stretching and bending vibrations	0.46	1.24	1629	O-H stretching and bending vibrations	0.64	1.42
1382	Weak O=N=O stretching	0.98	7.53	1411	Weak O=N=O stretching	0.66	1.78	1417	Weak O=N=O stretching	0.50	1.11
830	Broad adsorption	0.38	2.92	1124	Very weak N-H vibration	0.73	1.97	1122	Very weak N-H vibration	0.72	1.6

	bonds of Al-O, Cu-O-Al										
759	Broad adsorption bonds of Al-O, Cu-O-Al	0.13	1.00	766	Broad adsorption bonds of Al-O, Cu-O-Al	0.37	1.00	824	Broad adsorption bonds of Al-O,Cu-O-Al	0.50	1.11
560	Vibration of Cu-O stretching	0.26	2.00	617	Vibration of Cu-O stretching	0.39	1.05	621	Vibration of Cu-O stretching	0.45	1.00
-	-	-	-	474	Detection of Cerium doped oxide samples.	0.42	1.14	-	-	-	-

4.3. Thermogravimetric (TGA) analysis

Thermogravimetric (TGA) analysis is an analytical technique used in chemistry and material science to determine the composition of the sample at various temperatures. The process involves monitoring the weight of a sample as a function of temperature with time, while the same is subjected to a controlled temperature program under a restricted atmosphere of the experimental set-up. During a typical TGA experiment, a sample is heated at a programmed rate and corresponding changes in its normalized weight are recorded as a function of temperature or with time. The weight change can provide valuable information about various processes undergoing within the sample, such as decomposition, oxidation, reduction, dehydration or desorption (Vahid and Haghighi 2017).

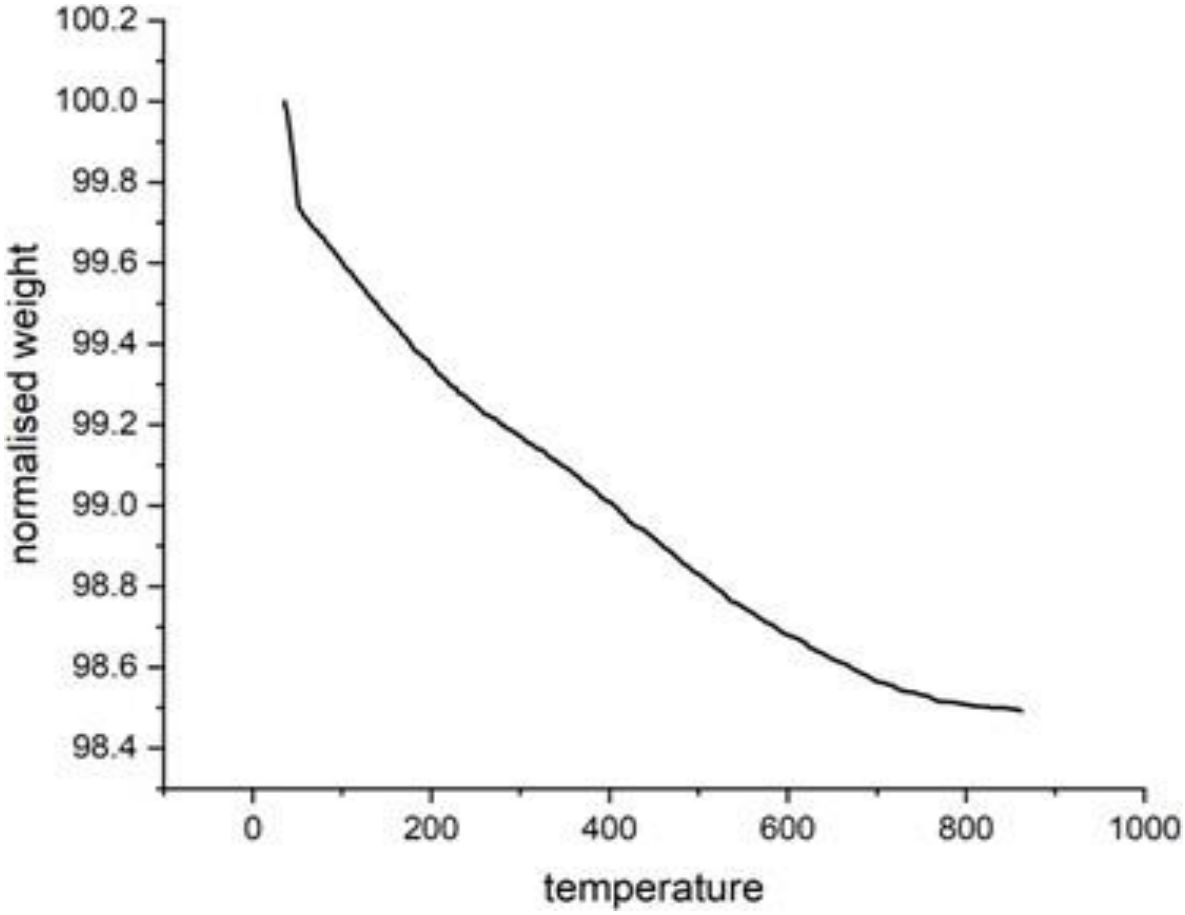
Thermogravimetric analysis (TGA) is performed on a *PerkinElmer instrument* (**Make**: Simultaneous thermal analyser; **Model**: STA 6000) in the UGC-Special Assistance Program [SAP] laboratory of Chemical Engineering department, Jadavpur University. The programmed heating range is set in between 40°C to 900°C, at a heating rate of 10°C/min under an inert nitrogen atmosphere. The measurement is carried out using 6-15 mg sample. TGA curves for all the three catalysts synthesized are shown in **Figure 4.5**. A consolidated curve of the three samples is plotted in **Figure 4.6**.

The mass reduction in Cu-CAT and Cu-A are almost same, around 3%, while for Cu-CA its around 2%. Overall reduction in weight in case of Cu-CA is less compared to the other two, indicating large amount of heat generated during the time of synthesis of this catalyst rather than the Cu-CAT and Cu-A. The reduction in the range of 100°C to 200°C in all of the samples is related to adsorbed water on the catalyst surface. Cu-CAT is treated at a reasonably high

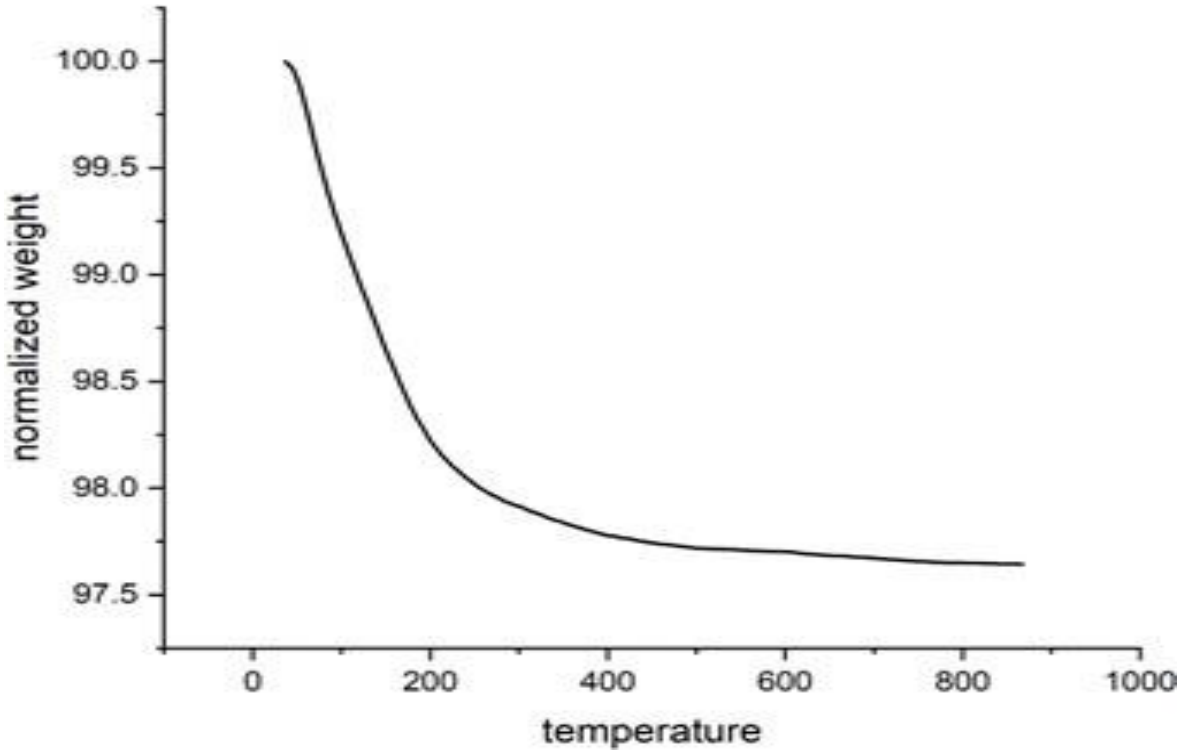
calcination temperature (800°C) so presence of moisture or water contents in this catalyst is very low. Therefore, the calibration curve of Cu-CAT is less steep as compared to the other two calibration curves of Cu-CA and Cu-A. In between the range of 200°C - 450°C, a significant decay is exhibited which indicates the removal of nitrogenous compound. Cu-CAT is synthesized by two step IWI method and this catalyst has the maximum percentage of nitrates.

Due to this, Cu-CAT shows a sharper exponential decay of weight in this range as compared to the other two. Partial decomposition of the nitrate, used as precursor, could be due to the less amount of heat generated by incomplete combustion. Also, results of FT-IR analysis show that many functional groups are present in Cu-CAT, Cu-CA and Cu-A [refer Table 4.3]. These inorganic compounds under high temperature, during TGA study, must have degraded causing some mass loss. But overall mass degradation of the three samples is less which is quite encouraging among the other characteristics, for the catalyst samples to be used for reduction of carbon monoxide (CO). It indicates that all the samples will work efficiently in reducing CO from the automobile exhaust. High temperature of the exhaust pipe cannot affect the mass of the catalysts any more. TGA analysis of the fourth catalyst, Cu/CA-S, is not carried out yet due to the non-availability of experimental slots in the UGC-SAP laboratory (Qiu, Li et al. 2011).

(a)


100.2
100.0
99.8
99.6
99.4
99.2
99.0
98.8
98.6
98.4
normalised weight
0
200
400
600
800
1000
temperature

(b)


100.0
99.5
99.0
98.5
98.0
97.5
normalized weight
0
200
400
600
800
1000
temperature

(c)

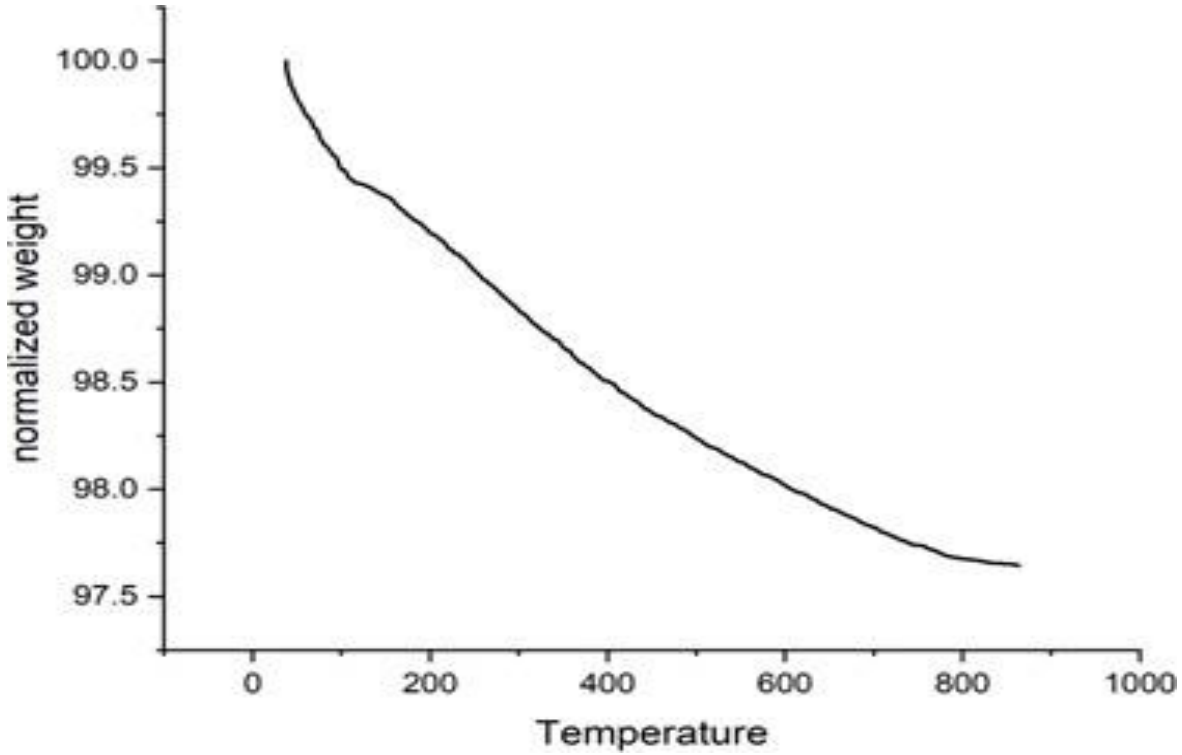


Figure 4.5: TGA plots of synthesized (a) Cu/CA, (b) Cu/CA-T, (c) Cu-A.

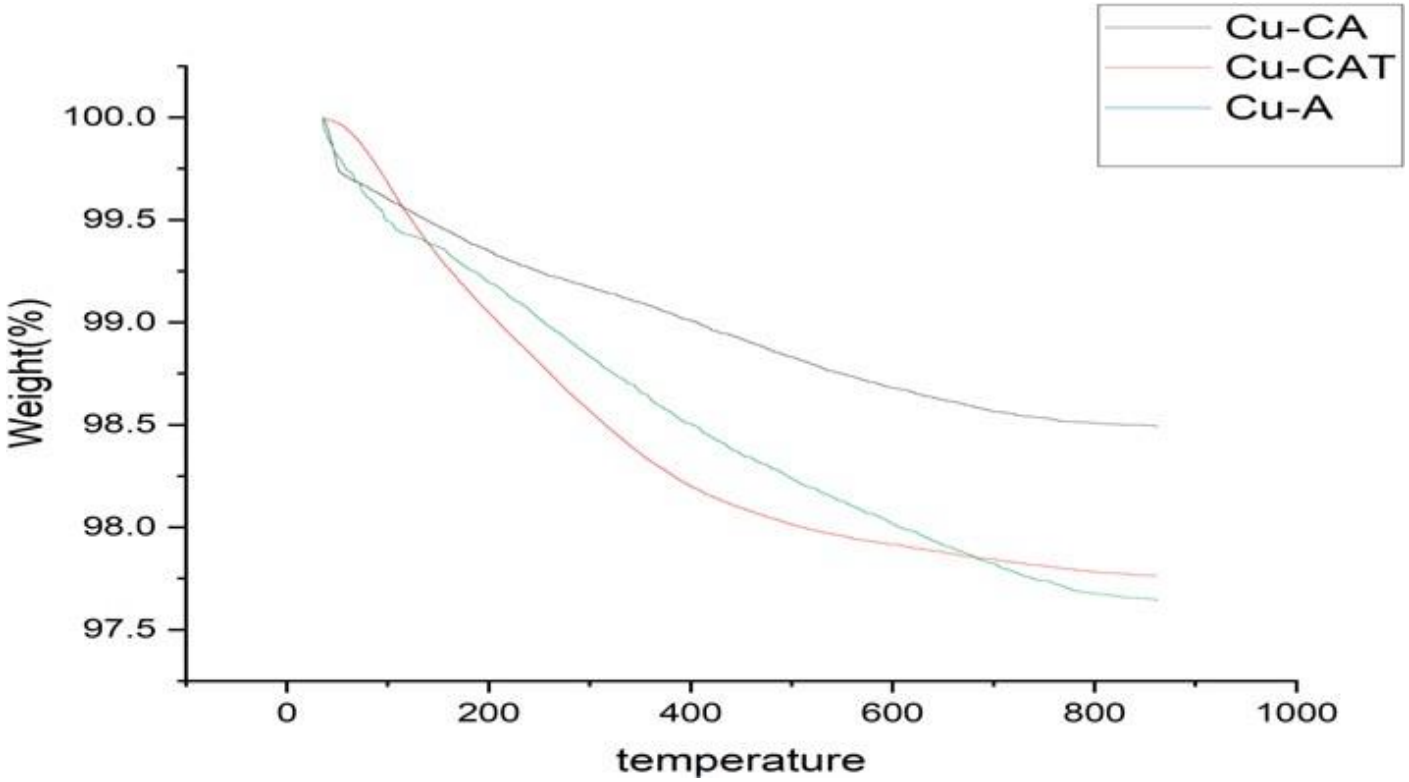


Figure 4.6: Consolidated TGA plots of synthesized (a) Cu-CA, (b) Cu-CAT, (c) Cu-A.

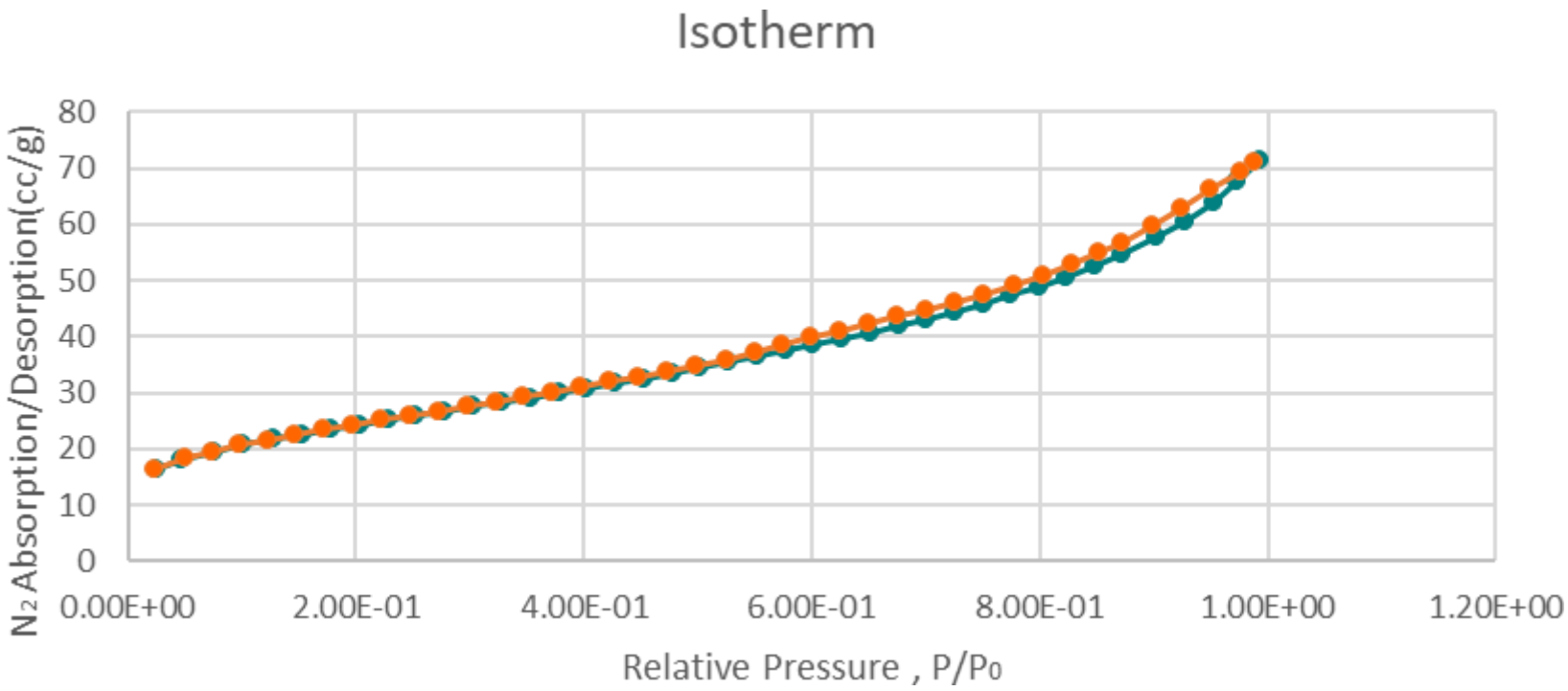
4.4. Surface area and pore volume analysis

BET surface area analysis refers to a technique used to measure the specific surface area of solid or powder materials. The term "BET" stands for Brunauer-Emmett-Teller, which is the name of the theory developed by the group of scientists namely Stephen Brunauer, Paul Emmett, and Edward Teller in the late 1930s. BET analysis is commonly used in the field of materials science and is particularly useful for characterizing porous materials such as catalysts, adsorbents, and powders. The technique is based on the physical adsorption of gaseous molecules onto the surface of a solid material. During BET analysis, an inert gas, typically nitrogen, is adsorbed onto the sample surface and pores under different ranges of relative pressures. The amount of gas adsorbed is measured, and this data is used to calculate the surface area of the material or the catalyst. The analysis relies on the assumption that the adsorption occurs in a monolayer formation on the material's surface. The BET equation, derived from the Brunauer-Emmett-Teller theory, is used to fit the experimental data and estimate the specific surface area. It provides information about the material's porosity, surface roughness, and active surface area. There are total five types of isotherms. Types II and III show large deviations from the Langmuir model, and hence BET model is proposed. In order to explain isotherm of type II and type III, Brunauer, Emmet and Teller extended the Langmuir approach by postulating multimolecular adsorption (Qiu, Li et al. 2011). BET surface area and pore volume of the synthesized catalysts are estimated using nitrogen adsorption/desorption isotherms generated in using a surface area analyzer [**Make**: Anton Paar; **Model**: Autosorb iQ Station 1] at 77 K and the characterization is carried out at *Chemical Engineering Department, IIT*

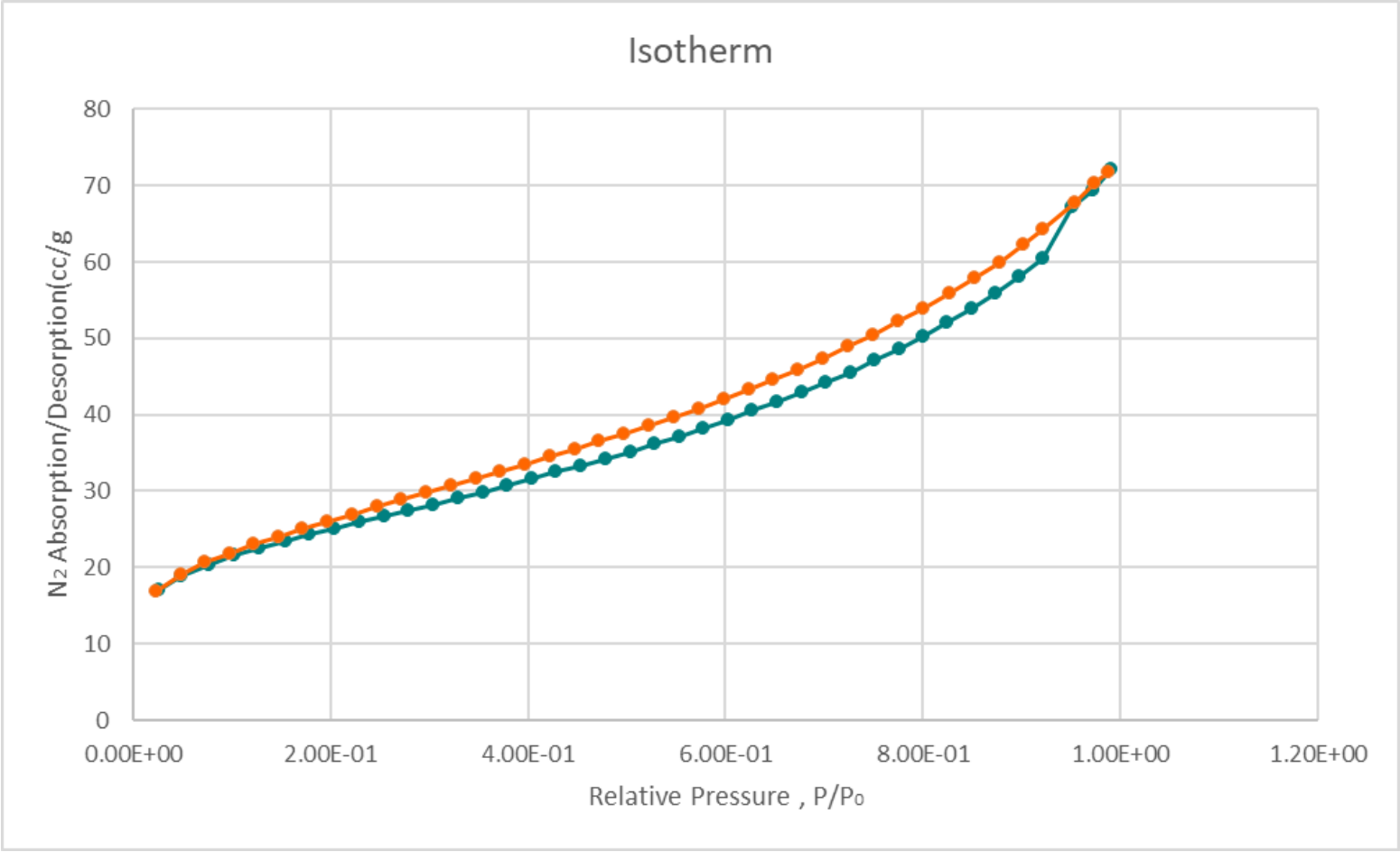
Kharagpur. The material is degassed at 393 K for 12 h before analysis and the maximum pressure is maintained at 100 kPa. The N_2 adsorption/desorption of Cu/CA, given in **Figure 4.7 (a)**, denotes type II isotherm. In the beginning, the macropores fill with inert nitrogen gas. The curve indicates that at low relative pressure monolayer formation takes place. At the knee, monolayer formation is beginning, and infinite multilayer formation occurs under medium pressure. At high p/p_0 the N_2 uptake gradually increases, which denotes the presence of intra-particle porosity. This explains that Cu/CA is primarily micro or mesoporous and this is the reason behind formation of the multilayers over the surface of the catalyst. The N_2 adsorption-desorption isotherms for Cu/CAT and Cu/A, shown in **Figure 4.7 (b)** and **Figure 4.7 (c)** give type II isotherms. Cu/CAT and Cu/A also show similar type of surface structure. This shows that the bimetallic catalyst is mostly microporous or mesoporous.

From BJH adsorption model, as shown in **Figure 4.8**, we can estimate the pore volume of the given catalyst. Pore volume of Cu/A is observed to be greater than Cu/CA and Cu/CAT. At any particular relative pressure, pore volume (cc/g) of Cu/A is little more than that of Cu/CA and Cu/CAT and hence the N_2 adsorption capacity increases. The results using the BJH model show that the specific surface area and pore volume decreases after cerium oxide treatment. Cu/A has a high surface area and a well-defined pore size distribution, which allows for the effective adsorption of nitrogen molecules. **Figure 4.8** shows the porosity of the three synthesized catalysts. Cu/CA has the highest porosity than the other two. From the pore radius data, we can evaluate that Cu/CA is mesoporous, while Cu/CAT and Cu/A are microporous in nature (Baneshi, Haghighi et al. 2014).

(a)


Isotherm
N2 Absorption/Desorption(cc/g)
80
70
60
50
40
30
20
10
0
0.00E+00
2.00E-01
4.00E-01
6.00E-01
8.00E-01
1.00E+00
1.20E+00
Relative Pressure , P/P0

(b)


Isotherm
80
70
60
50
40
30
20
10
0
N2 Absorption/Desorption(cc/g
0.00E+00
2.00E-01
4.00E-01
6.00E-01
8.00E-01
1.00E+00
1.20E+00
Relative Pressure , P/Po

(c)

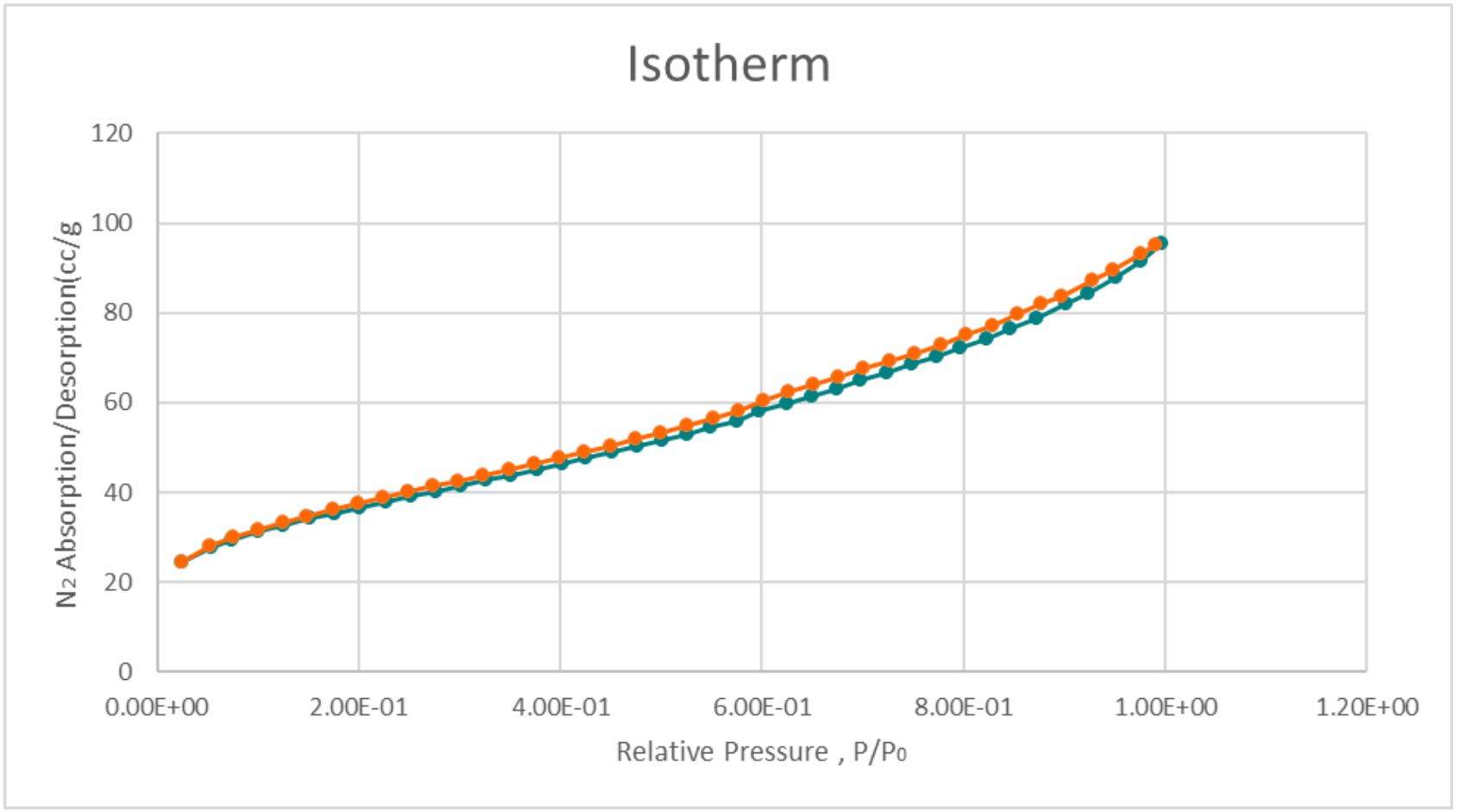
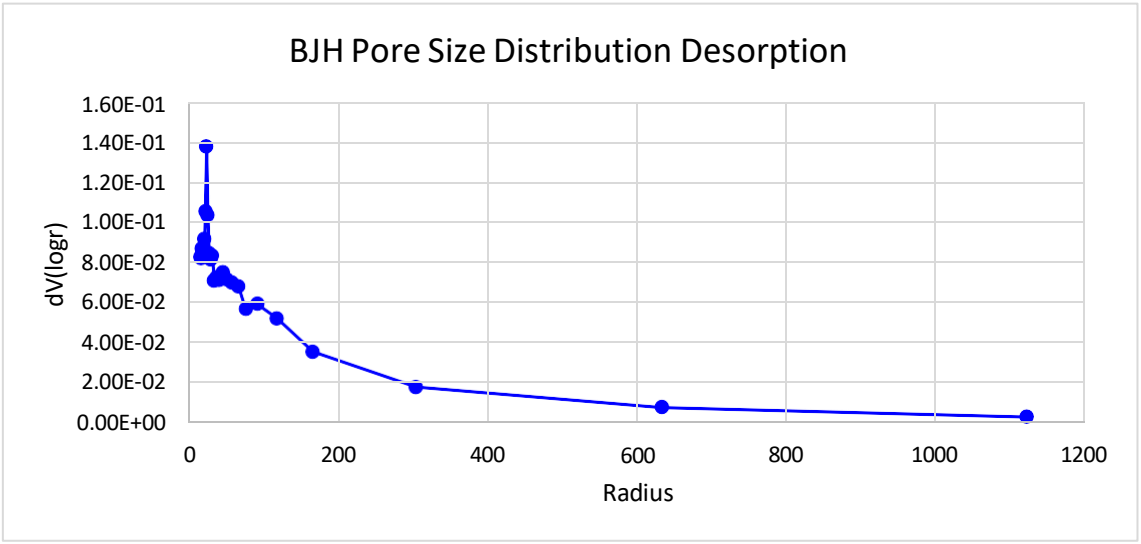
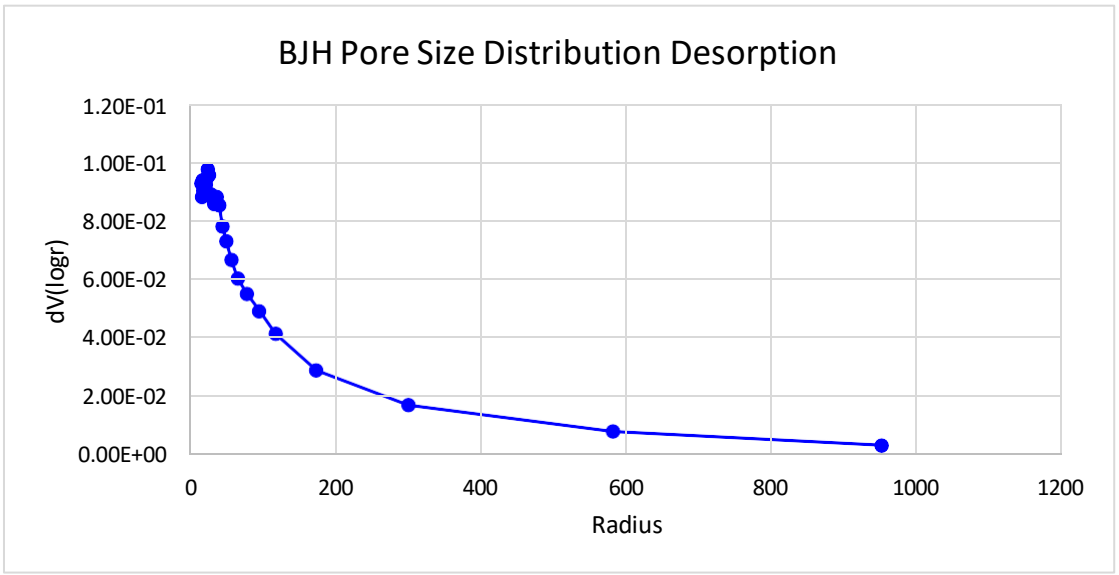


Figure 4.7: Nitrogen adsorption-desorption isotherms of (a) Cu/CA, (b) Cu/CAT, and (c) Cu/A.

(a)


BJH Pore Size Distribution Desorption
1.60E-01
1.40E-01
1.20E-01
1.00E-01
8.00E-02
6.00E-02
4.00E-02
2.00E-02
0.00E+00
dV(logr)
0
200
400
600
800
1000
1200
Radius

(b)


BJH Pore Size Distribution Desorption
1.20E-01
1.00E-01
8.00E-02
6.00E-02
4.00E-02
2.00E-02
0.00E+00
dV(logr)
0
200
400
600
800
1000
1200
Radius

(c)

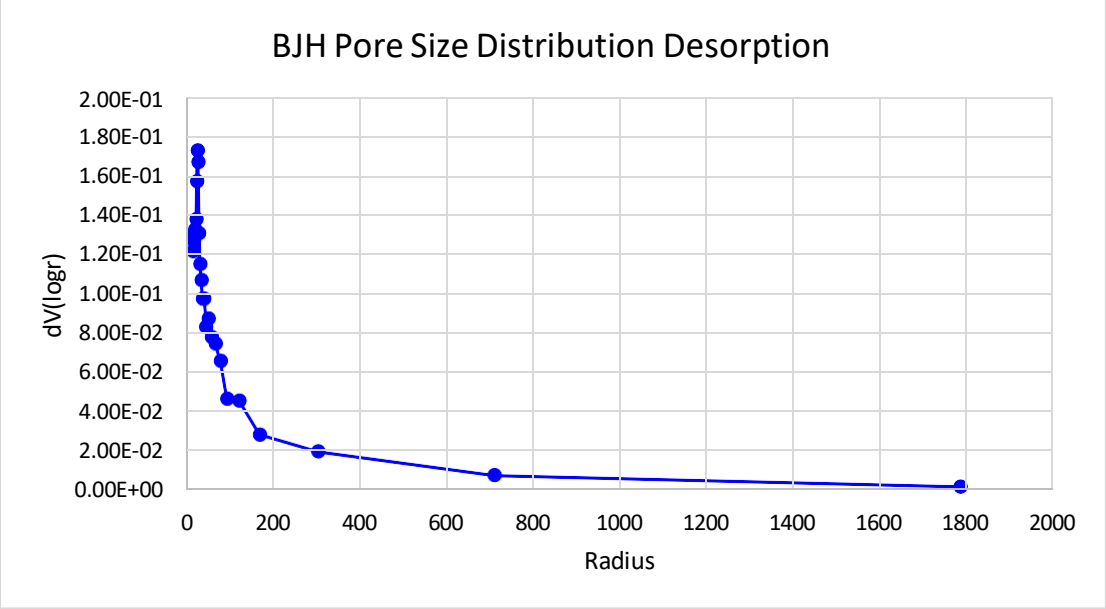


Figure 4.8: BJH pore size distribution curves of (a) Cu/CA, (b) Cu/CAT, and (c) Cu/A.

The BET surface area, pore volume and pore radius obtained from the nitrogen adsorption-desorption isotherms are summarized in **Table 4.4**. It shows that decrease in surface area and pore volume is due to the blockage of pores by the humic substances that are formed during the oxidation process (Vahid and Haghighi 2017). Comparing the surface area and pore volume of Cu/CA and Cu/CAT from Table 4.4, it is noticed that the surface area and pore volume are greater for Cu/CAT than the same for Cu/CA. It might be due to the uniform deposition of the active species CeO_2 two times in the novel T-IWI method. CeO_2 gets physisorbed on the surface of the microporous catalyst, thereby increasing the surface area and pore volume (Baneshi, Haghighi et al. 2014).

The pore size distributions obtained by fitting the experimental data in the Non-Local Density Functional Theory (NLDFT) are given in **Figure 4.9 (a)**. The same shows that maximum numbers of pores are located within the range 0.5 nm to 50 nm pore width,

which is both in the microporous and mesoporous region. Two visible peaks can be observed in the figure, both at the mesoporous region. Maximum cumulative numbers of pores exist in the mesoporous region.

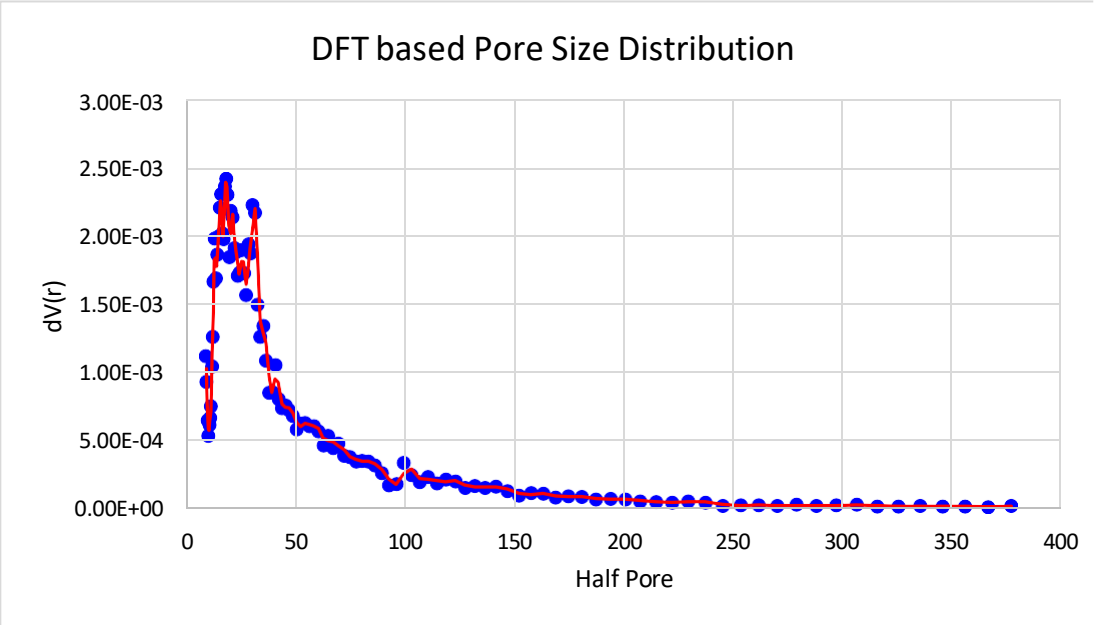
Table 4.3: Estimated data of Surface area, Pore volume and Pore radius of the synthesized catalysts.

Catalyst name	*Surface area(m^2/g)*	*Pore volume(cc/g)*	*Pore Radius(A°)*
Cu/CA	42.785	0.085	23.611
Cu/CAT	43.158	0.082	15.568
Cu/A	58.673	0.105	16.537

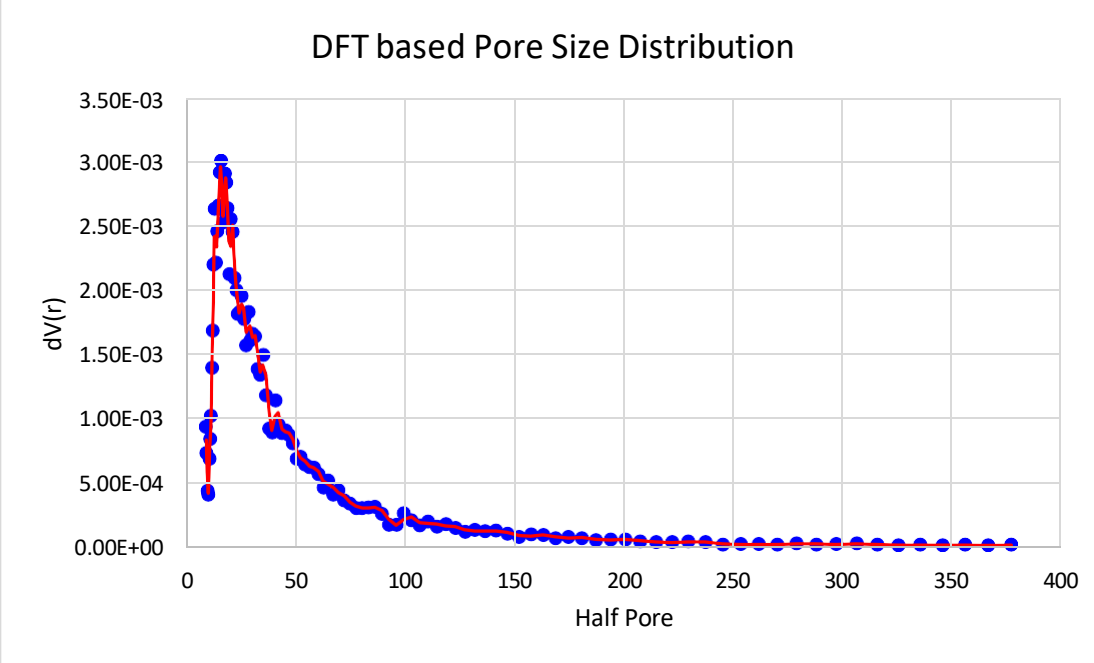
The pore size distribution shows that the number of mesopores decreases after modification of process during the synthesis of Cu/CAT catalyst, which is given in **Figure 4.9 (b)**. Corresponding shift for pore width is from 23.611 A° to 15.568 A°. The pore size distribution of Cu/CAT, as shown in **Figure 4.9 (b)** endorses that maximum cumulative number of pores are located in the microporous region (i.e. below 2 nm). A sharp peak can be observed at 15.568 A° (1.557 nm), which is in the microporous region. So, it can be concluded from the pore size distribution study that due to the updation of IWI method to the novel two-step IWI method, pore width/size of the catalysts decreases. The pore size distribution of Cu/A, obtained from NLDFT, as presented in **Figure 4.9 (c)**, shows a sharp peak at 16.537 A° (1.653 nm) pore-width. It is evident that the maximum number of pores are located in the microporous region (i.e. below 2 nm) for Cu/A. From DFT model we can understand that the pore size of all of the three catalysts is very low. This type of

observation supports the presence of type II isotherm. We get similar result from the BET model. This is due to the small pore size of each of the catalysts, conforming to the multilayer adsorption model.

(a)



(b)



(c)

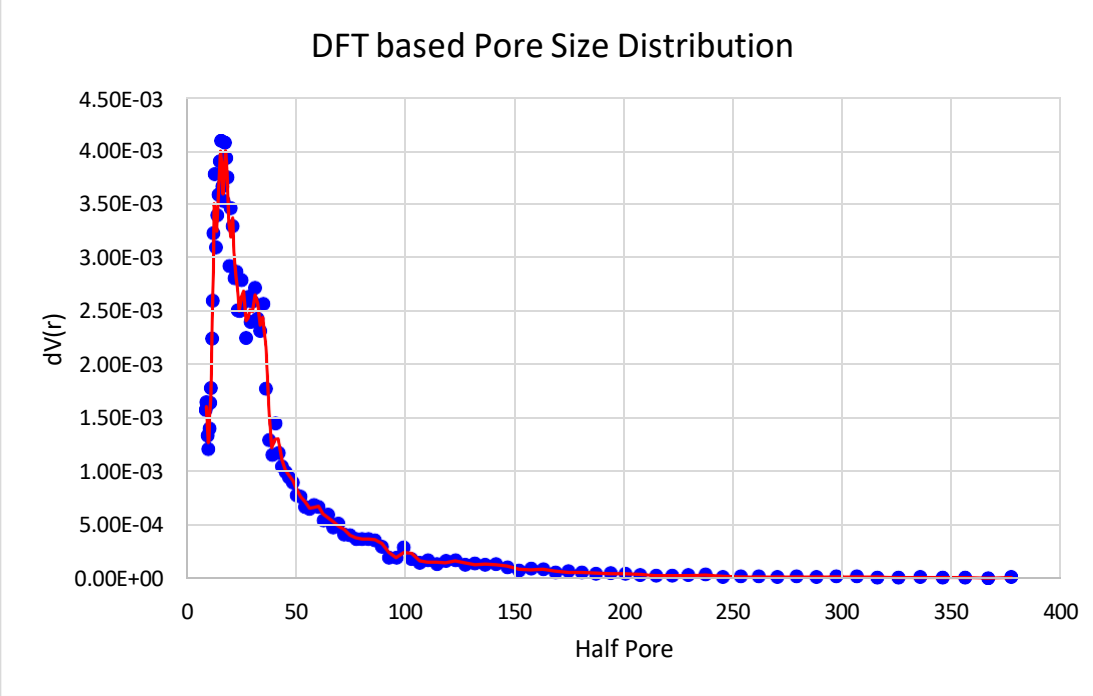


Figure 4.9: Density Functional Theory [DFT] based pore size distribution model curves of (a) Cu/CA, (b) Cu/CAT, and (c) Cu/A.

As adsorption of CO is a surface phenomenon, the same requires a catalyst which has large surface area. Cu/A has large surface area as compared to both Cu/CA and Cu/CAT, and it must adsorb more CO, and also reacts with more CO. However, its pore volume being bigger than both of Cu/CA and Cu/CAT, a negative impact is created on CO adsorption. If CO is captured on the pores of the catalyst, activity of the catalysts will decrease and catalyst will lose its longevity. Efficiency of the catalysts will be harmed. So, Cu/CA and Cu/CAT will work better if we consider the pore volume.

Surface area and pore volume analysis of the fourth catalyst named Cu/CA-S could not be carried out due to non-availability of slots for using the BET set-up on a time- sharing basis.

4.5. X-Ray Diffraction (XRD) analysis

X-rays can be considered waves of electromagnetic radiation. X-Ray Diffraction examination (XRD) could be a flexible non-destructive method utilized to dissect data point by point approximating the crystallographic structure, chemical composition, and physical properties of a Sample. It is based on the useful obstructions of monochromatic X-rays and determines the extent of crystallinity in the sample. X-rays are shorter wavelength electromagnetic radiation that are created when electrically charged particles with adequate vitality are decelerated. Concentrated diffracted beams scatter at distinctive points of crystals and the same are plotted to show a diffraction design. The diffraction design could represent all of the diffraction patterns at each stage.

The diffraction design of XRD characterization will be compared with the standard crystallographic databases such as the database of International Centre for Diffraction Data (ICDD), to compare the recognizable stage with the standard, estimate miller indices and identify crystalline phases of crystalline samples. The crests of the XRD design play an imperative part within the recognizable proof of the stages as well as the properties of the synthesized catalysts. Analysis of the crystalline size of nanoparticles is carried out to investigate the crystal structure of copper doped Cerium-Alumina samples. The characterization of three catalyst samples, with same components but different ratios, is performed with the aid of the XRD pattern by comparing the width of the peaks, crystal structures, phases of crystals, crystallites size and crystallinity percentage in XRD pattern. The Scherrer Eq. (1) is employed to determine the primary particle size of a given crystal

phase based on the most intense diffraction peak of cupric oxide, cerium oxide and alumina patterns:

$$\boldsymbol{D_{xrd} = \frac{k\lambda}{\beta \cos\theta}} \quad \textbf{..... (1)}$$

where *k* is the Scherrer constant; λ is the wavelength of the X-ray in nm; β is the line broadening factor; θ is the Bragg angle.Crystallinity index is required to understand that the catalyst is crystalline or amorphous. Crystallinity index from XRD data is calculated from the equation which is given below:

$$Crystallinity\ Index = \frac{Area\ \ of\ \ all\ \ the\ \ crystalline\ \ peaks}{Area\ of\ all\ crystalline\ and\ amorphous\ peaks} \quad \text{..... (2)}$$

The crystal phases of as-prepared catalysts were determined by the XRD technique. The crystalline structure of 4 catalysts were determined by powder X-ray diffraction (XRD) on a Siemens D 500 diffractometer operated at 40 kV and 30 mA with Cu Kα radiation (λ = 0.154 nm). Diffractograms were recorded in the 10–80° 2θ range and at a scanning rate of 0.02° s^{-1}. XRD analysis is done in Metallurgy department, Jadavpur University. Given diffraction patterns and phases are identified by ICDD database and JCPDS card numbers.

Figure 4.10 (a) represents the X-ray powder diffraction patterns of Cu/CA. The main peaks can be indexed to (111), (100), (422), (222), (113), (211). As per the $2\boldsymbol{\theta}$ vs intensity plot miller indices indicate that synthesized catalysts exhibit the large and sharp peaks of CeO_2 at 28.553°, Aluminium Nitride (AlN) at 33.206°, Copper Aluminium oxide ($CuAl_2O_3$) at 55.614° and Cerium Oxide (CeO_2) at 59.173°. Also, some small peaks of Cerium at 79.964° and Cerium Oxide (CeO_2) at 76.555 are identified by the Xray diffraction pattern. Detailed

analytical data is given in **Table 4.4 (a)**. As per the analysis, Cu/CA samples exhibited broad diffraction lines due to the cubic fluorite type phases of Ceria. Comparing Diameter of all the phases of crystals, CeO_2 has highest crystalline diameter compare to other phases. From the diffraction pattern, we notice that the Cu/CA give Sharp peaks which indicate towards crystallinity. *(Vahid and Haghighi 2017)*

Figure 4.10(b) represents the XRD patterns of Cu/CAT. The main peaks can be indexed to (111), (200), (400), (311), (116), (107). As per the $2\boldsymbol{\theta}$ vs intensity plot miller indices indicate that synthesized catalysts exhibit the large and sharp peaks of Cerium oxide (CeO_2) at 28.701°,33.196° and 56.445°, large and sharp peaks of Aluminium oxide (Al_2O_3) at 45.821° and two small peaks of copper aluminium oxide ($CuAlO_2$) and Aluminium oxide hydrate at 69.637° and 78.927°. Detailed analytical data is given in **Table 4.4 (b)**. From the crystallographic data Cu/CAT indicates same type of crystallographic structure with Cu/CA but the intensity of peaks of Cu/CAT is higher than the Cu/CA which indicates crystallinity of Cu/CAT is greater than the Cu/CA. Comparing Diameter of all the phases of crystals, CeO_2 has highest crystalline diameter compare to other phases.*(Vahid and Haghighi 2017)*

Figure 4.10 (c) represents the XRD patterns of Cu/A. The main peaks can be indexed to (110), (311), (202), (220), (311). As per the ICDD database, synthesized catalysts exhibit the small and broad peaks of copper oxide (CuO) at 32.541°, copper aluminium oxide ($CuAl_2O_4$) at 36.971° and Aluminium oxide (Al_2O_3) at 39.490°. Two large, strong and sharp peaks of Aluminium oxide (AlO) and copper oxide (CuO) are detected at 45.247° and 67.450°. Detailed analytical data is given in **Table 4.4 (c)**. XRD phase analysis reveal the

cubic crystal structure of Cu/A. Many peaks of Cu/A are broad. This type of peaks is indicating less crystalline size. In comparison with Cu/A, two other catalysts are more crystalline because of their sharp peaks. Peak's Intensity of this samples is also less compared to the other samples so it indicates the low crystal (grain) size.

Figure 4.10 (d) represents the XRD patterns of Cu/CA-S. The main peaks can be indexed to (220), (200), (116) and (311). As per the ICDD database, synthesized catalysts exhibit the strong and sharp peaks of copper azide (CuN_3) at 29.095°, Cerium oxide (CeO_2) at 33.359°, aluminium oxide (Al_2O_3) at 56.235° and Cerium oxide (CeO_2) at 56.515°. Detailed analytical data is given in **Table 4.4 (d)**. Most of the peaks of diffraction patterns are sharp so it indicates crystallinity structure of Cu/CA-S. Crystal phase of copper azide has the highest diameter among the all phases. Peak intensity of Cu/CA-S is less so it also has low crystal (grain) size but its crystal size is more than the Cu/A.

The average crystallite diameter of the 4 samples were evaluated by XRD diffraction by employing the Scherrer equation. The results shown in **Table 4.5**. Mean particle size resulted in 6.6800 nm, 7.6241 nm, 3.8299 nm and 7.4512 for the Cu/CA, Cu/CAT and Cu/A and Cu/CA-S. Cu/A exhibits the lowest mean crystallite size. When the Cerium dopped over the sample the average crystallite diameter increases. This happened in case of Cu/CA, Cu/CAT and Cu/CA-S. Cu/CAT and Cu/CA-S indicates nearly same Crystal size. As per analysis Crystallinity order of the three sample is Cu/CAT>Cu/CA-S >Cu/CA >Cu/A. **Table 4.6** shows the data of Crystallinity index of the 4 catalysts. Crystallinity order is

Cu/CA-S > Cu/A > Cu/CA > Cu/CAT. The highest crystallinity order is shown by Cu/CA-S (Baneshi, Haghighi et al. 2014).

Table 4.4: Phase analysis data of (a) Cu/CA, (b) Cu/CA-T, (c) Cu/A, and (d) Cu/CA-S.

	2-Theta	d (Å)	Height	Height%	Phase ID	JCPDS card no	(h k l)
(a)	28.553	3.1236	157	100.0	CeO_2	01-081-0792	(1 1 1)
	33.206	2.6958	52	33.1	AlN	01-076-0702	(1 0 1)
	55.614	1.6513	84	53.5	$CuAl_2O_4$	01-071-0966	(4 2 2)
	59.173	1.5601	69	43.9	CeO_2	01-081-0792	(2 2 2)
	69.964	1.3436	3	1.9	Ce	01-071-0439	(1 1 3)
	76.555	1.2435	4	2.5	Ce_2O_3	01-074-1145	(2 0 1)
(b)	28.701	3.1079	307	100.0	CeO_2	01-089-8436	(1 1 1)
	33.196	2.6966	80	26.1	CeO_2	01-089-8436	(2 0 0)
	45.821	1.9787	123	40.1	Al_2O_3	01-074-2206	(4 0 0)
	56.445	1.6289	105	34.2	CeO_2	01-089-8436	(3 1 1)
	69.637	1.2768	9	2.9	$CuAlO_2$	01-075-2356	(1 1 6)
	78.927	1.2119	6	1.9	$(Al_2O_3)_5(H_2O)$	01-073-1190	(1 0 7)
(c)	32.541	2.7494	21	12.4	CuO	01-080-0076	(1 1 0)
	36.971	2.4295	27	15.9	$CuAl_2O_4$	01-071-0966	(3 1 1)
	39.490	2.2801	20	11.8	Al_2O_3	01-074-2206	(2 0 2)
	45.247	2.0025	123	72.8	AlO	01-075-0278	(2 2 0)
	67.450	1.2810	169	100.0	CuO	01-080-0076	(3 1 1)

(d)	29.095	3.0667	90	100.0	CuN_3	01-085-0903	(2 2 0)
	33.359	2.6838	25	27.8	CeO_2	01-089-8436	(2 0 0)
	48.235	1.6345	24	26.7	Al_2O_3	01-071-1684	(1 1 6)
	56.515	1.6270	20	22.2	CeO_2	01-089-8436	(3 1 1)

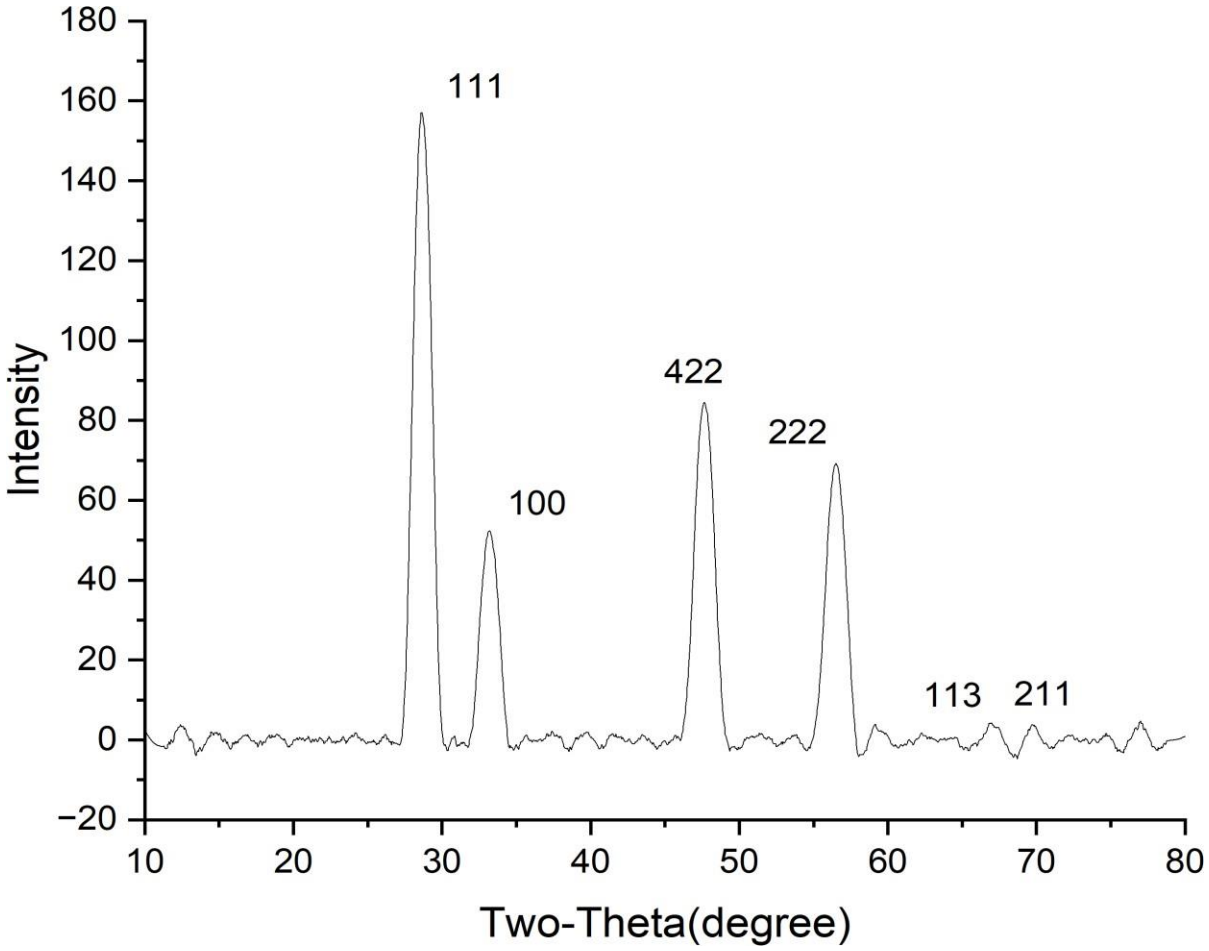
Table 4.5: Average crystalline size of the synthesized Catalysts.

Catalyst	Crystallite size D (nm)
Cu/CA	6.680026202
Cu/CA-T	7.624104962
Cu/A	3.829922826
Cu/CA-S	7.451270823

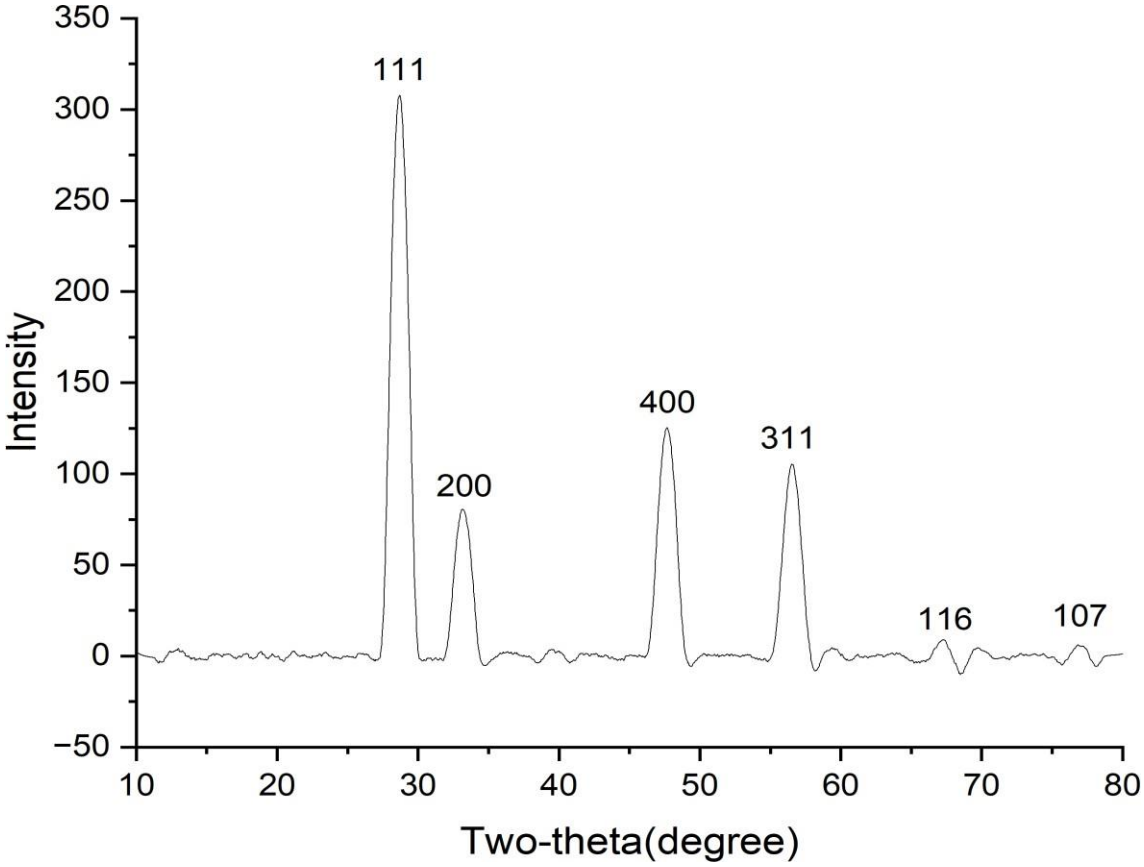
Table 4.6: Percentage of Crystallinity index of the catalysts

Catalyst	Crystallinity Index (%)
Cu/CA	69.5580423
Cu/CA-T	63.7046097
Cu/A	71.3262293
Cu/CA-S	74.5673399

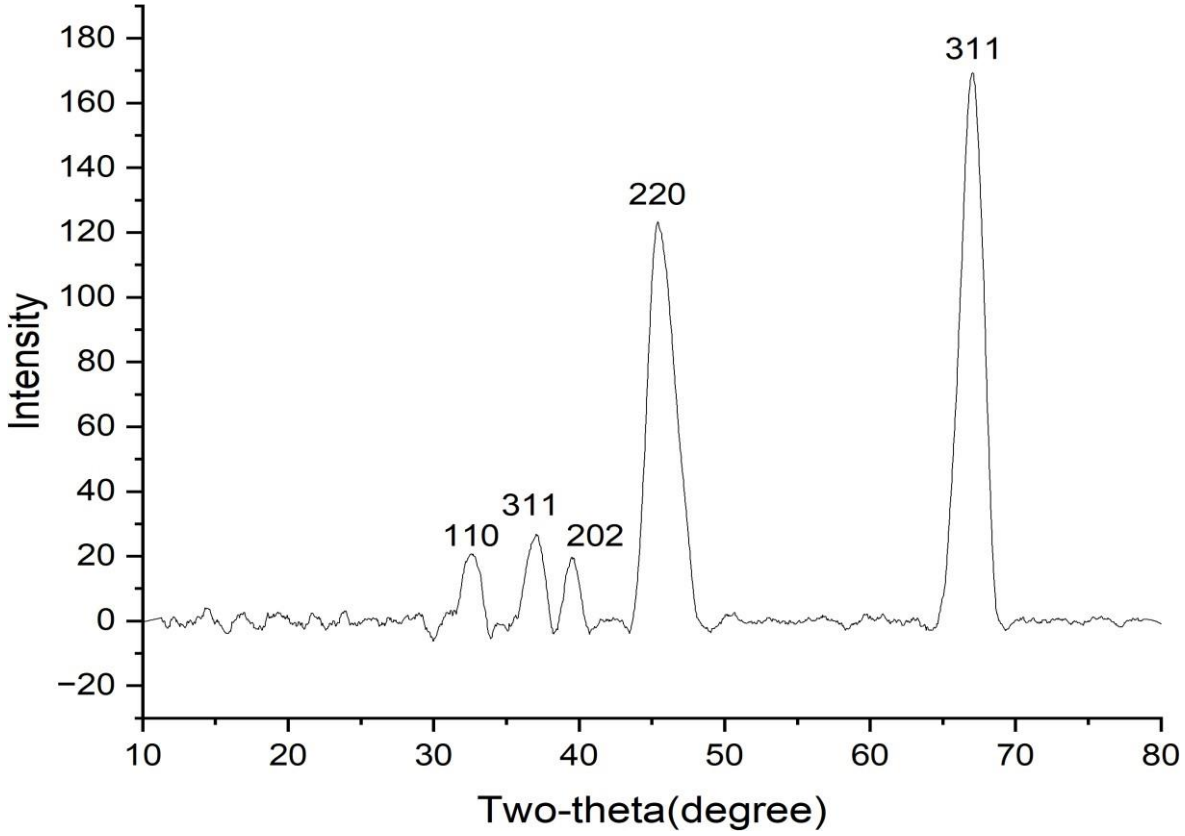
(a)


Intensity
Two-Theta(degree)
111
100
422
222
113
211
180
160
140
120
100
80
60
40
20
0
−20
10
20
30
40
50
60
70
80

(b)


Intensity
Two-theta(degree)
111
200
400
311
116
107
350
300
250
200
150
100
50
0
−50
10
20
30
40
50
60
70
80

(c)


Intensity
Two-theta(degree)
110
311
202
220
311
180
160
140
120
100
80
60
40
20
0
−20
10
20
30
40
50
60
70
80

(d)

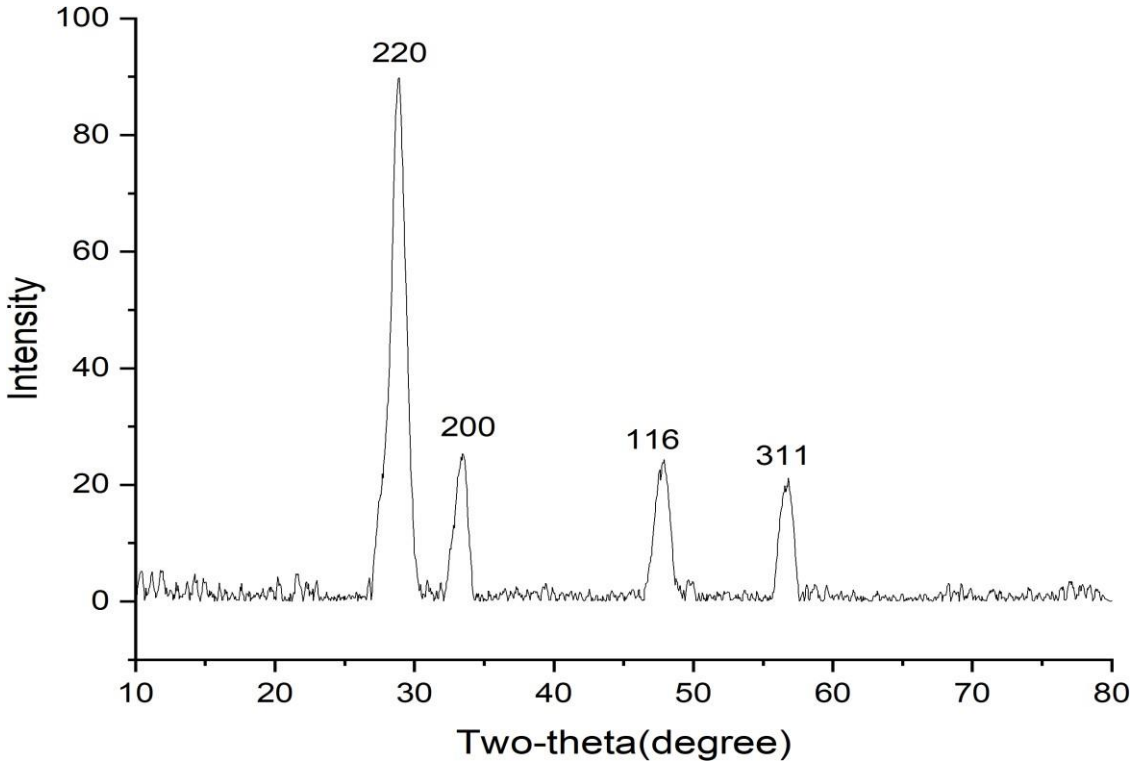


Figure 4.10: XRD patterns of (a)Cu/CA, (b)Cu/CA-T, (c)Cu/A, and (d)Cu/CA-S.

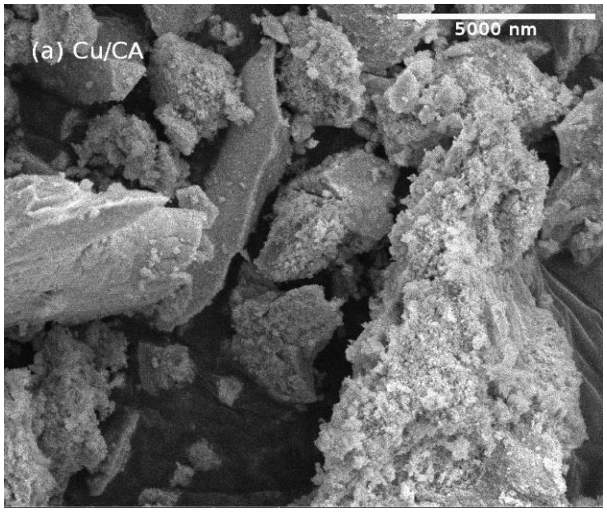
4.6. Field Emission Scanning Electron Microscopy (FESEM) analysis

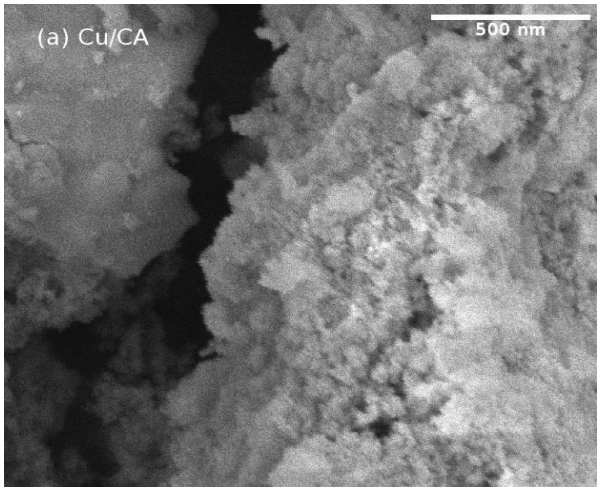
Textural characterization of the catalysts is carried out using a Field Emission Scanning Electron Micrograph (FE-SEM) [**Make**: ELECMI; **Model**: FEI INSPECT F50] at ×20,000 magnification for the image at 5 μm and at ×80,000 magnification for the image at 500 nm. **T**he analysis is carried out in the *Physics department, Jadavpur University*. FE-SEM analyses are carried out with the 4 synthesized catalysts to analysis the surface texture, particle size and actual loading capacity. Images from the FE-SEM analyser are then analysed using ImageJ and Origin software.

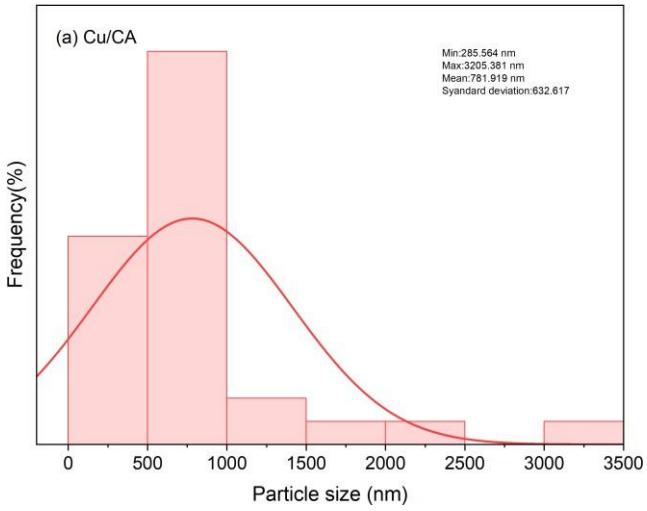
Figure 4.11 [(a), (b), (c) and (d)] shows the FESEM micrographs and histograms representing the corresponding particle size distributions of the synthesized catalysts. Metal particle size is one of the principal properties of the catalyst. Activity and selectivity of the catalyst strongly depends on it. Average particle size of the Cu/CA is 781.919 nm and is mostly concentrated in the range of 250 nm - 1250 nm. Particle size of Cu/CAT is 781.919 nm, on an average, and is mostly concentrated in the range of 300 nm - 1000 nm which is nearly same as observed in Cu/CA. However, in case of Cu/A, average particle size is 980.046 nm and most of the particles are present within the range of 300 nm - 1500 nm. According to this data, average particle size of Cu/A is greater than the Cu/CA and Cu/CA-T. It indicates that addition of ceria to the catalysts decrease the average particle size of the catalysts. Particles are more distributed in the Cu/A compare to others which indicates Cu/A has larger surface area to adsorb the CO. The average particle size of Cu/CA-S is 627.971 nm and the particles are distributed between the range of 250-900

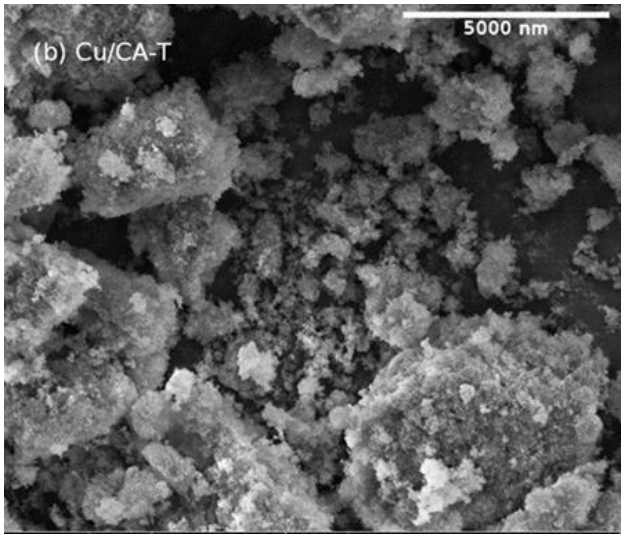
nm. Average particle size and range of distribution of particles in Cu/CA-S do not match with the same for the other three catalysts. From this data, we can infer that the catalysts synthesized using the sol-gel method generate smaller particles in size, while the catalysts synthesized by the IWI method evolved larger size particles in comparison. From the size distribution histogram, we can infer that particles of varying size and shape are present in all of the samples (Baneshi, Haghighi et al. 2014).

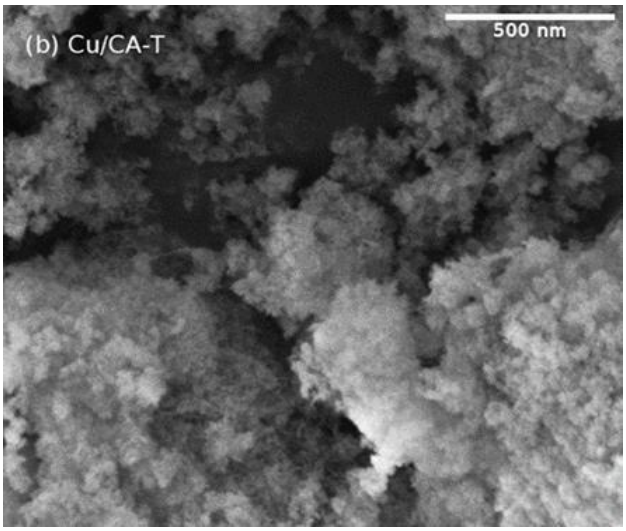
Image of **Figure 4.11 (a)** shows smooth surface of Cu/CA. Adsorption on this surface of Cu/CA will be very low because it cannot grab the gaseous particles of CO so easily due to the smoothness of the surface. Surface of the other three catalysts, as shown in **Figures 4.11 (a), (b), (c)** is rough so they will act as good adsorbents. Every catalyst has pores which can be identified by **Figures 4.11 (a), (b), (c)** and **(d)**, however, Cu/CA is found to be more porous as compared to the textures of the other three catalysts. It can be said from the FESEM analysis, Cu/CA may be less effective for catalytic activity as compared to the other three catalysts.

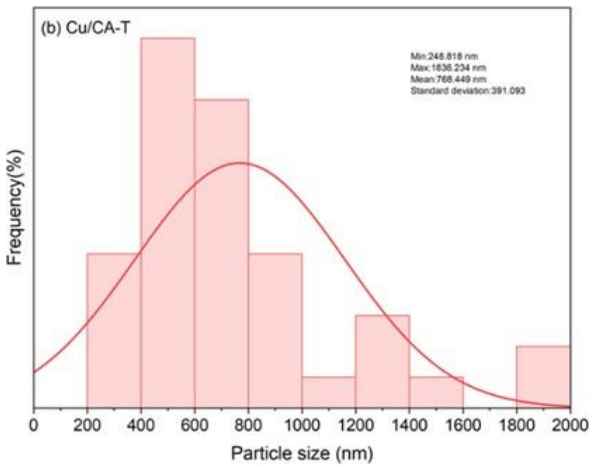

(a) Cu/CA
5000 nm

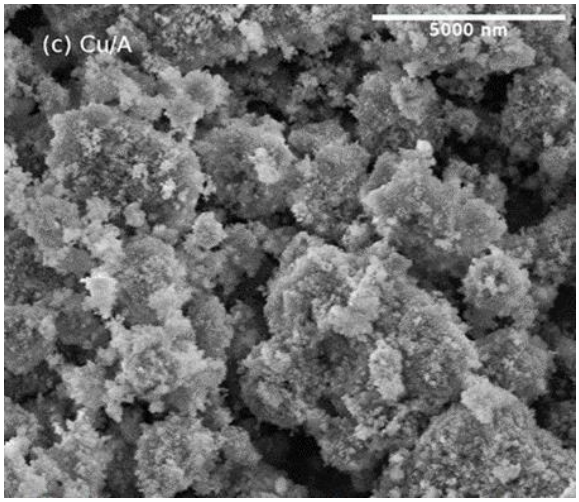

(a) Cu/CA
500 nm

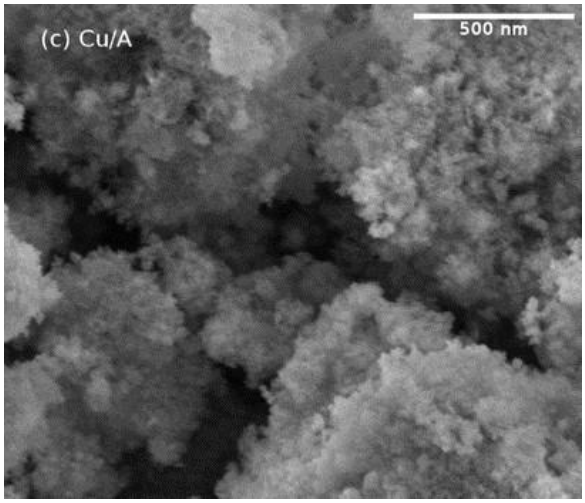

(a) Cu/CA
Min:285.564 nm
Max:3205.381 nm
Mean:781.919 nm
Syandard deviation:632.617
Frequency(%)
0
500
1000
1500
2000
2500
3000
3500
Particle size (nm)

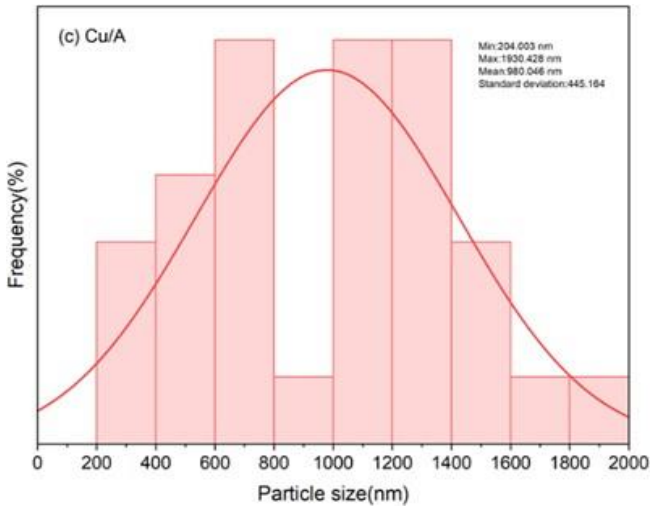

(b) Cu/CA-T
5000 nm


(b) Cu/CA-T
500 nm


(b) Cu/CA-T
Min:248.818 nm
Max:1836.234 nm
Mean:768.449 nm
Standard deviation:391.093
Frequency(%)
0
200
400
600
800
1000
1200
1400
1600
1800
2000
Particle size (nm)


(c) Cu/A
5000 nm


(c) Cu/A
500 nm


(c) Cu/A
Min:204.003 nm
Max:1930.428 nm
Mean:980.046 nm
Standard deviation:445.184
Frequency(%)
0
200
400
600
800
1000
1200
1400
1600
1800
2000
Particle size(nm)

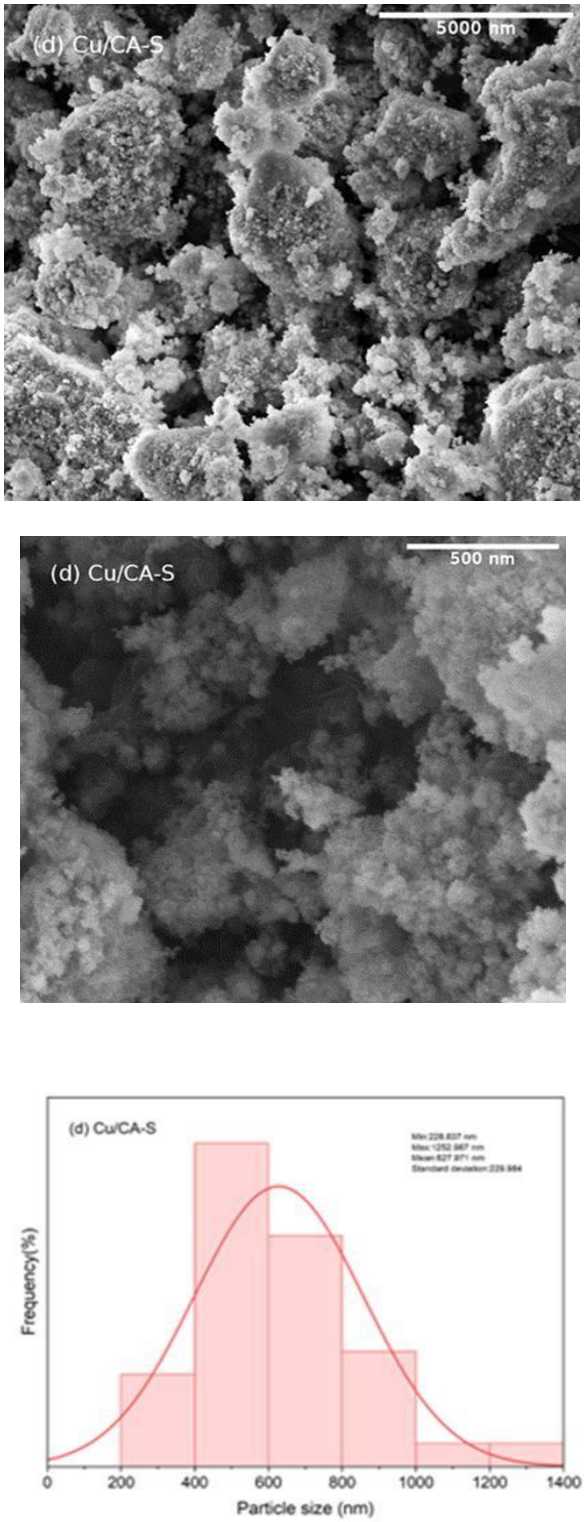


Figure 4.11: FESEM images and particle size distribution histogram of synthesized catalysts: (a)Cu/CA, (b)Cu/CA-T, (c)Cu/A, (d)Cu/CA-S.

Chapter 5

Control of Carbon Monoxide from vehicular exhaust: *In-situ control using portable packed bed filled with synthesized catalysts*

5.0. Introduction

Synthesis and characterization of a catalyst is the most essential part of our project. Practical test in the automobile vehicles using the synthesized catalysts is genuinely necessary to understand the efficacy of these catalysts. Large number of tests need to be carried out to evaluate the performance, efficiency, and effectiveness of the catalysts. Testing ensures that a particular synthesized catalyst meets the required standards and specifications for its intended application, making it a critical step in the development and application of novel catalytic materials. In the testing part, three numbers of catalysts synthesized (Cu/CA, Cu/CAT, and Cu/A) are discussed. A large number of portable packed-beds, with a specific length and diameter, are designed, containing specific amounts of each of these synthesized catalysts. The same are fitted within the exit of the silencer pipes of a 25 years old car [**Make**: Maruti-Suzuki; **Mod**el: 800 *DX*] and a large number of tests are carried out in a licensed Auto-Emission Laboratory of a registered petrol pump in Kolkata. All the necessary information, results related to the tests are discussed below.

5.1. IC engine details and generation of CO

Internal combustion engines (IC engines) are widely used in various applications, from automobiles to power generation. These engines operate by burning fuel within a combustion chamber to produce mechanical energy, which is then converted into useful work. There are different types of IC engines, including gasoline engines (spark-ignition engines) and diesel engines (compression-ignition engines), each with its own operating principles and characteristics.

Here is a brief overview of the main components and operation of a typical IC engine:

a. Combustion Chamber: This is where the fuel-air mixture is ignited and burned. In gasoline engines, a spark plug ignites the air-fuel mixture, while in diesel engines, the air is compressed until it reaches a temperature where diesel-fuel injected into the chamber ignites spontaneously.
b. Piston: The piston moves up and down within the cylinder, converting the pressure generated by the combustion process into mechanical energy. This movement is transferred to the crank-shaft via a connecting rod.
c. Cylinder: The combustion chamber is housed within the cylinder, where the piston moves. IC engines can have multiple cylinders arranged in various configurations (inline, V, flat, etc.).
d. Valves: In four-stroke engines (most common in automotive applications), there are intake and exhaust valves that open and close at specific times to allow air-fuel mixture into the cylinder and exhaust gases to come out.
e. Fuel System: This includes components such as fuel injectors (in diesel engines) or carburettors/fuel injectors (in gasoline engines), which deliver the correct amount of fuel into the combustion chamber.

f. Ignition System (gasoline engines only): Consists of a spark plug and associated components to ignite the air-fuel mixture at the right moment.

g. Cooling System: IC engines generate a significant amount of heat during operation, so a cooling system (usually involving a radiator and a specified coolant) is necessary to prevent overheating.

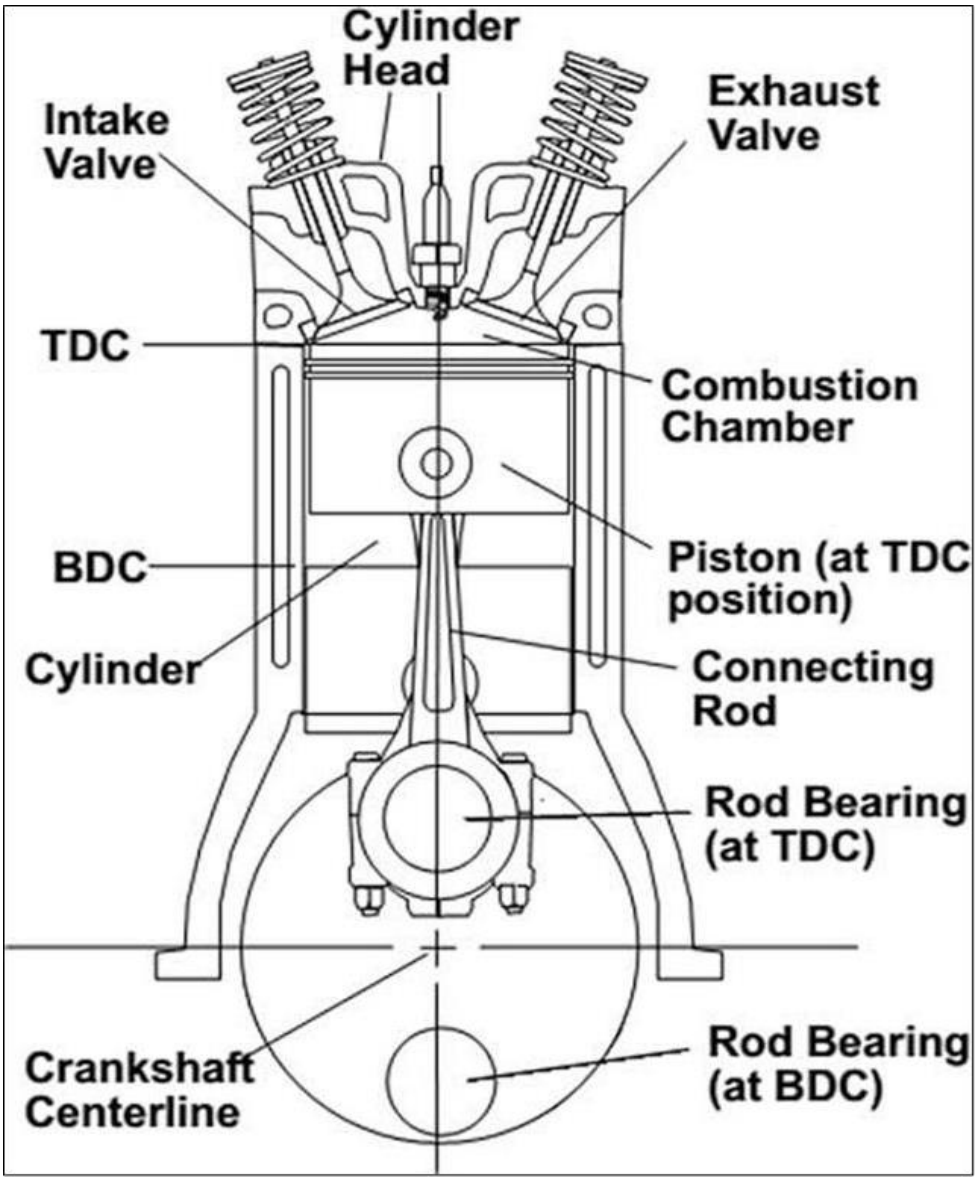


Figure 5.1: Schematic diagram of an IC engine.

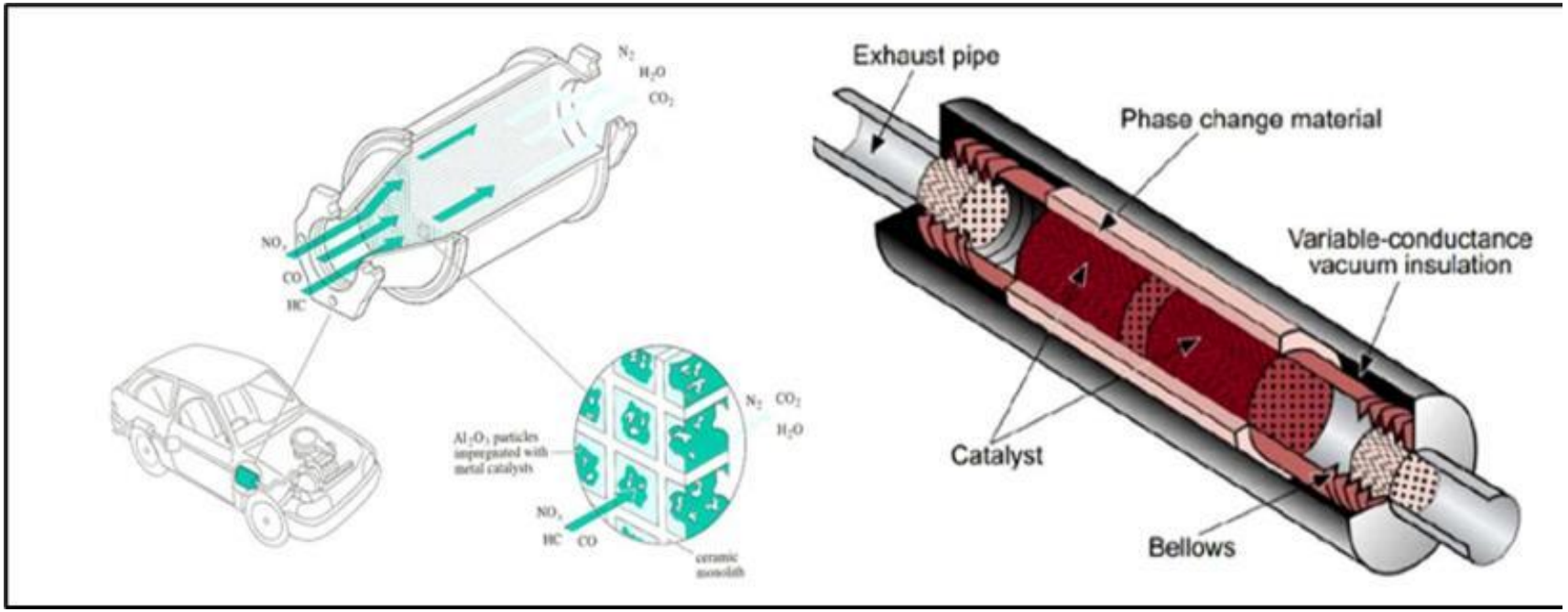


Figure 5.2: Inner Structure of the catalytic converter present in a car exhaust pipe.

5.1.1. Generation of CO (Carbon Monoxide)

Carbon monoxide (CO) is a toxic gas produced during the incomplete combustion of carbon-containing fuels. In IC engines, CO is primarily generated when there is not enough oxygen available to completely oxidize the carbon present in the fuel to carbon dioxide (CO_2). Several factors can contribute to the generation of CO:

(a) Incomplete Combustion: When the air-fuel mixture in the combustion chamber is not properly mixed or when combustion conditions (such as temperature or pressure) are not optimally adequate, incomplete combustion occurs, leading to the production of CO instead of CO_2.

(b) Rich Fuel Mixture: Running an engine with a fuel-rich mixture (more fuel relative to air) can result in higher CO emissions because there is not enough oxygen available to completely burn all the fuel.

(c) Poor Engine Tuning: Incorrect ignition timing, faulty spark plugs, or other issues with the ignition system of the IC engine can lead to inefficient combustion, thereby increasing CO emissions.

(d) Exhaust System Malfunction: Problems with the exhaust system, such as a clogged catalytic converter, can hinder the conversion of CO to less harmful gases like CO_2, leading to higher CO emissions.

Reducing CO emissions from IC engines typically involves optimizing the combustion processes, improving engine design, and tuning, and ensuring proper maintenance of engine components and exhaust systems. Additionally, the use of catalytic converters in

gasoline engines helps convert CO to CO_2 and water vapor, reducing harmful emissions. The three (3) numbers of catalysts that are synthesized in this project, are used as within a cotton-bed to control the CO emission. The cotton bed is wrapped in an aluminium mesh of a specified length and diameter. The mesh containing the catalytic bed is then installed at the tail of the exhaust pipe and reduction in the generated CO is continuously monitored.



Figure 5.3: The vehicle [**Make**: Maruti-Suzuki; **Mod**el: 800 *DX*] used for testing.

5.2. Design of the experiments

Portable cylindrical packed beds of diameter 1 inch and height 2.5 inches are prepared using Aluminium mesh sheets, as shown in **Figure 5.1**. Inside the hollow bed, packings are made using raw cotton layers inside which each variety of the synthesized catalysts are embedded. The raw cotton is first cut into small square shapes of dimension 2x2 sq inches and is then separated into thin layers. The catalyst is spread/dispersed evenly onto the cotton layer surface and the same is covered using another layer on top. This unit is then rolled into a cylindrical shape and is inserted into the hollow Aluminium cylindrical bed. The cylindrical bed has one of its ends open and the other closed. Many such portable beds are prepared using different quantities of catalysts and are then subjected to a pollution-under-control (PUC) tests for a 25-year-old car [**Make**: Maruti-Suzuki; **Mod**el: 800 DX; **Engine class**: BS II] at a nearby petrol pump and the CO emission percentage is estimated.

At first, CO [%] emissions are recorded without using any catalyst [*control*] in the tailpipe of the car. The car is started and the detector pipe is then immediately inserted inside the tailpipe. For the first 60 seconds the reading is taken at 10 kmph speed and then for the next 60 seconds the car speed is maintained at 20 kmph. The recorded CO emission [%] for the entire 120 seconds duration is digitally displayed on the recorder which is connected to a computer. After the first test, the second test is repeated following a similar protocol using the catalytic packed beds containing different quantities of the catalyst (0.5 g and 1 g) being inserted into the tailpipe. The following **Table 5.1** shows the

recorded CO emissions [%] with respect to time for all the three synthesized catalysts with quantities 0.5 g and 1 g at two difference acceleration speeds of 10 km/h and 20 km/h. Due to non-availability of slots, analysis using the fourth catalyst could not be carried out.

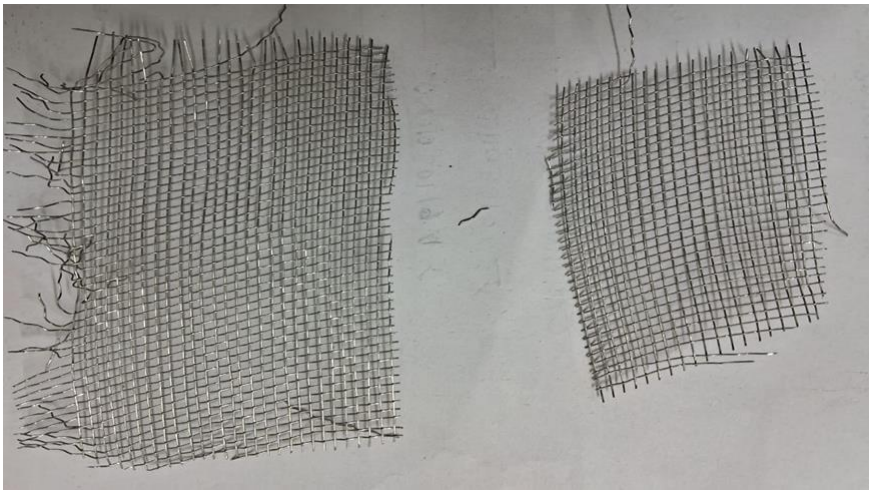


Figure 5.4. Raw material of the external structure of the cylindrical packed bed (Aluminium Mesh).

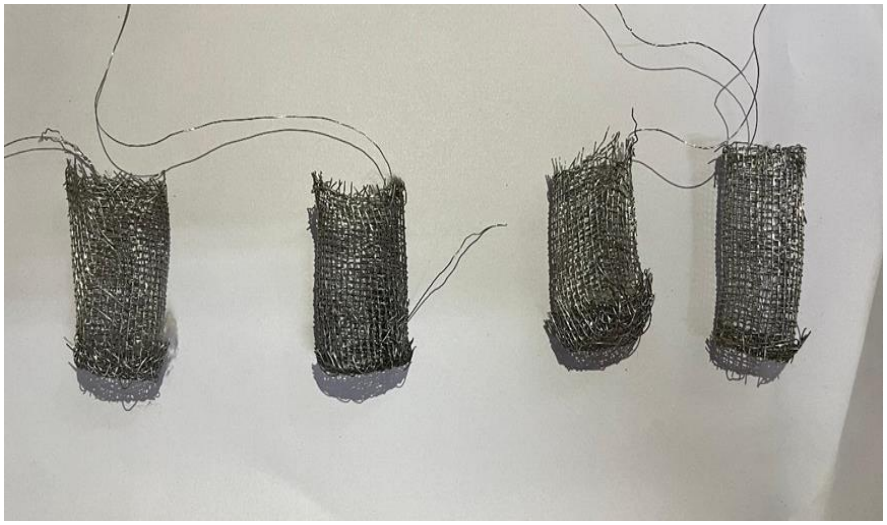


Figure 5.5: Cylindrical envelopes for storing the cotton beds packed with synthesized catalysts.

(a)



(b)



(c)

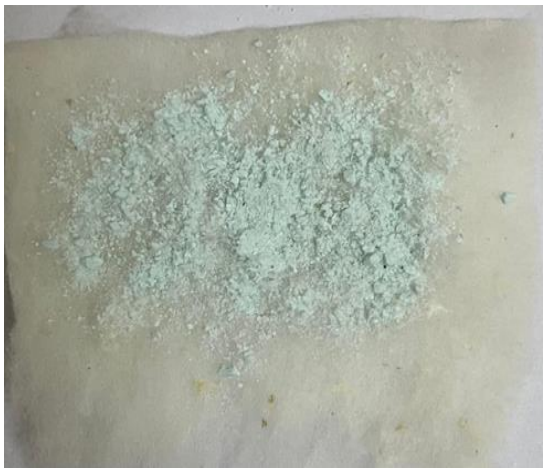


Figure 5.6: Catalysts dispersed over the cotton bed for (a) Cu/CA, (b) Cu/CAT, (c)Cu/A.

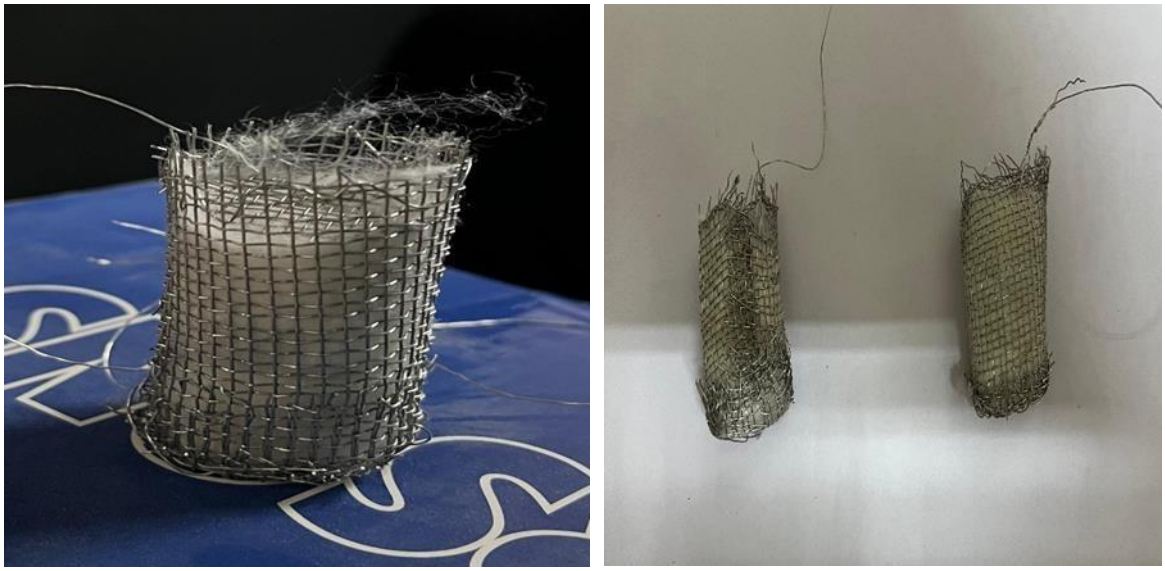


Figure 5.7: Cylindrical packed-bed stuffed with well-dispersed synthesized catalysts.

5.2.1. Parameters for Testing

a. Weather condition (Temperature, humidity)
b. Quantity of the catalysts used
c. Accelerated speed of the used car (more the acceleration, the levels of emission of CO increases)
d. Time duration of testing
e. Diameter of the cylindrical packed bed (less than the tail-pipe diameter)
f. Quality of the bed material (i.e. Cotton is used in our bed)
g. Condition of the IC engine of the used car (PUC failed car or the car which used for more than 15 years is suitable for this)



Figure 5.8: Installation of the packed-bed filled with catalysts at the tailpipe.

5.3. Results and Discussion

Table 5.1: CO emission testing without using any catalyst [Control].

Acceleration speed of the used car	Time(sec)	Emission of CO (%)
10 km/h	0	0.593
	5	0.612
	10	0.639
	15	0.652
	20	0.699
	25	0.713

	30	0.762
	35	0.782
	40	0.802
	45	0.820
	50	0.831
	55	0.837
	60	0.850
20 Km/h	0	0.487
	5	0.501
	10	0.526
	15	0.548
	20	0.559
	25	0.560
	30	0.562
	35	0.567
	40	0.571
	45	0.578
	50	0.611
	55	0.615
	60	0.632



Figure 5.9: Pictures of monitoring of CO, testing and recording the data-sets.

Table 5.2: Control of CO emissions using Catalyst 1 (Cu/CA).

Acceleration speed of used car	Quantity of used catalyst	Time(sec)	Emission of CO (%)
		0	0.248
		5	0.251
		10	0.266
		15	0.267
		20	0.280

10 km/h	0.5 gm	25	0.307
		30	0.308
		35	0.348
		40	0.350
		45	0.344
		50	0.367
		55	0.411
		60	0.456
	1.0 gm	0	0.017
		5	0.021
		10	0.021
		15	0.023
		20	0.023
		25	0.030
		30	0.034
		35	0.038
		40	0.049
		45	0.53
		50	0.058
		55	0.062
		60	0.081
20 km/h	0.5 gm	0	0.341
		5	0.340
		10	0.360
		15	0.383
		20	0.412
		25	0.435
		30	0.452

		35	0.512
		40	0.536
		45	0.545
		50	0.591
		55	0.631
		60	0.655
	1.0 gm	0	0.058
		5	0.064
		10	0.067
		15	0.070
		20	0.076
		25	0.078
		30	0.085
		35	0.088
		40	0.096
		45	0.111
		50	0.135
		55	0.151
		60	0.211

Table 5.3: Control of CO emissions using Catalyst 2 (Cu/CA-T).

Acceleration speed of used car	Quantity of used Catalyst	Time(sec)	Emission of CO (%)
10 km/h	0.5 gm	0	0.412
		5	0.436
		10	0.458
		15	0.491

		20	0.512
		25	0.534
		30	0.538
		35	0.551
		40	0.568
		45	0.591
		50	0.594
		55	0.597
		60	0.612
	1.0 gm	0	0.253
		5	0.268
		10	0.299
		15	0.315
		20	0.345
		25	0.361
		30	0.411
		35	0.425
		40	0.458
		45	0.481
		50	0.502
		55	0.545
		60	0.561
		0	0.125
		5	0.138
		10	0.154
		15	0.181
		20	0.210
		25	0.228

20 km/h	0.5 gm	30	0.235
		35	0.248
		40	0.261
		45	0.288
		50	0.315
		55	0.327
		60	0.345
	1.0 gm	0	0.172
		5	0.185
		10	0.217
		15	0.245
		20	0.248
		25	0.257
		30	0.264
		35	0.287
		40	0.288
		45	0.291
		50	0.301
		55	0.320
		60	0.325

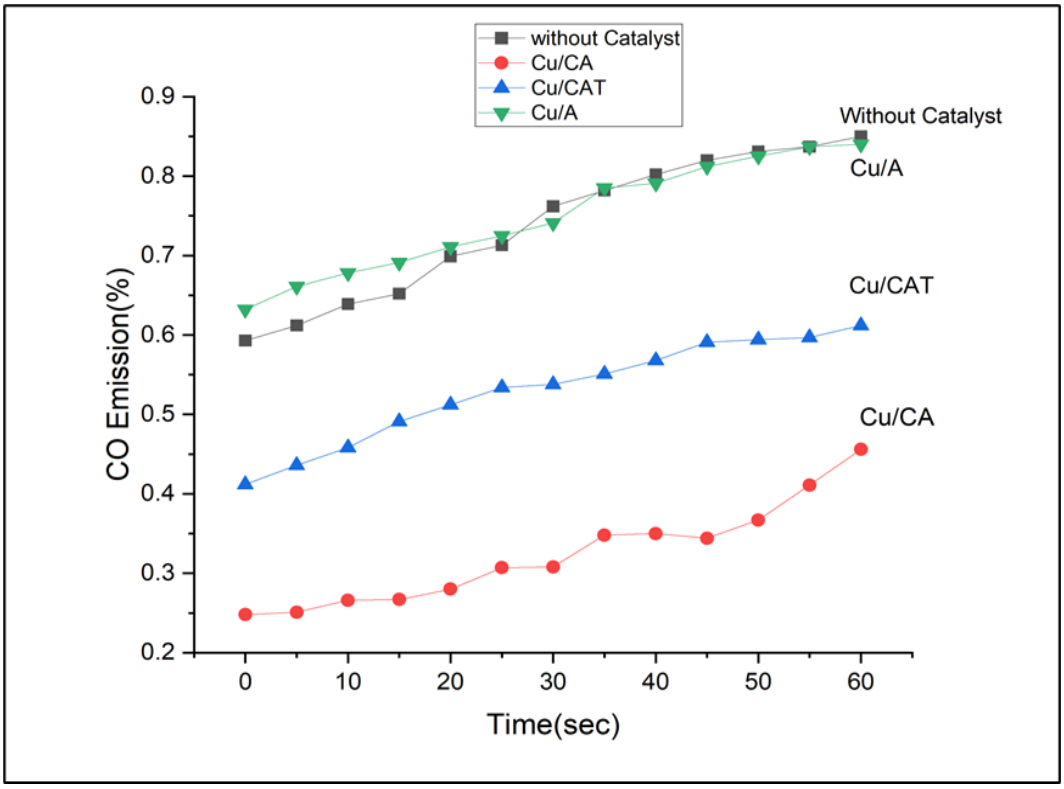
Table 5.4: Control of CO emissions using Catalyst 3 (Cu/A).

Acceleration speed of used car	Quantity of used catalyst	Time(sec)	Emission of CO (%)
		0	0.632
		5	0.661
		10	0.678

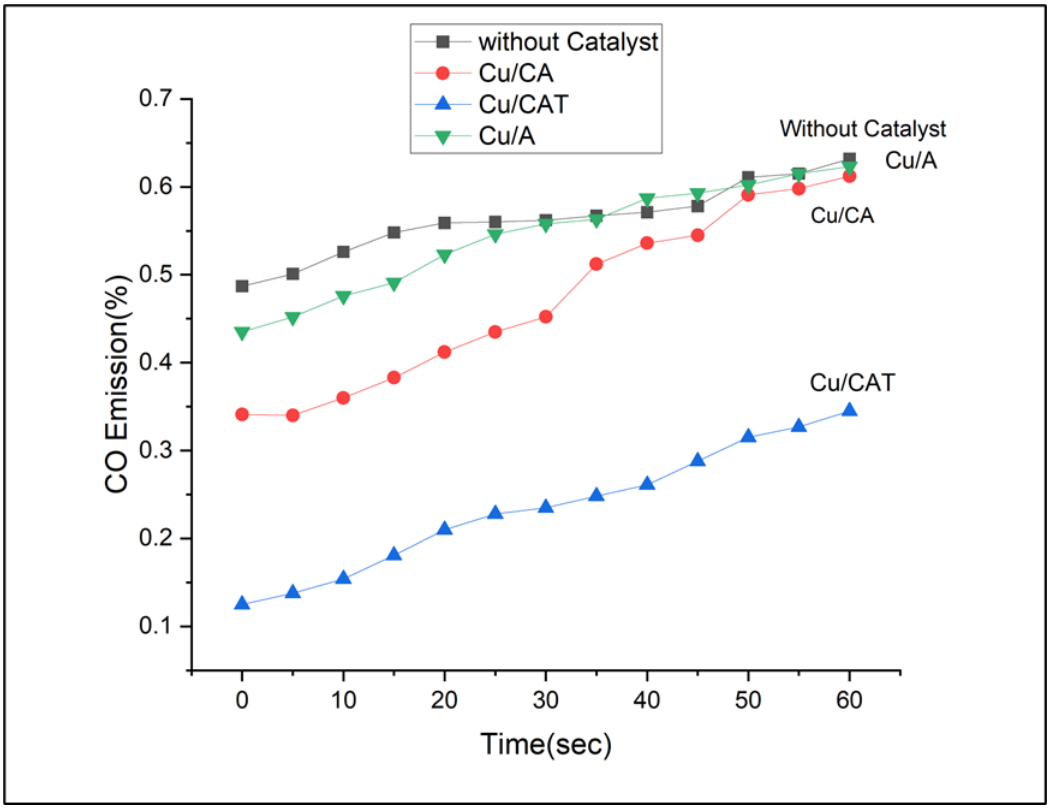
10 km/h	0.5 gm	15	0.691
		20	0.711
		25	0.725
		30	0.741
		35	0.785
		40	0.791
		45	0.812
		50	0.825
		55	0.837
		60	0.840
	1.0 gm	0	0.052
		5	0.071
		10	0.084
		15	0.121
		20	0.137
		25	0.145
		30	0.168
		35	0.195
		40	0.213
		45	0.232
		50	0.245
		55	0.268
		60	0.295
		0	0.435
		5	0.452
		10	0.476
		15	0.491
		20	0.523

20 km/h	0.5 gm	25	0.546
		30	0.558
		35	0.563
		40	0.587
		45	0.593
		50	0.602
		55	0.615
		60	0.623
	1.0 gm	0	0.048
		5	0.053
		10	0.058
		15	0.064
		20	0.067
		25	0.071
		30	0.076
		35	0.079
		40	0.080
		45	0.081
		50	0.084
		55	0.092
		60	0.095

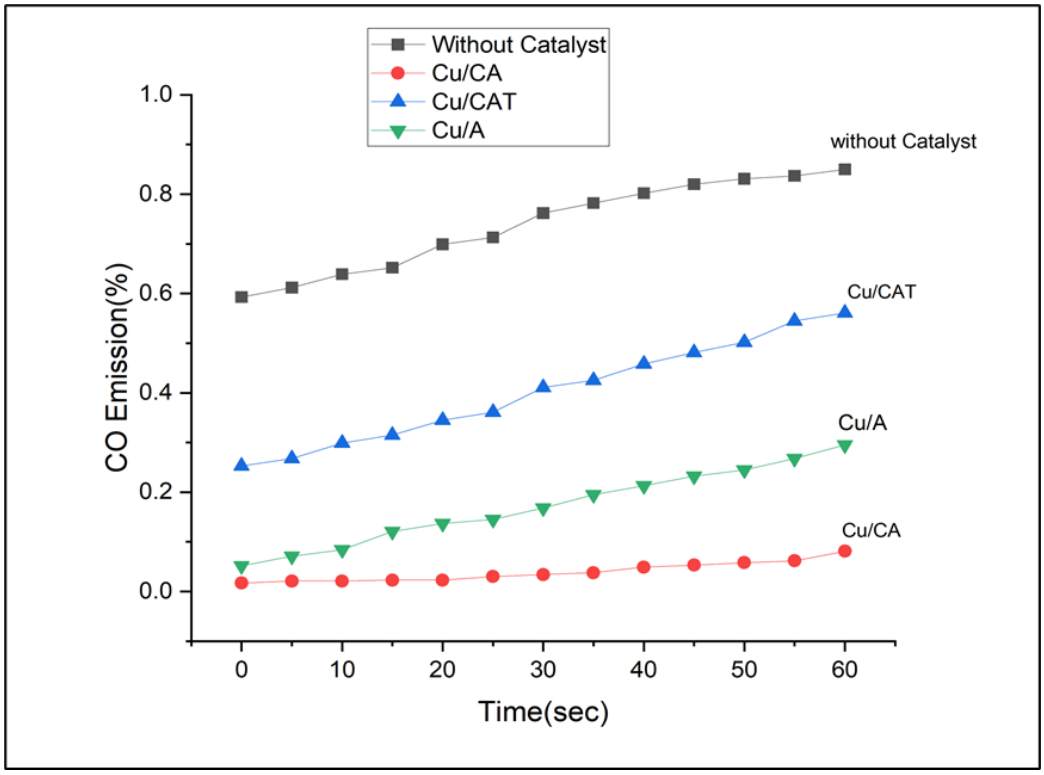
(a)


without Catalyst
Cu/CA
Cu/CAT
Cu/A
Without Catalyst
Cu/A
Cu/CAT
Cu/CA
CO Emission(%)
Time(sec)
0.2
0.3
0.4
0.5
0.6
0.7
0.8
0.9
0
10
20
30
40
50
60

(b)


without Catalyst
Cu/CA
Cu/CAT
Cu/A
Without Catalyst
Cu/A
Cu/CA
Cu/CAT
CO Emission(%)
Time(sec)
0.1
0.2
0.3
0.4
0.5
0.6
0.7
0
10
20
30
40
50
60

(c)



(d)

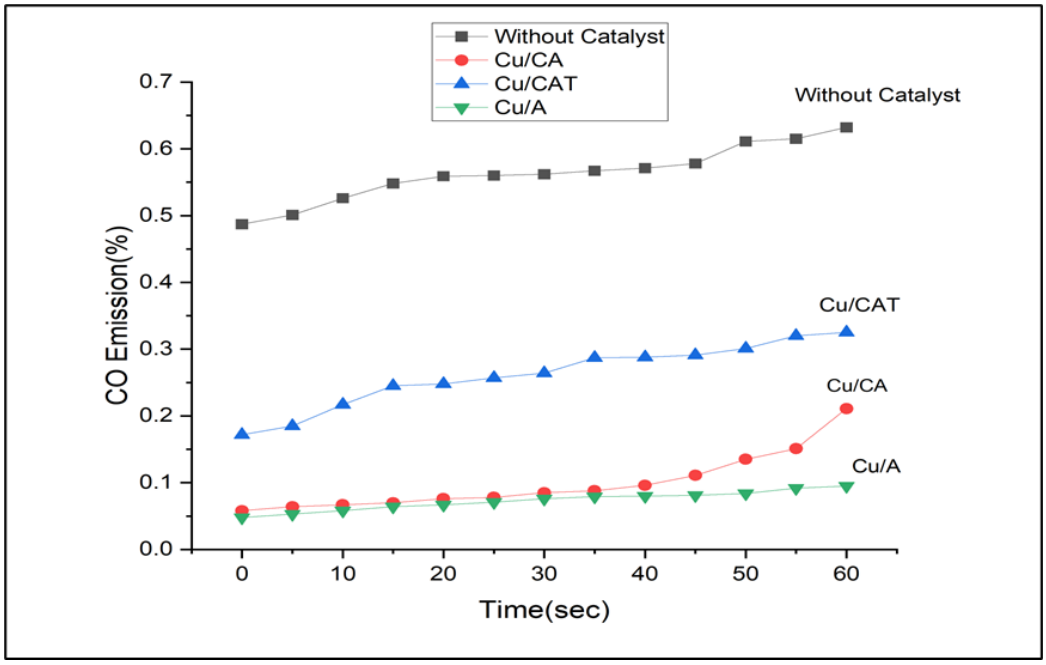


Figure 5.10: Comparison plots of CO emissions with various quantity of catalysts and accelerated speed: (a) Quantity=0.5 gm, Speed=10 km/h, (b) Quantity=0.5 gm, Speed=20 km/h, (c) Quantity=1.0 gm, Speed=10 km/h, (d) Quality=1.0 gm, Speed=20 km/h.

CO emissions are recorded at two different speeds, viz, 10 kmph and 20 kmph. At first CO emission for the car is recorded without using any catalyst. **Table 5.1** shows the continuous data for CO emissions without using any catalyst [Control] while **Table 5.2**, **Table 5.3**, and **Table 5.4** show the continuous data for control of CO using Catalyst 1 (Cu/CA), Catalyst 2 (Cu/CA-T), and Catalyst 3 (Cu/A) respectively.

On observing **Figure 5.3 (a)** we see that the emissions of CO are around 0.6% - 0.85% at a speed of 10 kmph and the same are around 0.5% - 0.65% at a speed of 20 kmph speed [refer **Figure 5.3 (b)**] while no catalyst was used. In **Figure 5.3 (a)** we clearly see that on using 0.5 g quantity of each catalyst and at 10 km/h speed, Cu/CA stands out to be the best choice among all three (3) catalysts. Catalyst Cu/CA-T also gives satisfactory result while Cu/A could not reduce the CO emissions at all. Cu/CA reduce the CO emission significantly as compared to both Cu/CA-T and Cu/A.

In **Figure 5.3 (b)**, the speed of the car is maintained at 20 kmph. In this case 0.5 g quantity of each catalyst is used. Here we find that catalyst Cu/CA-T gives the best result in terms of control of CO emissions as compared to the other catalysts. Catalyst Cu/CA also controlled the emission but not to a significant extent. Again, catalyst Cu/A is seen to be unable to reduce the CO emissions at all. At high speed, Cu/CA-T works better than Cu/CA. In both the speeds 0.5 g of Cu/A cannot contribute significantly to control CO emissions.

In **Figure 5.3 (c)** speed is kept at 10 kmph and catalyst quantity used is 1.0 g each. In this case Cu/CA exhibits the best result. But, Cu/A and Cu/CA-T also show quite satisfactory performance in terms of control of CO emissions from auto exhaust.

In **Figure 5.3 (d)**, car speed is maintained at 20 kmph and quantity of catalyst used is 1.0 g each. Here we observe that Cu/CA and Cu/A both exhibit the best results and the optimum reduction in CO values are also very similar. Catalyst Cu/CA-T also reduced the CO emission quite significantly.

Considering process parameters like car speed, catalyst quantity and running time into consideration, catalysts Cu/CA-T and Cu/CA are able to reduce CO emissions quite significantly and consistently, while the performance of catalyst Cu/A is not that satisfactory when the quantity of the catalysts is low. At higher quantity of Catalysts (i.e. 1.0 gm) all the three catalysts show significantly better results. From this we can understand that high quantity of Cu/A must be used in order to control emissions of CO.

Chapter 6:

Conclusion and Recommendations for Future-work

6.1. Conclusion

The major objectives of our work were to prepare supported metal catalysts with superior 'low-temperature activity,' excellent 'thermal stability', and 'high-level selectivity' that would effectively reduce harmful carbon monoxide gas from auto-exhaust of the vehicles that cause severe negative impact to human and animal lives all around the world. Keeping these major objectives in mind, four novel metal catalysts were prepared namely, Cu/CA, Cu/CA-T, Cu/A, and Cu/CA-S using conventional synthesis methods like the Wet Impregnation method, Sol-Gel method and some modified form of these methods like the Two-Step Wet Impregnation method. These catalysts, after being put through several physical characterization processes like CHNS, FT-IR, TGA, BET, XRD, etc. their elemental properties, surface morphology, thermal stability, pore volume, surface area, the particle-size distributions were evaluated. Catalysts Cu/CA and Cu/CA-T had the lowest pore volumes suggesting them to be used as more selective catalysts in terms of reducing CO emissions, as compared to Cu/A. Various pore size distribution models like BET, BJH, and NLDFT also indicated that majority of the pores are in the microporous region. After carrying out the emission control tests, it was finally concluded that under varying process

parameters like the quantity of the specific catalyst, car accelerator speed, length, diameter, and porosity of the packed-bed, running time, etc. catalysts Cu/CA and Cu/CA-T both were able to control the CO emission much better as compared to Cu/A. But it was also found that while using higher quantities of catalysts, catalyst Cu/A could also control the emission quite satisfactorily along with Cu/CA and Cu/CA-T. All the catalysts also showed excellent thermal stability even after being subjected to thermogravimetric analysis at very high temperatures. The portable cylindrical packed-beds containing the synthesized catalyst wrapped in cotton-pads, were also found to be quite useful in carrying out the emission control tests successfully after being inserted into the tail-pipe of the 25 year old car efficiently.

6.2. Recommendations for Future Work

All the catalysts were satisfactorily able to control carbon monoxide emissions from the vehicular exhaust. Even after this, there remain a few areas which should be further explored in the future to improve the methodologies for treating CO emissions, in particular.

- ✓ It would be interesting to find out if the catalysts could also control the emission of other gases like CO_2, SO_x, NO_x, etc. which are also quite harmful.
- ✓ Interference with CO_2 while CO gets converted using the synthesized catalysts is another important aspect to be studied.

- ✓ Apart from noble or base metals, if any other metal could be used to prepare the catalysts, that could effectively control CO emissions, remains an area of further research.
- ✓ Another area of research could be optimization of the synthesis processes using advanced Design of Experiments statistical tools like RSM and other relevant Machine Learning tools.
- ✓ Researchers could also investigate how they could optimize and correlate the activity and selectivity of the catalysts by considering various parameters like distribution of particle size, properties of support-material, and textural properties of catalyst.
- ✓ During emission control tests, it is also necessary to check the activity of synthesized catalysts using initial-rate and other relevant methods under varying car accelerator speed (which would change the exhaust CO concentrations), and using different quantities of the catalysts.
- ✓ We will have to check the catalysts at different weather conditions too.
- ✓ Also, it will be a crucial concern to check on the aging factor, probability of regeneration and re-use of the spent catalysts. Through this, we can estimate the efficiency and effectiveness of the catalysts.

These would eventually lead to a cleaner transportation system and a greener earth.

References

[1] National Institutes of Health (NIH). 2016. TOXNET: Toxicology Data Network. NIH, U.S. National Library of Medicine. @ http://toxnet.nlm.nih.gov/. Accessed 4/6/2017

[2] Rose, C. S., R. A. Jones, L. J. Jenkins Jr and J. Siegel. 1970. The acute hyperbaric toxicity of carbon monoxide. Toxicology and Applied Pharmacology 17(3): 752-760.

[3] Badr, O. and S. Probert (1994). "Carbon monoxide concentration in the Earth's atmosphere." Applied Energy **49**(2): 99-143.

[4] Chowdhury, I. R. (2015). "Scenario of vehicular emissions and its effect on human health in Kolkata city." International Journal of Humanities and Social Science Invention **4**(5): 1-9.

[5] Dey, S., et al. (2019). "Ambient temperature complete oxidation of carbon monoxide using hopcalite catalysts for fire escape mask applications." Advanced Composites and Hybrid Materials **2**: 501-519.

[6] Dey, S. and N. Mehta (2020). "Automobile pollution control using catalysis." Resources, Environment and Sustainability **2**: 100006.

[7] Mineau, P., et al. (2001). "Pesticide acute toxicity reference values for birds." Reviews of Environmental Contamination and Toxicology **170**: 13-74.

[8] Mishra, A. (2023). "Clearing the Air: India's National Clean Air Programme and the Path Forward." Policy.

[9] Morris, G. L., et al. (1985). "Weanling pigs under sublethal concentrations of atmospheric carbon monoxide." Journal of animal science **61**(5): 1080-1087.

[10] Patel, K. D., et al. (2022). "Design and development of automotive catalytic converter using non-nobel catalyst for the reduction of exhaust emission: A review." Materials Today: Proceedings **57**: 2465-2472.

[11] Raub, J. A. (1999). "Health effects of exposure to ambient carbon monoxide." Chemosphere - Global Change Science **1**(1): 331-351.

[12] Ravindranath, N., et al. (2011). "Biofuel production and implications for land use, food production and environment in India." Energy policy **39**(10): 5737-5745.

[13] Schafer Jr, E. W. and W. A. Bowles Jr (2004). Toxicity, repellency or phytotoxicity of 979 chemicals to birds, mammals and plants, National Wildlife Research Center.

[14] Aghamohammadi, S., et al. (2017). "Sequential impregnation vs. sol-gel synthesized Ni/Al2O3-CeO2 nanocatalyst for dry reforming of methane: Effect of synthesis method and support promotion." Molecular Catalysis **431**: 39-48.

[15] Lykaki, M., et al. (2018). "Ceria nanoparticles shape effects on the structural defects and surface chemistry: Implications in CO oxidation by Cu/CeO2 catalysts." Applied Catalysis B: Environmental **230**: 18-28.

[16] Maciel, C. G., et al. (2012). "Effect of nature of ceria support in CuO/CeO2 catalyst for PROX-CO reaction." Fuel **97**: 245-252.

[17] Phutthakoon, P., et al. (2022). "Effects of preparation method on catalytic activities of the CuO/CeO2-Al2O3 catalyst for the selective CO oxidation reaction." Journal of Engineering and Innovation **15**(3): 197-207.

[18] Xie, S., et al. (2021). "Highly active and stable palladium catalysts on novel ceria–alumina supports for efficient oxidation of carbon monoxide and hydrocarbons." Environmental Science & Technology **55**(11): 7624-7633.

[19] Arif, M., et al. (2021). "A complete characterization of microalgal biomass through FTIR/TGA/CHNS analysis: An approach for biofuel generation and nutrients removal." Renewable Energy **163**: 1973-1982.

[20] Baneshi, J., et al. (2014). "Homogeneous precipitation synthesis of CuO–ZrO2–CeO2–Al2O3 nanocatalyst used in hydrogen production via methanol steam reforming for fuel cell applications." Energy Conversion and Management **87**: 928-937.

[21] Escribano, V. S., et al. (2008). "A study of a ceria–zirconia-supported manganese oxide catalyst for combustion of Diesel soot particles." Combustion and Flame **153**(1-2): 97-104.

[22] Fadeeva, V., et al. (2008). "Elemental analysis of organic compounds with the use of automated CHNS analyzers." Journal of analytical chemistry **63**: 1094-1106.

[23] Qiu, F., et al. (2011). "Heterogeneous solid base nanocatalyst: preparation, characterization and application in biodiesel production." Bioresource technology **102**(5): 4150-4156.

[24] Topsøe, N.-Y. and H. Topsøe (1999). "FTIR studies of dynamic surface structural changes in Cu-based methanol synthesis catalysts." Journal of Molecular Catalysis A: Chemical **141**(1-3): 95-105.

[25] Vahid, B. R. and M. Haghighi (2017). "Biodiesel production from sunflower oil over MgO/MgAl2O4 nanocatalyst: effect of fuel type on catalyst nanostructure and performance." Energy Conversion and Management **134**: 290-300.

[26] Amelkovich, Y. A., O. Nazarenko, A. Sechin and V. P.M (2015). "Characterization of copper nanopowders after natural aging." IOP Conference Series: Materials Science and Engineering **81**.

[27] Selvamani, A., K. Shanthi, D. Santhanaraj, C. Babu, V. Srinivasan, P. Thirukumaran, V. Ramkumar, A. Shakilaparveen and R. Balasubramanian (2018). "Effective removal of automobile exhausts over flower-like Ce1− xCuxO2 nanocatalysts exposed active {100} plane." Journal of Rare Earths **36**(6): 603-612.

[28] Dey, S. and G. C. Dhal (2019). "Catalytic conversion of carbon monoxide into carbon dioxide over spinel catalysts: An overview." Materials Science for Energy Technologies **2**(3): 575-588.

[29] Dey, S. and G. C. Dhal (2020). "Controlling carbon monoxide emissions from automobile vehicle exhaust using copper oxide catalysts in a catalytic converter." Materials Today Chemistry **17**: 100282.

[30] Dey, S., G. C. Dhal, R. Prasad and D. Mohan (2017). "Effect of nitrate metal (Ce, Cu, Mn and Co) precursors for the total oxidation of carbon monoxide." Resource-efficient technologies **3**(3): 293-302.

Annex-I

Boehm Titration

Determination of carbon surface chemistry, based on classical analytical chemistry, was first developed by Boehm. He proposed to neutralize the surface functionalities based on their acid strength. In this method, sodium bicarbonate, $NaHCO_3$ (pK_a = 6.37), sodium carbonate, Na_2CO_3 (pK_a = 10.25), sodium hydroxide, NaOH (pK_a = 15.74), and sodium ethoxide, $NaOC_2H_5$ (pK_a = 20.58) are used as bases. In this acid/base titration, sodium bicarbonate neutralizes carboxylic acids, sodium carbonate neutralizes carboxylic acids and lactones, and sodium hydroxide neutralizes carboxylic acids, lactones and phenols. However, sodium ethoxide reacts with all oxygen species, even extremely weak acids (pK_a < 20.58). But, because of the difficulties in using sodium ethoxide due to its non-aqueous media and oxygen free conditions, Boehm titration is limited to the determination of carboxylic groups, lactones, and phenols.

Experimental procedure

The adsorbent materials (GAC and FACs) weighing 0.2 g each are taken in a 100 ml beaker. 0.1 N NaOH, 0.1 N Na_2CO_3 and 0.1 N $NaHCO_3$ are prepared and 25 ml of each of this solution is added to the beaker containing GAC and FACs. Then, this mixture is kept for 72 h for complete reaction. The amount of base consumed by the acidic groups present on the surface of the adsorbent materials, is determined by back-titration method. 0.1 N HCl is used to neutralize the unreacted bases that are left after reaction

with the acidic functional groups of activated carbon. A solution of NaOH is prepared beforehand, as a secondary standard to determine the strength of HCl used here. The strength of NaOH is determined by the primary standard of oxalic acid. The amount of acidic groups present on the surface of GAC and FACs are determined by milli-equivalent unit.

Calculation

At first, the strength of secondary standard NaOH is determined by titration with oxalic acid as a primary standard. Then, the strength of HCl is determined by titration with NaOH. The amount of NaOH consumed by carboxylic group is determined by back titration with HCl. As we know,

1L 1(N) $NaHCO_3$ ≡ 84 g $NaHCO_3$

Hence, we can calculate the amount of $NaHCO_3$ in gm by calculating the normality of $NaHCO_3$and with the quantity of HCl before and after reaction. This weight of $NaHCO_3$ is divided by the molecular weight of $NaHCO_3$ to convert it to g or milli equivalent of $NaHCO_3$. Similarly, the strength of Na_2CO_3 can be calculated by titration with HCl. We know,

53 g-equivalent of Na_2CO_3≡ 84 g-equivalent of $NaHCO_3$

So, the amount of Na_2CO_3 consumed by the acidic group can be converted to milli-equivalent of $NaHCO_3$. Consequently, the amount of carboxylic and lactonic groups can be determined in terms of $NaHCO_3$. By knowing the difference of the amount of $NaHCO_3$ required, the estimation of lactonic group present on the surface of GAC and FACs can be

obtained. Again, we know,

40 g-equivalent of NaOH ≡ 84 g-equivalent of $NaHCO_3$

So the amount of NaOH consumed by the acidic functional groups can be converted in terms of $NaHCO_3$. Similar to the above method, the amount of phenolic group can be estimated from the difference in the amounts of $NaHCO_3$ required, as NaOH reacts with all carboxylic, lactonic and phenolic groups.